Deep Learning for Spatial Multi-Omics: Predicting Cardiomyocyte Differentiation Efficiency at Single-Cell Resolution

by

Tumo Kgabeng

submitted in accordance with the requirements

for the degree of

Master of Engineering

in the department of

Mechanical, Bioresources and Biomedical Engineering

at the

UNIVERSITY OF SOUTH AFRICA

SUPERVISOR: Prof Thanyani Pandelani

CO-SUPERVISOR: Prof Harry Ngwangwa

EXTERNAL-SUPERVISOR: Prof Lulu Wang

2026

DECLARATION

Name:	Tumo Kgabeng
Student number:	28346416
Degree	Master of Engineering (90121)

Exact wording of the title of the thesis as appearing on the electronic copy submitted for examination:

Deep Learning for Spatial Multi-Omics: Predicting Cardiomyocyte Differentiation Efficiency at Single-Cell Resolution

I declare that the above thesis is my own work and that all the sources that I have used or quoted have been indicated and acknowledged by means of complete references.

I further declare that I submitted the thesis to originality checking software, and it falls within the accepted requirements for originality.

I further declare that I have not previously submitted this work, or part of it, for examination at UNISA for another qualification or at any other higher education institution.

(*The thesis will not be examined unless this statement has been submitted.*)

SIGNATURE	DATE
	6/03/2026

ACKNOWLEDGEMENTS

I extend my heartfelt gratitude to all those who have contributed to the successful completion of this thesis. This journey would not have been possible without the support, guidance, and encouragement of numerous individuals and institutions who have shaped both my academic development and this research endeavour.

I am profoundly grateful to my supervisory team for their exceptional guidance throughout this research journey. To Prof Thanyani Pandelani, Prof Lulu Wang, and Prof Harry Ngwangwa, whose visionary leadership and deep expertise provided the foundational direction for this work. Your ability to bridge theoretical concepts with practical applications has been instrumental in shaping this work. Your patience in explaining complex methodological concepts and your encouragement during challenging phases of model development have been invaluable.

My deepest gratitude goes to my parents, whose unwavering love, support, and sacrifice have made this academic journey possible. Your belief in the importance of education and your constant encouragement throughout the years of study have been the bedrock of my perseverance. Your understanding during the countless hours spent on research, writing, and analysis, and your patience during moments of academic stress, have been invaluable. The values of hard work, integrity, and dedication that you instilled in me have guided every aspect of this research. This achievement is as much yours as it is mine.

I am deeply grateful to the University of South Africa for providing the framework, resources, and academic environment that made this research possible. The university's commitment to excellence in postgraduate research and its support for innovative computational biology research have been essential to the success of this work.

I am grateful to my fellow graduate students and research colleagues who provided intellectual stimulation, technical discussions, and moral support throughout this journey. The collaborative environment and exchange of ideas have enriched both the research process and my understanding of computational biology and regenerative medicine.

TABLE OF CONTENTS

ABBREVIATIONS

AI	Artificial Intelligence
GAT	Graph Attention Network
GCN	Graph Convolutional Network
XAI	Explainable Artificial Intelligence
scRNA-seq	Single-cell RNA Sequencing
PCA	Principal Component Analysis
LSTM	Long Short-Term Memory
MC	Monte Carlo
UQ	Uncertainty Quantification
SHAP	SHapley Additive exPlanations
GNN	Graph Neural Network
RNN	Recurrent Neural Network
iPSC	Induced Pluripotent Stem Cells
CM	Cardiomyocyte
GATA4	GATA Binding Protein 4
MEF2C	Myocyte Enhancer Factor 2C
TBX5	T-box Transcription Factor 5
NKX2-5	NK2 Homeobox 5
FKBP1A	FK506 Binding Protein 1A
MYL2	Myosin Light Chain 2
PLN	Phospholamban
CPU	Central Processing Unit
GPU	Graphics Processing Unit

RAM	Random Access Memory
VRAM	Video Random Access Memory
SSD	Solid-State Drive
NVMe	Non-Volatile Memory Express
ERC	Ethics Review Committee
DOI	Digital Object Identifier
UNISA	University of South Africa

DEFINITION OF TERMS

Cardiomyocyte	A specialised muscle cell that forms the contractile tissue of the heart
Cardiomyocyte differentiation	The biological process through which pluripotent or progenitor cells progressively develop into specialised cardiomyocytes
Cardiomyocyte differentiation efficiency	The proportion of stem cells that successfully differentiate into functional cardiomyocytes under a given differentiation protocol
Cell-Cell communication	The exchange of biomechanical signals between neighbouring cells that regulate cellular behaviour, differentiation, and tissue organisation.
Induced Pluripotent Stem Cells (iPSCs)	Somatic cells that have been programmed into pluripotent state, enabling them to differentiate into various specialised cell types, including cardiomyocytes.
iPSC-Derived Cardiomyocytes (iPSC-CMs)	Heart muscle cells generated through the differentiation of induced pluripotent stem cells.
Single-cell resolution	The ability to measure and analyse biological processes at the level of individual cells rather than bulk tissue samples
Spatial multi-omics	The combined measurement and analysis of multiple molecular data types (such as transcriptomics, epigenomics, proteomics, metabolomics) while preserving spatial location of cells within tissue architecture

TABLE OF FIGURES

LIST OF TABLES

LIST OF EQUATIONS

ABSTRACT

Cardiovascular diseases remain the leading cause of global mortality, with limited regenerative capacity of adult cardiac tissue presenting significant therapeutic challenges. The primary cause of death worldwide is still cardiovascular diseases, and treating these conditions is extremely difficult due to the adult heart tissue's limited capacity for regeneration. Cardiomyocytes derived from human induced pluripotent stem cells (hiPSC-CMs) present promising potential for cardiac regenerative medicine; however, existing differentiation protocols are highly inconsistent and do not have accurate predictive evaluation techniques. By integrating the analysis of temporal gene expression data and spatial transcriptomics, this study developed a novel hybrid deep learning architecture that combines Graph Neural Networks (GNNs) and Recurrent Neural Networks (RNNs) to predict the outcomes of cardiomyocyte differentiation. RNN components analysed temporal gene expression trajectories across 800 samples and 10 time points, while GNN components processed spatial transcriptomics data from 752 tissue spots to capture spatial relationships. Three fusion strategies - concatenation, attention-based, and ensemble approaches - were meticulously evaluated. With an accuracy of 96.67%, the ensemble fusion approach outperformed the state-of-the-art computational approaches by a significant margin (+13.47% compared to the top GNN approaches and +6.97% compared to specialised biological models).

Keywords: Cardiomyocyte differentiation; Spatial transcriptomics, Spatial multi-omics; Single-cell biology; Deep learning; Graph Neural Networks; Recurrent Neural Networks; Stem cells; Artificial Intelligence; Cardiac biology

PUBLISHED RESEARCH OUTPUT

- Kgabeng T, Wang L, Ngwangwa HM, Pandelani T. Integrating Spatial Omics and Deep Learning: Toward Predictive Models of Cardiomyocyte Differentiation Efficiency. Bioengineering (Basel). 2025 Sep 27;12(10):1037. doi: 10.3390/bioengineering12101037. PMID: 41155036; PMCID: PMC12561129.
- Kgabeng T, Wang L, Ngwangwa H, Pandelani T. HeartMAP: A multi-chamber spatial framework for cardiac cell-cell communication. Comput Struct Biotechnol J. 2025 Nov 8;27:4976-4991. doi: 10.1016/j.csbj.2025.11.015. PMID: 41322007; PMCID: PMC12661431.
- Modelling the 4D Space-Time of Cardiac Differentiation Using a Hybrid Graph-Recurrent Neural Network. AI, Computer Science and Robotics Technology Journal (IntechOpen), (*under peer review*)
- GRAIL-Heart: A Graph Attention Network for Inferring Ligand-Receptor Interactions in Spatial Transcriptomics. MethodsX (under peer review, preprint published, DOI: 10.2139/ssrn.6137179)
- GRAIL-Heart v2: A Graph Neural Network Framework for Inverse Modelling of Cell-Cell Communication in Cardiac Tissues. Biomedical Signal Processing and Control (*under peer review*)

1. CHAPTER 1: INTRODUCTION

1.1.BACKGROUND

Cardiovascular diseases (CVDs) remain the leading cause of global mortality, accounting for around 20.5 million deaths in 2021 alone, with over 75% of deaths occurring in low and middle-income nations[1]. This strain is mostly caused by ischaemic heart disease and stroke, which reflects structural difficulties in prevention, treatment, and innovative therapeutics[1]. CVDs, which are caused by diabetes, hypertension, and socioeconomic shifts, take 215 lives every day in South Africa[2], more than all malignancies combined. The adult heart's regenerative ability is quite restricted[3], even with the best medical treatment, making it difficult to heal injured cardiac tissue, which is why this epidemic highlights the urgent need for sophisticated regenerative techniques. These alarming statistics highlight ongoing deficiencies in CVD prevention, early detection, and treatment, particularly in areas with limited resources. Because human cardiomyocytes seldom return to the cell cycle after an ischaemic event, injured myocardium is replaced by fibrotic scar, causing fibrosis and unfavourable cardiac remodelling, increasing the risk of heart failure. This pathophysiological cascade underscores the urgent need for regenerative approaches capable of restoring functional cardiac tissue rather than merely managing disease progression.

With the potential to produce infinite quantities of patient-specific cardiomyocytes without the moral limitations relating to embryonic sources, human induced pluripotent stem cells (hiPSCs) have become a transformative platform for cardiac regenerative medicine[4]. Recent developments in growth factor-guided and small molecule modulator-based directed differentiation protocols have produced impressive results; in suspension culture systems, some of these techniques have been able to achieve >90% cardiomyocyte purity[5]. With yields of roughly 2.4 cardiomyocyte per input hiPSC, the most recent optimised protocols achieved >90% cardiac troponin T-positive cells, signifying significant efficiency gains[5]. Additionally, cutting-edge techniques like reseeding at the cardiac progenitor stage have shown 10-20% absolute increases in cardiomyocyte purity without impairing sarcomere structure or contractility[6]. These hiPSC-derived cardiomyocytes (hiPSC-CMs) demonstrate critical morphological and functional characteristics of native heart cells, including spontaneous contractility, calcium handling machinery, and expression of cardiac-specific transcription factors, positioning them as promising candidates for cell therapy and tissue engineering applications[6], [7]. However, significant challenges persist in translating this potential into clinical reality[8]. Significant batch-to-batch variability is present in current differentiation protocols, and reproducibility under various experimental conditions is impacted by significant intra- and inter-batch variability in cardiomyocyte purity[5], [9]. The therapeutic efficacy of hiPSC-CMs is further limited by their electrical and contractile characteristics, which exhibit significant heterogeneity and frequently resemble immature foetal rather than adult cardiomyocytes[5], [9], [10], [11]. The continuous need for reliable predictive methodologies to maximise protocol outcomes is demonstrated by recent developments in monitoring differentiation efficiency using cutting-edge techniques like Raman spectroscopy of conditioned media[12]. A

thorough understanding of the molecular processes controlling cardiomyocyte differentiation efficiency and maturation is necessary to fully realise their regenerative potential[11].

The development of spatial multi-omics technologies has revolutionised our ability to analyse cellular behaviour and microenvironmental control within intact tissue architectures[13]. Spatial transcriptomics platforms, particularly 10X Genomics Visium technology, enable simultaneous mapping of gene expression patterns to precise anatomical locations, preserving critical spatial context that is lost in traditional single-cell approaches[14], [15], [16], [17]. The intricate cellular communities that make up the developing heart have been made visible by recent developments in spatial transcriptomics[13], [17]. Research has shown that various cardiac cell populations interact spatially to coordinate the development of the ventricular wall[18]. These technologies have revealed spatially restricted regulatory networks, such as local signalling hubs that coordinate lineage commitment through intricate interactions between the Notch and Wnt/β-catenin pathways during cardiomyocyte differentiation[19], [20]. Comprehensive spatial transcriptomic atlases of cardiac development have identified critical spatiotemporal genes such as Igf2, H19, and Tcap, along with transcription factors Tcf12 and Plagl1, which may be associated with the loss of myocardial regeneration ability during early heart development[21], [22], [23]. The dynamic gene expression cascades that propel cardiomyocyte commitment and maturation have been elucidated by temporal profiling of differentiation trajectories using single-cell RNA-sequencing, which complements spatial approaches[24]. Recent single-cell analyses have established comprehensive maturation trajectories, revealing that cardiomyocytes form engineered tissues exhibit various maturation states characterised by sequential changes in developmental, structural, and metabolic gene expression programs[25]. Critical developmental checkpoints have been identified by time-course analyses, which also show how key cardiac transcription factors including NKX2-5, GATA4, and TBX5 coordinate their physical and functional connections to sequentially activate cardiac gene programs[26], [27], [28], [29]. These transcription factors work synergistically; NKX2-5 and GATA4 work together through specific protein-protein interactions, while TBX5 and NKX2-5 work together to control the expression of downstream cardiac gene expression[26], [27], [28], [29]. Novel metrics such as transcriptomic entropy have emerged as robust approaches for quantifying cardiomyocyte maturation status, demonstrating that transcriptomic entropy decreases progressively as cardiomyocytes mature from fetal to adult states[30]. However, integrating these spatial and temporal datasets into predictive models of differentiation efficiency remains a formidable challenge[31].

Deep learning frameworks have demonstrated remarkable success in interpreting high-dimensional biological datasets, offering unprecedented opportunities for understanding complex cellular behaviours[32], [33], [34]. With its ability to capture neighbourhood-dependent gene expression patterns and cell-cell communication networks inside tissue slices, Graph Neural Networks (GNNs) have emerged as particularly powerful tools for spatial transcriptomics analysis[35], [36]. SpaInGNN is one of the latest advancements in GNN architectures created particularly for spatial transcriptomics, it uses advanced graph generation approaches to combine

spatial location data, histology information, and gene expression profiles[37]. With techniques like SpatialGlue attaining >90% accuracy in recognising spatial domains across various tissue types and technology platforms, advanced GNN frameworks have proven to perform better in spatial domain delineation[34], [38]. Meanwhile, Recurrent Neural Networks (RNNs) excel at modelling temporal dependencies in sequential data, making them ideally suited for analysing gene expression trajectories during differentiation processes[34]. Hybrid approaches combining GNN and RNN architectures have shown exceptional performance in biological applications, with studies demonstrating that GNN-RNN combinations can achieve >98% accuracy in complex biological prediction tasks[39], [40].

Despite these technological advancements, current computational approaches for predicting cardiomyocyte differentiation outcomes suffer from significant limitations[41], [42], [43], [44]. Models trained exclusively on transcriptomic data typically achieve only 65-75% accuracy in classifying maturation stages, highlighting the need for more sophisticated integration strategies[45]. Recent machine learning approaches for cardiovascular disease prediction have achieved accuracies of 98.5% using optimised ensemble methods, demonstrating the potential for advanced computational approaches when applied to cardiac biology[46]. Furthermore, existing architectures often ignore important spatial relationships and temporal dynamics that fundamentally govern cellular fate decisions[46]. The integration of explainable artificial intelligence (XAI) methodologies with GNN architectures has shown promise in identifying critical molecular pathways and spatial interaction patterns, with frameworks achieving significant improvements in biological interpretation while maintaining predictive accuracy[47], [48]. This is an entirely computational study, it does not include wet-lab experiments, new data collection, and clinical trials, it's confined to the development, training, and evaluation of a hybrid deep learning model using existing, publicly available datasets. Throughout this study, "differentiation efficiency" refers to the proportion of input hiPSCs that successfully commit to and mature into cardiomyocyte lineage under a given protocol. In the computational context of this study, differentiation efficiency is operationalised as the model's classification of a cell or sample into one of the labelled cardiomyocyte maturation stages (early, mid, or late) derived from the Elorbany et al. (2022)[49] temporal scRNA-seq dataset, where stage labels serve as proxy indicators of protocol success. This definition is used consistently throughout the chapters and subchapters.

1.2.PROBLEM STATEMENT

The lack of reliable computational frameworks that can predict and optimise differentiation efficiency significantly hinders the translation of hiPSC-derived cardiomyocyte technology from the lab bench to the clinical bedside. While temporal profiling and spatial transcriptomics technologies have generated unprecedented datasets documenting the dynamics of cardiomyocyte differentiation, there is currently no integrated computational approach to leverage these complementary data modalities for accurate outcome prediction.

Three significant flaws in current predictive models hinder their clinical application:

First, modality isolations represent a fundamental challenge in existing approaches, spatial transcriptomics data and temporal gene expression are typically analysed separately, missing crucial synergistic regulatory patterns that results from their integration. The spatiotemporal coordination of molecular events that determines the success of differentiation is not captured by this reductionist approach. With SpatialGlue exhibiting exceptional performance across variety of tissue types, recent developments in spatial multi-omics integration have shown that approaches incorporating multiple data modalities can achieve far higher accuracy than single-modality approaches[38]. There is a substantial knowledge gap, nonetheless, as these approaches have not been systematically applied to predict cardiomyocyte differentiation.

Second, most existing integration methods lose crucial spatial positioning information during data fusion, a phenomenon known as context blindness. Cell fate decisions are largely influenced by the microenvironmental context, which included physical constraints, signalling gradients, and cell-cell communication networks. However, these spatial relationships are often disregarded in favour of more simplified analytical approaches; In complex biological prediction tsks, advanced GNN architectures have demonstrated an impressive capacity to preserve spatial context while attaining >85% accuracy[50]. The failure to incorporate spatial neighbourhood information represents a major limitation in current differentiation prediction approaches.

Third, temporal discontinuity limits the predictive ability of static analytical methods. Over the course of days to weeks, developmental checkpoints are sequentially activated during cardiomyocyte differentiation, while early regulatory events determining the results of subsequent maturity. These dynamic processes cannot be modelled by static snapshots, which leads to an insufficient understanding of differentiation trajectories. Hybrid GNN-RNN architectures have demonstrated exceptional performance in modelling biological temporal dependencies, with recent studies achieving >90% accuracy in time-series biological predictions[51]. The absence of such temporal modelling in current differentiation prediction represents a critical methodological gap.

These limitations pose a challenge in optimising the differentiation protocols required to produce clinical-grade cardiomyocytes with consistent quality and functional properties. Delays in delivering regenerative medicines to patients in dire need result from resource waste, prolonged development timelines, and the inability to predict which experimental conditions will yield high-efficiency differentiation. Conservative estimates suggests that predictive optimisation could address current impediments to clinical translation by enhancing functional outcomes and lowering manufacturing costs by 30-40%.

1.3.PURPOSE OF THE STUDY

By developing a novel hybrid deep learning framework that integrates temporal gene expression data with spatial transcriptomics, this study seeks to close the crucial gap in cardiomyocyte differentiation prediction and attain hitherto unheard-of-levels of accuracy in differentiation outcome prediction. The goal of this research is to develop a novel comprehensive computational platform for spatiotemporal analysis of cardiomyocyte differentiation at single-cell resolution by

combining the temporal sequence modelling power of Recurrent Neural Networks with the spatial pattern recognition capabilities of Graph Neural Networks.

The hybrid GNN-RNN architecture is specifically designed to capture the intricate interactions between temporal gene expression dynamics and spatial microenvironmental variables, which together impact differentiation efficiency. This framework incorporates cutting-edge attention mechanisms and graph construction techniques to optimise predictive accuracy while preserving biological interpretability, drawing on recent developments in spatial multi-omics integration and explainable AI methodologies[37], [47]. By using this comprehensive approach, the study hopes to uncover critical spatiotemporal molecular markers, optimise differentiation protocols through data-driven insights, and offer explainable predictions that can guide clinical translation and experimental design.

The research leverages established public datasets and proven deep learning architectures to ensure reproducibility and enable comparison with existing literature, while advancing the field through novel integration strategies and comprehensive validation approaches. This work has the potential to revolutionise hiPSC-based cardiac therapy and establish new benchmarks for computational approaches in regenerative medicine by achieving the target 95% accuracy in differentiation prediction.

1.4.RESEARCH QUESTIONS

This study is guided by four fundamental research questions that address critical knowledge gaps in computational analysis of cardiomyocyte differentiation:

i. How do spatially restricted gene expression patterns influence transcriptional heterogeneity within differentiating cardiomyocyte populations, and can these spatial relationships be effectively captured through advanced GNN architectures?

Complex cellular communities within cardiac tissues have been revealed by recent advanced in spatial transcriptomics, with specific spatial domains showing distinct transcriptional signatures that correlate with functional outcomes. By using sophisticated graph construction approaches, advanced GNN architecture like SpalnGNN have shown exceptional performance in capturing spatial relationships[37]. This question addresses whether these advanced spatial modelling approaches can identify the microenvironmental factors that drive differentiation success.

ii. Does the integrated analysis of spatial transcriptomics and temporal gene expression data significantly improve prediction accuracy of differentiation outcomes compared to unimodal analytical approaches, and what is the magnitude of this improvement?

While spatial multi-omics integration approaches such SpatialGlue have achieved >90% accuracy in identifying spatial domains across a variety of tissue types[38], its potential for predicting temporal differentiation has not yet been investigated. In addition to establishing

benchmarks for computational approaches in regenerative medicine, this question quantifies the added value of multi-modal integration.

iii. Which combinations of spatial neighbourhood features and temporal expression dynamics correlate most strongly with successful cardiomyocyte differentiation trajectories and functional maturation?

Key spatiotemporal regulators of cardiac development have been discovered by recent studies, including critical transcription factor networks including NKX2-5, GATA4, and TBX5[27], [28]. Leveraging the pattern recognition capabilities of hybrid deep learning architectures, this question aims to identify novel spatiotemporal biomarkers that might not be visible using conventional analytical approaches.

iv. Can hybrid GNN-RNN architectures identify biologically relevant molecular markers that align with established cardiac development pathways, and do these computational predictions provide actionable insights for protocol optimisation?

The integration of XAI methodologies with advanced neural network architectures has shown promise in biological applications[47], [48]. To ensure that the framework offers interpretable insights for experimental validation, this question addresses the biological validity of computational predictions as well as their translational potential for improving differentiation protocols.

1.5.RESEARCH OBJECTIVES

This study aims to achieve the overarching goal through six specific objectives that systematically address the technical; and biological challenges of spatiotemporal differentiation modelling:

i. Develop a hybrid deep learning model that combines RNNs for temporal modelling of gene expression trajectories during cardiomyocyte differentiation with GNNs for spatial analysis of intercellular communication patterns.
ii. Achieve superior prediction accuracy by demonstrating that hybrid spatial-temporal modelling significantly outperforms individual modalities, targeting >95% accuracy in cardiomyocyte differentiation stage classification.
iii. Implement and compare multiple fusion strategies, including concatenation-based, attention-weighted, and ensemble approaches, to identify optimal methods for combining spatial and temporal biological information.
iv. Identify spatiotemporal molecular markers by leveraging spatial transcriptomics datasets and temporal differentiation profiles to discover spatially restricted gene expression patterns and temporal transcription factor networks that correlate with differentiation efficiency.
v. Deploy XAI methodologies, including Shapley Additive exPlanations (SHAP) analysis and attention mechanism visualisation to highlight important regulatory pathways and

spatial interaction patterns that drive differentiation success, ensuring biological interpretability of model predictions.

vi. Validate computational predictions through identification of established cardiac biomarkers and comparison with known developmental pathways, confirming the biological relevance and translational potential of discovered spatiotemporal patterns.

1.6.SIGNIFICANCE OF THE STUDY

This study addresses a critical challenge in cardiac regenerative medicine by providing a novel computational framework for spatiotemporal analysis of cardiomyocyte differentiation. The significance of this works extends across multiple domains, offering both immediate scientific contributions and long-term clinical impact.

By demonstrating how hybrid deep learning architectures can integrate heterogeneous biological data types to achieve unprecedented predictive accuracy, this study advances computational biology from a scientific standpoint. With ramifications that go beyond cardiac biology to other stem cell differentiation systems, the novel combination of spatial and temporal modelling approaches establishes a new paradigm of analysing developmental processes. Studies in spatial multi-omics integration have demonstrated the power of sophisticated computational approaches[38], but their application to temporal prediction in regenerative medicine represents a significant methodological advancement.

The technological innovation represents a significant advancement in the application of artificial intelligence to regenerative medicine. By targeting >95% differentiation prediction accuracy, this framework aims to surpass current computational approaches and establish new benchmarks for the field. Recent cardiovascular machine learning studies have demonstrated remarkable performance[46], indicating the potential for advanced computational approaches when applied systematically to cardiac biologically. Translating computational insights into experimental validation is made easier by using XAI, which ensures that predictions maintain their biological interpretability. According to conservative estimates, predictive optimisation could address current challenges in clinical translation by improving functional outcomes and reducing manufacturing costs by 30-40%. This advancement is in line with global priorities for cardiovascular research, particularly the growing emphasis on novel therapeutic approaches for heart failure and the emerging frameworks for precision medicine in cardiovascular care. To address the global burden of cardiovascular disease, the World heart Federation's vision for cardiovascular health by 2030 places a strong emphasis on innovation and technology, with specific recognition of the potential for precision-engineered cellular therapies[52], [53].

The broader impact extends to establishing proof-of-concept for spatiotemporal modelling approaches that could accelerate integration of stem cell technologies into clinical trials. This study offers a roadmap for similar applications across regenerative medicine by bridging the gap between multi-omics measurement and functional prediction, potentially benefiting patients with diverse degenerative diseases. The framework's emphasis on explainable predictions addresses the critical

need for interpretable AI in healthcare, ensuring that computational insights can be effectively translated into experimental protocols and clinical applications.

The urgency of this research is highlighted by the global health context. With cardiovascular diseases remaining the leading cause of death worldwide and projected to increase substantially over the coming decades[54], [55], [56], novel approaches to cardiac regeneration represent an important component of comprehensive cardiovascular care strategies. The necessity of developing cost-effective regenerative therapies that could be scaled globally is highlighted by the disproportionate burden of cardiovascular disease in low- and middle-income nations, making this framework's protocol optimisation capabilities particularly valuable.

1.7.DELIMINATIONS OF THE STUDY

This study focuses on specific data types, analytical approaches, and biological systems to ensure depth and rigor while maintaining feasibility.

i. Data Modality

This study is limited to spatial transcriptomics and temporal gene expression data, representing the most mature and available spatial omics technologies. While other modalities such as spatial proteomics or metabolomics could provide additional insights, current spatial multi-omics platforms lack the resolution and standardisation necessary for reliable integration. While acknowledging the potential of future expansion to additional modalities, recent developments in spatial multi-omics technologies have validated the effectiveness of transcriptomics-based approaches across diverse tissue types and platforms[38]. This focus leverages the complementary capabilities of temporal profiling (differentiation dynamics) and spatial gene expression mapping (tissue organisation) while avoiding the technical complications associated with less established technologies.

ii. Biological Scope

The framework focusses on the differentiation of human iPSC-derived cardiomyocytes, which was selected due to it established experimental approaches and direct clinical significance. To maintain translational focus and prevent confounding variables associated with different developmental pathways, this focus excludes other cardiac cell types (fibroblasts, endothelial cells, smooth muscle cells) as well as alternative stem cell sources (embryonic stem cells, direct reprogramming approaches). Comprehensive approaches for hiPSC-CM differentiation with >90% efficiency have been developed recently[5], ensuring the clinical relevance of the findings while offering a robust experimental foundation for computational modelling.

iii. Data Sources

The analysis utilises well-characterised public datasets, specifically temporal differentiation data that captures the development trajectories of cardiomyocytes and spatial transcriptomics data from recent comprehensive cardiac studies. This approach avoids the cost and technical

challenges of developing new multi-omics datasets while ensuring reproducibility and enabling comparison with existing literature. The selection of established datasets with proven quality and biological relevance ensures that computational methods can be rigorously validated against known biological processes[18], [29].

iv. Computational Architecture

The hybrid approach is limited to GNNs and RNNs based on their proven effectiveness in spatial and temporal biological data analysis, respectively. This architecture choice is well justified by recent developments in GNN architectures for spatial transcriptomics and successful hybrid biological applications. While transformer-based architectures and other deep learning approaches could potentially offer advantages, the GNN-RNN combination offers an ideal balance of interpretability, performance, and computational efficiency for the target application, with documented success in similar biological prediction tasks reaching >85% accuracy[34], [37], [39], [50].

v. Performance Benchmarks

The study targets >95% differentiation prediction accuracy, representing a substantial improvement over current approaches that typically achieve 65-75% accuracy. This target is informed by recent developments in machine learning for cardiovascular applications[46], where highly effective ensemble approaches have revealed that high-accuracy biological prediction is feasible when the right computational approaches are systematically applied.

2. CHAPTER 2: LITERATURE REVIEW

2.1.INTRODUCTION

Understanding cardiac biology and regenerative medicine has undergone a paradigm shift due to the convergence of deep learning techniques with spatial multi-omics technology. To address fundamental challenges in cardiac regeneration, this literature review looks at how advanced AI techniques, specifically GNNs and RNNs, can be integrated with spatially resolved transcriptomics, epigenomics, and multi-modal datasets. The scope includes deep learning applications in single-cell and spatial biology, recent developments in spatial omics technologies applied to cardiac tissues, and predictive modelling techniques for differentiation efficiency in iPSC-CMs.

The four primary themes that this study focuses on are cardiomyocyte differentiation and regenerative medicine constraints, spatial multi-omics technical advancements in cardiac biology, deep learning applications in spatial and temporal genomics, and predictive modelling for differentiation efficiency. The inclusion criteria give priority to research addressing the difficulties of cardiac regeneration and iPSC-CM maturation, AI techniques pertinent to single-cell and spatial genomics modelling, and studies employing spatial omics in cardiac biology.

2.2.CARDIOMYOCYTE DIFFERENTIATION AND REGENERATIVE MEDICINE

2.2.1. Cardiomyocyte Biology and Development

Cardiac development is a highly orchestrated process involving intricate transcriptional hierarchies and signalling pathways[57]. The molecular regulation of cardiomyocyte differentiation comprises of a cascade of transcription factor activation; the first step is the primitive streak stage, where Mesoderm Posterior 1 (Mesp1) is activated by the T-box transcription factor Eomesodermin (Eomes)[58], [59]. Through the coordinated expression of important transcription factors such as Nkx2-5, Gata4, and other T-box transcription factors, this regulatory cascade creates cardiac specification[58], [59].

Four unique stages of cardiomyocyte differentiation have been identified using temporal analysis, each of which is distinguished by specific patterns of chromatin alteration[60]. With the discovery of unique pre-activation chromatin patterns at cardiac muscle genes, these demonstrate the connection between chromatin structure and gene expression[61], [62]. Gata4 and Meis1's transcriptional synergism has become a crucial regulatory mechanism, and Brg1, a chromatin remodelling factor, works alongside Polycomb repressive complexes to play a crucial role in cardiac differentiation[63].

Recent genomic studies show E-box-binding homeobox 1 (ZEB1) as a crucial regulator during early cardiomyocyte differentiation, especially during the transition from mesoderm to cardiac mesoderm[64], [65], [66], [67]. FGF, BMP, and Wnt are examples of signalling pathways that play biphasic roles in cardiomyocyte differentiation; patterns of temporal activation and inhibition are crucial for accurate cardiac fate determination[68].

2.2.2. iPSC-Derived Cardiomyocytes (iPSC-CMs)

Although differentiation protocols have advanced significantly, iPSC-CMs still have fundamental drawbacks that limit their clinical translation[69]. One of the main challenges is the immature phenotype, as iPSC-CMs differ from mature in vivo cardiomyocytes in terms of electrophysiological parameters, contraction patterns, and gene expression profiles[69], [70], [71], [72]. These cells usually blend atrial, ventricular, and nodal-like phenotypes within the same differentiation culture, exhibiting heterogeneous action potential properties[72], [73].

The efficiency of differentiation protocols based on temporal modulation of the Wnt/β-catenin pathway has increased, and some of these procedures have been able to obtain cardiomyocyte purity of >90%[5]. However, there is still a great deal of variation among differentiation batches, iPSC lines, and laboratories[74]. Given that different iPSC lines have optimal cell seeding densities that vary by a factor of four, cell seeding density has become a crucial metric[75]. Standardisation and scalability are made more difficult by this variation, which also affects post-thaw functional properties and cryopreservation survival rates[5].

While diverse methods can produce contracting cardiomyocytes, thorough morpho-functional comparisons of differentiation protocols have shown that there are notable variations in the consistency of marker expression, sarcomeric organisation, and electrophysiological accessibility[76]. The use of bioreactor-based(figure 1) techniques has demonstrated potential for enhancing functional maturity and reproducibility, with stirred suspension cultures yielding more reliable results than monolayer approaches[5].

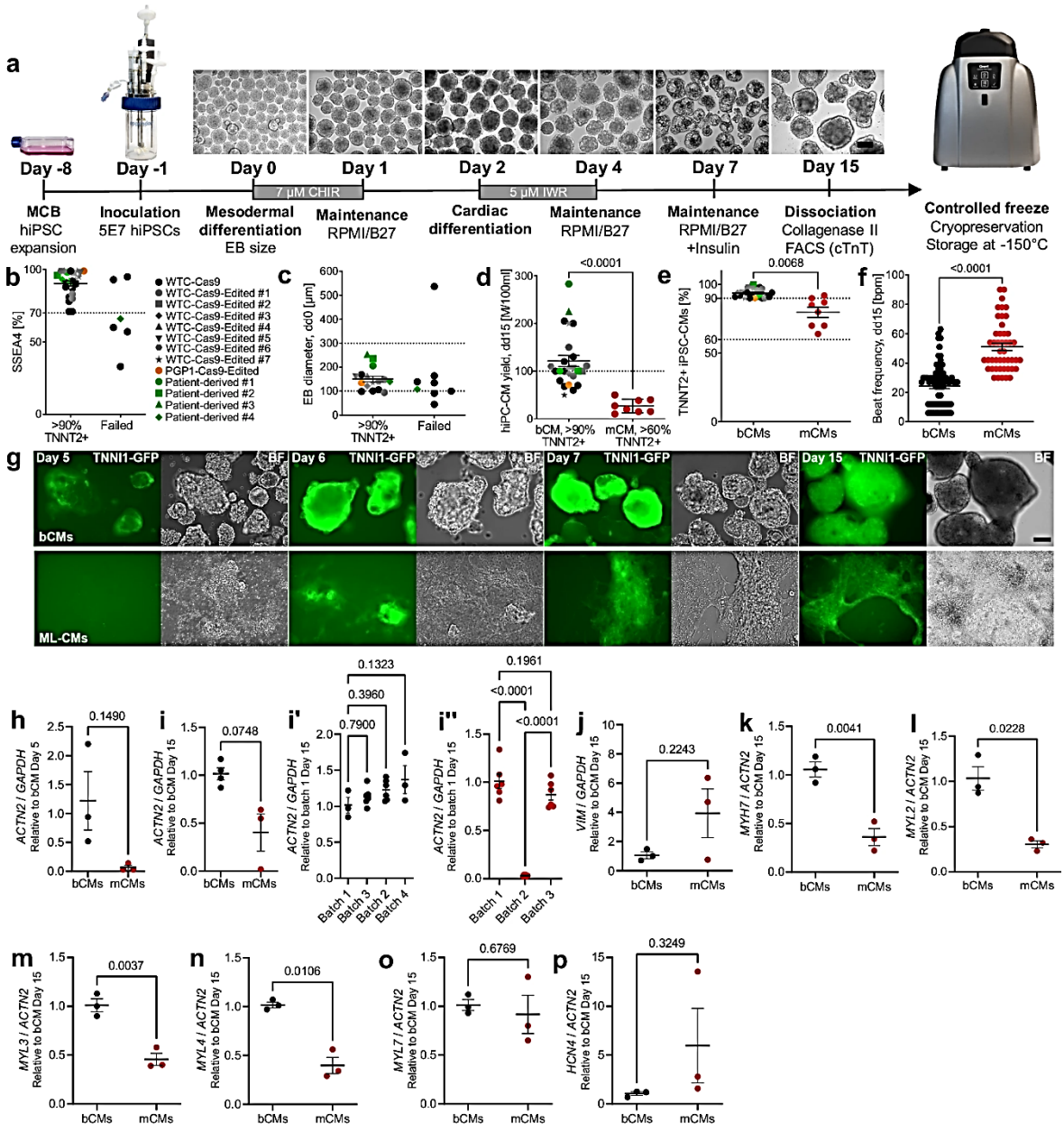

Figure 1: Optimised stirred bioreactor cardiac differentiation protocol showing efficient and reproducible generation of human iPSC-derived cardiomyocytes and cardiac organoids in stirred suspension systems[5].

2.2.3. Challenges in Cardiac Regeneration

Cardiomyocyte renewal rates in the adult human heart are only about 0.5% annually, indicating a severely limited capability for regeneration[3], [77]. This stands in stark contrast to the estimated one billion or more cardiomyocytes lost after myocardial infarction[72]. Cardiomyocyte generation in end-stage heart failure is modest, occurring at rates 10-50 times lower than in healthy hearts, according to recent studies employing nuclear bomb test-derived ^{14}C[77].

Remarkably, compared to healthy hearts, patients with left ventricular assist device (LVAD) support exhibited a six-fold increase in cardiomyocyte renewal, indicating that mechanical unloading can release latent regenerative potential[77]. According to this study, the cardiac microenvironment in heart failure may actively inhibit regenerative processes. Therefore, targeting these environmental variables with therapeutic interventions may improve endogenous repair mechanisms[77], [78], [79].

Technical difficulties in cell replacement treatments exacerbate the restricted ability for regeneration[3]. Large-scale iPSC-CM generation has advanced significantly, but problems with engraftment, electrical integration, and arrhythmogenicity still pose serious obstacles to clinical application[80]. The outcomes of recent clinical trials using cell injection therapies and cardiac patches have been inconsistent, and insufficient controls and small sample sizes have made it difficult to draw firm conclusions regarding their effectiveness[80].

2.3.ADVANCES IN SPATIAL MULTI-OMICS TECHNOLOGIES

2.3.1. Spatial Transcriptomics

Studies on cardiac biology have been transformed by spatial transcriptomics, which provides whole-transcriptome or tailored gene expression data while preserving spatial context[81]. The 10x Genomics Visium platform, which supports tissue slices up to 6.5 mm x 6.5 mm with over 5,000 detection points per capture area, has become a key method for spatial transcriptomics in cardiac research[82], [83]. Cellular heterogeneity and spatial organisation in both healthy and pathological cardiac tissues have been successfully mapped using this method[84].

Unprecedented insights into cardiac electro-anatomy and immunology have been uncovered by recent applications in human cardiac research[85]. Using a combination of single-cell and spatial transcriptomics, a thorough mapping of eight cardiac regions has revealed unique ion channel and G-protein-coupled receptor repertoires as well as cellular niches within the cardiac conduction system[85].

Unprecedented insights into cardiac electro-anatomy and immunology have been uncovered by recent applications in human cardiac research[85]. Using a combination of single-cell and spatial transcriptomics, a thorough mapping of eight cardiac regions has revealed unique ion channel and G-protein-coupled receptor repertoires as well as cellular niches within the cardiac conduction system[85], [86], [87]. It has been demonstrated that the sinoatrial node is divided into a core composed of glial cells that promote glutamatergic signalling, fibroblasts, and pacemaker cells[85], [88]. Spatial transcriptomics has been shown to be particularly useful for studying cardiac development and disease progression[89], [90]. 31 coarse- and 72 fine-grained cell states have been found in studies of the growing human heart, and they have been mapped to highly resolved cardiac cellular niches[91]. This method has described hitherto unidentified cardiac cell types, such as resident chromaffin cells, and offered new insights into the development of the atrial septum, heart valves, and cardiac pacemaker-conduction system[91].

Different cardiomyocyte transcriptional states have been identified in disease contexts by spatial transcriptomics of infarcted mouse hearts, establishing a controlled multistep progression from remote zone to border zone populations[92]. Understanding the spatial organisation of heart repair mechanisms has been made possible by the accurate mapping of cellular composition changes after myocardial infarction, enabled by the merging of spatial and single-cell data[92].

2.3.2. Spatial Epigenomics

One new era of study in cardiac biology is the integration of spatial and epigenomic data. Although chromatin accessibility landscapes during cardiac differentiation have been revealed by the classical single-cell ATAC-seq (scATAC-seq), the inclusion of spatial context holds promise for illuminating the differences in epigenetic regulation among heart tissues[81], [93].

The ability to simultaneously profile chromatin accessibility, histone modifications, and gene expression in the same tissue segment has been made possible by recent advancements in spatial-ATAC sequencing and multi-modal techniques[94], [95], [96]. These technologies have demonstrated that cardiac tissues' chromatin accessibility patterns exhibit both local variances and global commonalities that correlate to functional cardiac regions[97]. Studies on hypertrophic cardiomyopathy have shown that certain transcription factors exhibit fetal-like enrichment patterns, and that foetal gene reprogramming occurs at both transcriptome and chromatin accessibility levels[97].

Using scATAC-seq to study cardiac reprogramming has shown that chromatin accessibility dramatically changes during cell fate conversion[98]. Pseudotime trajectory analysis based on principal curves has demonstrated rapid opening of cardiac-related cis-regions and closing of fibroblast-related regions, with transient opening of neurogenic process-associated regions[98]. By integrating scATAC-seq and scRNA-seq data, significant regulators, including Tcf21 and Fos, have been identified, while revealing the bimodal function of Smad3 at various phases of cardiac reprogramming[98].

2.3.3. Integration of Multi-Omics at Single-Cell Level

A major computational and technical challenge is integrating several omics modalities at single-cell resolution[99], [100], [101]. Histone modifications, chromatin accessibility, transcriptome, and protein panels are among the five modalities that can now be profiled simultaneously in the same tissue segment thanks to recent methodological advancements[102]. These methods mine intrinsic tissue properties as supervisory information and use self-supervised learning to create a proxy without the need for extra data[50], [102]. Multi-modal spatial omics integration faces several technical obstacles, including data normalisation across modalities, resolution variations between technologies, and computing scalability[81], [103]. Through probabilistic alignment, novel computational frameworks like SIMO have been created for the chromatin accessibility and DNA methylation modalities that were not previously spatially profiled[103].

Novel fibroblast subpopulations in post-myocardial infarction tissues have been identified using cardiac-specific applications of multi-omics integration[93]. Integrating scRNA-seq and scATAC-seq data revealed GATA5/ISL1 + fibroblasts, which are essential for cardiac repair and have both fibroblast and cardiomyocyte signatures[93]. Functional validation showed that GATA5 and ISL1 co-regulate Wnt signalling pathways to facilitate fibroblast transformation into functional cardiomyocytes.[93], [104]. Beyond cellular identity, cardiac tissues exhibit heterogeneity in terms of functional characteristics and environmental responses[105], [106]. Researchers have been able to uncover layers of heterogeneity by the integration of scRNA-seq with spatial transcriptomics, providing a thorough understanding of the functional dynamics and cellular interactions within the heart[81]. This approach has been particularly useful for locating uncommon cell populations and figuring out where they are located in cardiac tissues[81].

2.3.4. Spatial-Temporal Biological Benchmarks and Datasets

As spatial multi-omics technologies have grown, a multitude of datasets have been produced that offer previously unheard-of insights into cardiac development, regeneration, and disease. This sub-section offers a thorough summary of the spatial-temporal omics datasets that are currently available and pertinent to cardiac biology, with a focus on resources that integrate temporal dynamics and spatial context, which are crucial for understanding the processes of cardiac differentiation and regeneration. The landscape of spatial-temporal cardiac datasets includes different species, developmental stages, and technological approaches. Recent advancements have yielded datasets covering everything from adult cardiac homeostasis and disease states to early embryonic development[90], [107], [108], [109]. To validate computational approaches and understand the intricate spatiotemporal dynamics of cardiac biology, these resources serve as essential standards. Table 1 shows the summary of datasets used for spatiotemporal analysis of cardiac tissues.

Table 1: Summary of datasets used for spatiotemporal analysis of cardiac tissues, including modality, tissue type, and temporal information.

Dataset	Modality	Tissue	Temporal Info	Citation
Human Cell Atlas Heart Development	scRNA-seq + Spatial Transcriptomics	Human embryonic heart	Yes (5.5 – 14 Weeks Post Conception (WPC))	[110]
Spatial dynamics of developing human heart	scRNA-seq + MERFISH	Human embryonic heart	Yes (9 – 16 WPC)	[18]
Adult human heart cell atlas	scRNA-seq + snRNA-seq	Adult human heart	No (Adult)	[111]
Spatially resolved multiomics of	scRNA-seq + snATAC-seq + Spatial Transcriptomics	Adult human heart	No (Adult)	[85]

human cardiac niches				
Spatial multi-omic map of human MI (Myocardial Infarction)	snRNA-seq + snATAC-seq + Spatial Transcriptomics	Human infarcted heart	Yes (Post-MI timepoints)	[112]
Mouse Heart Spatiotemporal Atlas (Stereo-seq)	Spatial Transcriptomics (Stereo-seq)	Mouse heart	Yes (embryonic day 20 (E20), postnatal day 1 (P01), postnatal day 4 (P04), postnatal day 14 (P14))	[22]
Mouse heart spatial transcriptomics (Visium)	scRNA-seq	iPSC-derived cardiomyocytes	Yes (pluripotency (day 0), germ layer specification (day 2), progenitor cardiac cell state (day 5), committed cardiac cell state (day 15), definitive cell state (day 30))	[113]
Human heart spatial transcriptomics (Disease)	Spatial Transcriptomics	Human heart (disease)	No (Disease states)	[113], [114]
Developing human heart (EGA)	snRNA-seq + Spatial Transcriptomics + ISS	Human embryonic heart	Yes (4.5, 6.5, 9 WPC)	[114]
Human heart organoids spatial atlas	scRNA-seq + Spatial transcriptomics	Human heart organoids	Yes (approximately 3 days after seeding (day 0) – day 20 of differentiation)	[115]
iPSC-CM scRNA-seq + scATAC-seq	scRNA-seq + scATAC-seq	iPSC-derived cardiomyocytes	Yes (Day 0 - 30)	[116]

Human SAN Cell Atlas	scRNA-seq + scATAC-seq	Human sinoatrial node (iPSC)	Yes (Differentiation)	[117]
Zebrafish heart regeneration atlas	scRNA-seq + Spatial Transcriptomics (Stereo-seq)	Zebrafish heart	Yes (8 time-points of zebrafish heart regeneration stages)	[118]
Human cardiac conduction system	scRNA-seq + Spatial Transcriptomics	Human cardiac conduction system	No (Adult)	[85], [91], [119]

Human Developmental Cardiac Datasets

With 80,000 individual cells and 70,000 spatially barcoded tissue regions between 5.5- and 14-weeks post-conception, the *Human Cell Atlas Heart Development dataset* is the most extensive spatial-temporal resource for human cardiac development[110]. This dataset offers a previously unheard-of resolution of cardiac morphogenesis by combining single-cell RNA sequencing with 10x Genomics Visium spatial transcriptomics[110]. The atlas offers new insights into the evolution of the heart valve, the atrial septum, and the pacemaker-conduction system by identifying 31 coarse- and 72 fine-grained cell states that are mapped to highly resolved cardiac cellular niches[91], [110].

MERFISH technology is used in the *Spatial Dynamics of Developing Human Heart dataset* to map the development of the heart at subcellular resolution between 9- and 16-weeks post-conception[18]. This resource lists 75 distinct cell states, including resident chromaffin cells and other cardiac cell types that were previously unidentified[18]. The dataset offers insights into multicellular signalling mechanisms that coordinate spatial organisation during cardiac morphogenesis and demonstrates the intricate laminar organisation of ventricular cardiomyocyte subpopulations across the ventricular wall[18].

The *Developing Human Heart (EGA) dataset* represents a groundbreaking effort combining three complementary approaches: Spatial transcriptomics, single-cell RNA sequencing, and in situ sequencing[120]. This resource, which is accessible to the public via the European Genome-Phenome Archive, includes the three crucial developmental periods of 4.5-5, 6.5-, and 9-weeks post-conception[120], [121]. The dataset has laid the groundwork for further developmental cardiac research and offers organ-wide gene expression patterns with single-cell spatial resolution[120], [121].

Adult Human Cardiac Resources

The Adult Human Cell Atlas, which examines roughly 500,000 distinct cells from six anatomical regions, offers the most thorough description of the cellular variety of the adult human heart[85]. This resource reveals different atrial and ventricular fractions with a range of developmental

origins while highlighting the cellular heterogeneity of cardiomyocytes, pericytes, and fibroblasts[85], [122], [123]. The atlas has developed into a key resource for understanding both the mechanisms underlying disease and normal cardiac function.

To identify cellular niches within eight regions of the adult human heart, the *Spatially Resolved Multiomics of Human Cardiac Niches dataset* combines spatial transcriptomics, single-cell RNA sequencing, and single-cell ATAC sequencing[85]. This database identifies unique repertoires of ion channels and G-protein-coupled receptors in cardiac conduction system cells, offering new insights into cardiac electro-anatomy and immunology[124], [125]. The dataset shows that the sinoatrial node is compartmentalised, containing glial cells that facilitate glutamatergic signalling, fibroblasts, and specialised pacemaker cells[126].

Disease-Focused Cardiac Datasets

The Spatial Multi-Omics Map of Human Myocardial Infarction represents the most thorough multi-modal analysis of human cardiac injury, which maps the cellular and molecular alterations that occur after myocardial infarction by combining single-nucleus RNA sequencing, single-nucleus ATAC sequencing, and spatial transcriptomics[112]. This dataset reveals relationships between fibroblast and myeloid cells and defines various cell niches, such as fibrotic, inflammatory, and myogenic regions[112]. To understand cell-cell interactions during cardiac remodelling and repair, the resource provides spatial context[112].

Model System Datasets

The Mouse Heart Spatiotemporal Atlas (Stereo-seq) provides a comprehensive spatial transcriptome data from both relatively mature and regeneration-capable neonatal hearts at four crucial timepoints (embryonic day 20 (E20), postnatal day 1 (P01), postnatal day 4 (P04), postnatal day 14 (P14))[22]. This dataset defines 14 different cell types and includes 330,857 cell bins in 22 high-quality sections[22]. The resource shows how fibroblasts and cardiomyocytes' gene expression varies dynamically as they go from regenerative to non-regenerative stages.

With 569,896 cells/spots spanning eight regeneration stages, the *Zebrafish Heart Regeneration Atlas* is the most extensive spatial-temporal resource for understanding cardiac regeneration[118]. This dataset uses single-cell RNA sequencing and spatial transcriptomics (Stereo-seq) to describe the series of cardiomyocyte cell states that lead to the development of regenerated myocardium[118]. A 4D "virtual regenerating heart" is provided by the resource, which is a useful tool for studies on cardiovascular regeneration[118].

iPSC-Derived Cardiac Datasets

The *Human iPSC-CM Differentiation Time Series* offers a comprehensive single-cell transcriptional profiling of human induced pluripotent stem cells traversing from pluripotency through cardiac differentiation[113]. This dataset identifies stage-specific changes in cell state by capturing 43,168 cells at five crucial timepoints (days 0, 2, 5, 15, and 30)[113]. The database sheds

light on the genetic regulation of cardiovascular development and the transcriptional foundation of cardiac differentiation[113].

One of the earliest multi-modal assessments of iPSC-derived cardiomyocyte differentiation, the iPSC-CM scRNA-seq + scATAC-seq dataset combines transcriptional and epigenetic profiles throughout the differentiation timeline[127], [128]. This resource offers insights on the proliferation-maturation transition during cardiac development by identifying six cardiomyocyte subpopulations with heterogeneity based on cell cycle and maturation states[127], [128].

Organoid-Based Cardiac Resources

By applying spatial transcriptomics to engineered cardiac tissues, the *Human Heart Organoid Spatial Atlas* sheds light on how geometric restrictions affect the formation and function of organoids[115]. With circular patterns promoting more robust cardiac organoid creation than angular geometries, this dataset shows that template geometry considerably changes cardiac function and structure[115]. This resource provides a foundation for understanding structure-function relationships in cardiac tissue engineering.

Technical Considerations and Data Integration Challenges

For integrated analysis, the diversity of technologies and experimental methodologies used in these datasets offers both opportunities and challenges. Platform-to-platform resolution variations range from subcellular (MERFISH: ~100nm) to spot-level (10x Visium: ~55μm), necessitating careful attention when comparing findings[84]. There is a wide range of temporal sampling techniques; some datasets concentrate on certain developmental stages, while others offer extensive temporal coverage (daily timepoints).

The distinctions between the cardiac development schedules of zebrafish, mice, and humans highlight the difficulty of cross-species integration. By using dynamic temporal warping approaches to synchronise developmental stages across species, it has been discovered that, depending on the cell type examined, mouse cardiac development from E9.5 to E13.5 correlates with human development from 5 to 15 weeks post-conception[129]. To manage the various data types, noise properties, and batch effects that come with integrating transcriptomics, epigenomics, and spatial information, multi-modal data integration calls for sophisticated computational approaches[130]. While some of these issues have been resolved by recent advancements in integration techniques like SIMO and MoSSL, standardised solutions for multi-modal cardiac data integration remain an active area of development[131].

Data Accessibility and Reproducibility

These datasets' accessibility varies greatly; some are accessible through public repositories, while others require certain access permissions. Data integration and sharing are made easier by the Huma Cell Atlas initiative's standardised data formats and submission procedures. Spatial

transcriptomics datasets, however, frequently require certain computational resources and visualisation tools, which could restrict wider accessibility[132], [133].

The intricacy of spatial transcriptomics protocols creates reproducibility issues, as variables like tissue preparation, sectioning quality, and library preparation have a big impact on data quality[134], [135], [136]. One of the field's continuous priorities is the development of standardised procedures and quality control measures.

2.4.DEEP LEARNING IN SINGLE-CELL AND SPATIAL OMICS

2.4.1. Deep Learning in Single-Cell Omics

Deep learning has become a transformative approach for single-cell omics data analysis, overcoming issues with the datasets' inherent high dimensionality, sparsity, and noise[137], [138]. Recurrent Neural Networks (RNNs) are excellent at processing sequential biological data, such as DNA sequences, whereas Convolutional Neural Networks (CNNs), which were initially developed for image analysis, have been modified to capture local and global patterns in genomic data[139]. Recent developments in single-cell clustering have shown that deep learning approaches outperform conventional approaches[137], [138], [140], [141], [142]. By iteratively optimising a clustering objective function, the DESC algorithm clusters scRNA-seq data in an unsupervised deep embedding approach[138]. DESC achieves a proper balance between clustering accuracy and stability with minimal memory footprint by gradually eliminating batch effects while preserving biological signal through iterative self-learning[138].

Dual-topology adjacency graphs, which combine node distribution information into conventional adjacency graphs, have been implemented into novel architectures like scG-cluster[137]. Dual-topology adaptive graph convolutional networks (TAGCNs) with residual connections and attention mechanisms are used in this approach to prevent over-smoothing while maintaining the capacity to discern minute variations in cell expression profiles[137]. Extensive tests consistently show better performance in terms of clustering accuracy and scalability as compared to current state-of-the-art methods[137].

Using methods like scMUG, the inclusion of gene functional module information has significantly improved clustering performance[143]. This method filters expression profiles using gene functional correlations and adds new similarity metrics that include global distribution and local density similarities[143]. This kind of functional integration has proven effective for identifying hierarchical structures in scRNA-seq datasets and identifying rare cell types [143].

2.4.2. GNNs for Spatial Biology

Because GNNs naturally depict cellular linkages and geographical interactions, they have completely changed the way spatial data is being analysed[50]. The primary benefit of GNNs is their capacity to concurrently represent spatial neighbourhood information and gene expression similarity, making them perfect for spatially resolved transcriptomics analysis[36], [144]. The effectiveness of GNN-based approaches for cell-type deconvolution and spatial domain

identification has been shown by the recent applications in spatial transcriptomics[50]. Real spots can be adapted from pseudo-spots by dual graph construction employing expressive and spatial information according to the STdGCN framework (shown in figure 2), which builds comprehensive graphs with both pseudo-spots and real spots as individual nodes[145]. This approach has demonstrated exceptional effectiveness in predicting cell-type proportions across a variety of spatial transcriptomics platforms[145].

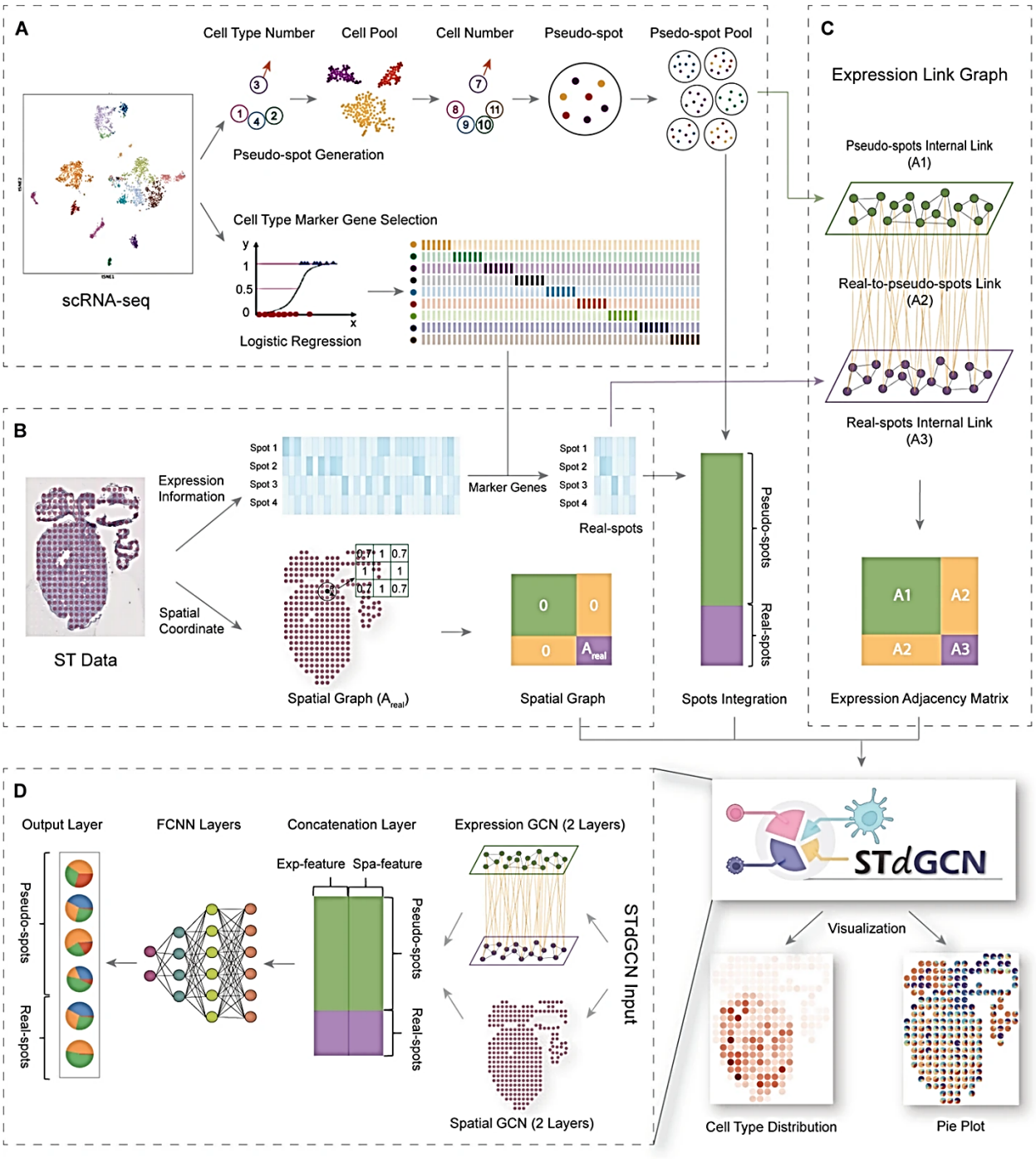

Figure 2: Schematic view of the STdGCN framework. The model integrates spatial and expression information to infer cell type composition in spatial transcriptomics data. It first uses a single-cell RNA-seq reference profiles to identify cell-type specific marker genes and build a pseudo-spot pool. Two graphs are then created, a spatial graph capturing relationships among spots and an expression graph representing gene expression correlations. These graphs are jointly processed by the STdGCN model, where fully connected layers handle expression features, spatial graph convolutional network (GCN) layers model spatial dependencies, and expression GCN layers learn

gene relationships. The combined outputs are used to predict cell type proportions and produce interpretable visualisations[145].

A major development in spatial biology is the emergence of specialised GNN architectures for the inference of cell-cell communication[146], [147]. CellNEST, shown in figure 3, presents relay-network communication detection, which uses attention mechanisms to find patterns of ligand-receptor-ligand-receptor communication[147]. This approach has shown potential in identifying intricate intercellular signalling networks by successfully detecting T cell homing signals in human lymph nodes and identifying aggressive cancer communication patterns[147].

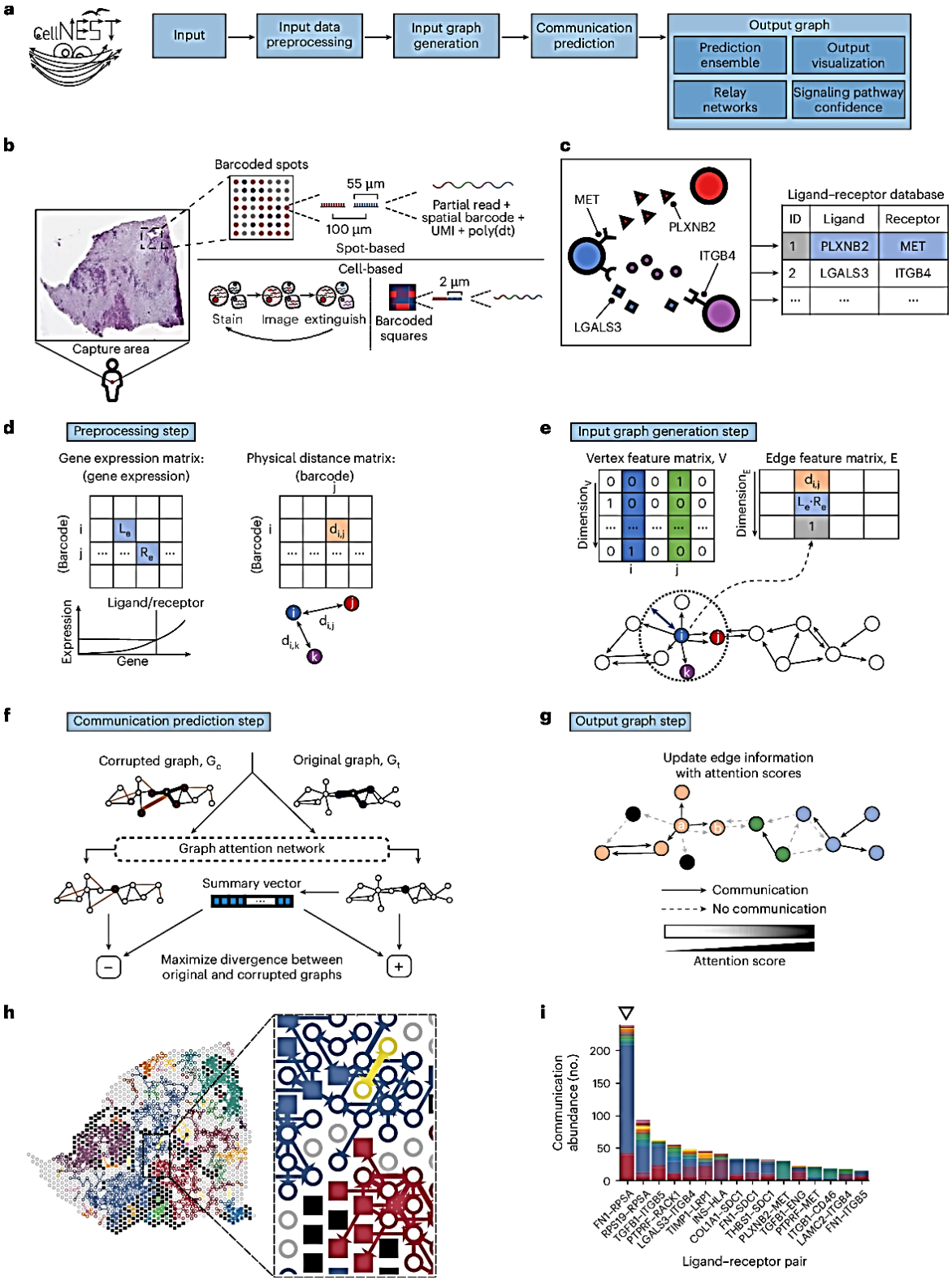

Figure 3: Overview of CellNEST framework for predicting ligand-receptor mediated cell-cell communication from spatially resolved gene expression data[147].

To detect active ligand-receptor signalling among neighbouring cells, adaptive graph models like spaCI(shown in figure 4) have integrated both spatial locations and gene expression profiles[146]. When compared to current approaches, spaCI performs better on simulation and real-world spatial transcriptomics datasets and offers insights on upstream transcriptional variables that mediate active interactions[146]. Robust inference of cellular communications from sparse spatial data is made possible by the combination of triplet loss functions and attention mechanisms[146].

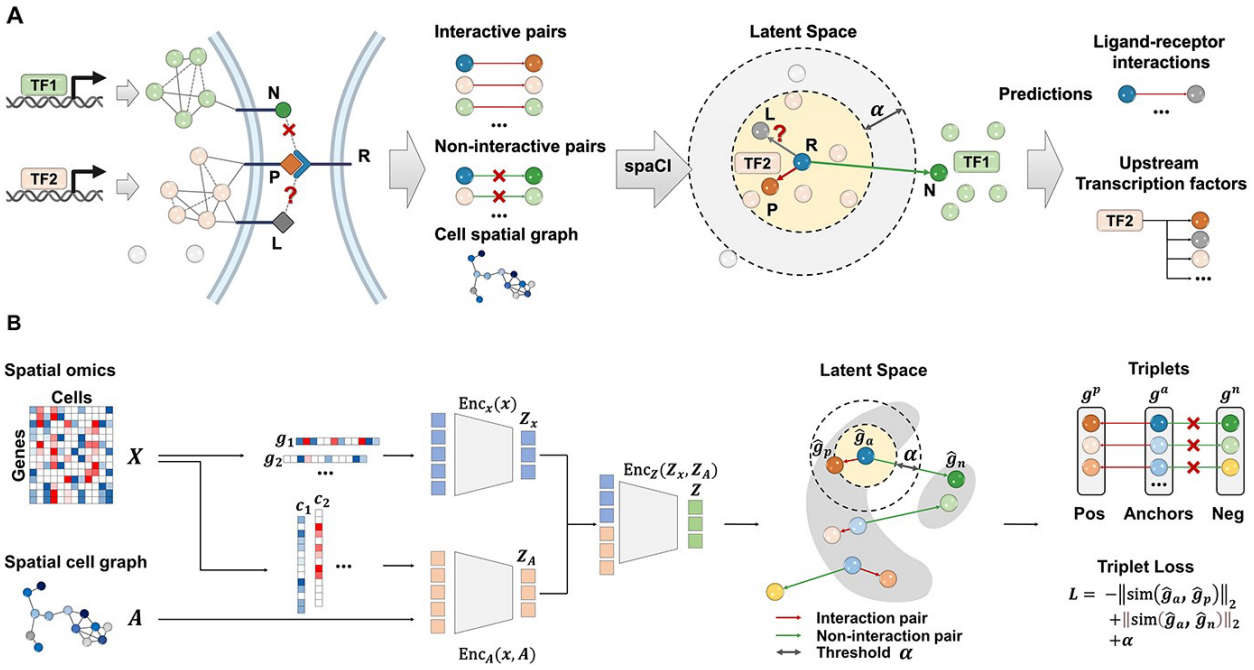

Figure 4: Schematic overview of spaCI, the model exploits both the spatial organisation of cells and comprehensive gene expression profiles to infer ligand-receptor interactions within tissue contexts. spaCI embeds gene features into a latent representation via two complementary components: a gene-centric linear encoder and a cell-centric attentive graph encoder, this approach enables simultaneous integration of transcriptional patterns and spatial cellular proximities within the latent space[146].

2.4.3. RNNs for Temporal Modelling

Specialised uses for recurrent neural networks include simulating the temporal dynamics of differentiation trajectories and gene expression[148]. RNNs are well-suited for capturing sequential dependencies and predicting future cellular states based on historical gene expression patterns because of the temporal nature of biological processes, especially cellular differentiation[149]. Recent studies have shown the application of dual attention RNN models to predict gene temporal dynamics from synthetic time series data derived from gene regulatory networks[148], [150]. These models produce remarkably accurate predictions across various network architectures, while the attention mechanism offers comprehensible insights on gene interactions[151], [152], [153]. Different gene regulatory network architectures can be distinguished hierarchically using graph theory to analyse attention patterns[148].

Predicting cell-cell interactions from spatial transcriptomics data has been explored using the combined capabilities of Long Short-Term Memory (LSTM) and GNNs[149], [154]. This hybrid approach leverages the graph-based potential of GNNs for spatial context modelling and the sequence learning capabilities of LSTM[155], [156]. When compared to conventional methods, rigorous testing has shown improved predictive capabilities, with backwards search integration producing optimal performance[157].

Moreover, LSTM networks have been used to predict protein subcellular localisation from DNA sequences, outperforming earlier benchmark models that lacked human-engineered features in terms of accuracy[158], [159], [160]. The versatility of RNN architectures in genomics applications has been demonstrated by the successful resolution of sequence-based biological problems through the integration of convolutional layers between raw data and LSTM inputs[161], [162], [163].

2.4.4. Multi-Modal Deep Learning Frameworks

Multi-modal deep learning frameworks that integrate spatial and temporal dimensions offer a state-of-the-art approach for comprehending intricate biological systems[164], [165], [166]. These frameworks address the challenge of modelling multi-modality spatio-temporal data with dynamic heterogeneity across space, time, and data modalities[167]. Multi-modality data augmentation is used in conjunction with global and modality-specific self-supervised learning paradigms in recent advancements like MoSSL (Multi-modality Spatio-Temporal learning via Self-Supervised Learning)[168]. Compared to single-view methods, these approaches allow for the thorough use of spatial transcriptomic data from multiple perspectives, resulting in a more accurate identification of spatial expression patterns[164], [165], [166].

Transformer-based architectures have become effective tools for enhancing spatial transcriptomics[169]. stEnTrans mines intrinsic tissue properties as supervisory information and uses self-supervised learning to create proxy tasks on gene expression profiles[170]. This method outperforms conventional interpolation approaches by offering thorough predictions for gene expression in unmeasured regions while boosting expression in original spots[170]. The combination of temporal convolutional networks and GNNs has shown potential for simulating spatiotemporal dynamics in intricate biological systems[151]. With applications ranging from transcriptomics to neuroimaging and other spatially resolved biological datasets, this combination allows end-to-end learning from both spatial and temporal components of biological data[151].

Current multi-modal frameworks face significant gaps when employed in cardiac tissue engineering applications[152]. While current approaches excel at handling individual data modalities, the unique challenges in cardiac differentiation prediction necessitate specialised structures that can combine spatial, temporal, and multi-omics data in a biologically meaningful manner[153]. Studies are still ongoing to develop interpretable frameworks that maintain predictive accuracy while offering biological insights[154], [155].

2.4.5. Hybrid GNN-RNN Architectures in Spatiotemporal Modelling: Cross-Domain Inspiration and Biological Applications

The integration of graph and recurrent neural networks represents a convergence of temporal sequence learning and spatial relationship modelling that has shown impressive results in a variety of application domains[156], [157], [158], [159]. To apply these hybrid architectures to cardiac regeneration and spatial multi-omics applications, it is crucial to comprehend their theoretical underpinning and real-world applicability in non-biological settings.

Foundational Architectures in Traffic and Urban Systems

The pioneering work for hybrid GNN-RNN architectures in traffic forecasting was laid by the groundbreaking work of Spatio-Temporal Graph Convolutional Networks (STGCN) shown in figure 5[160], [161], [162]. By using a full convolutional structure in place of conventional recurrent units, STGCN tackles the fundamental problem of modelling both the temporal dynamics of traffic flow and the spatial connections among road network nodes[160], [161], [162].

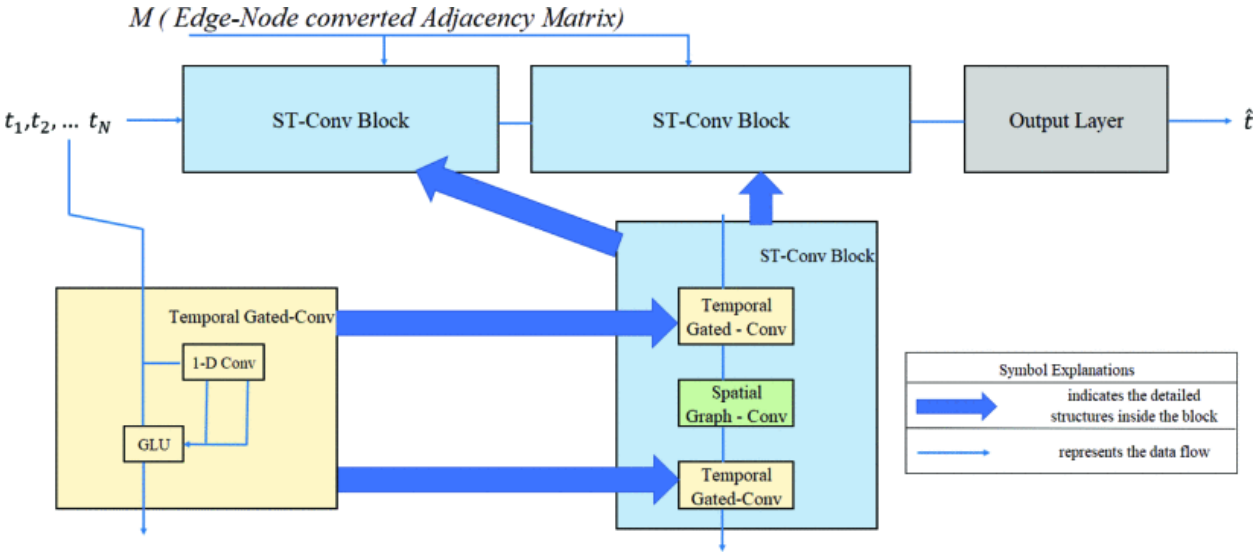

Figure 5: STGCN Architecture [163], [164].

In contrast to conventional methods, the framework's spatio-temporal convolutional blocks (ST-Conv blocks) combine temporal gated convolution layers with spatial graph convolution layers to enable significantly faster training speeds with fewer parameters[163], [165], see figure 6.

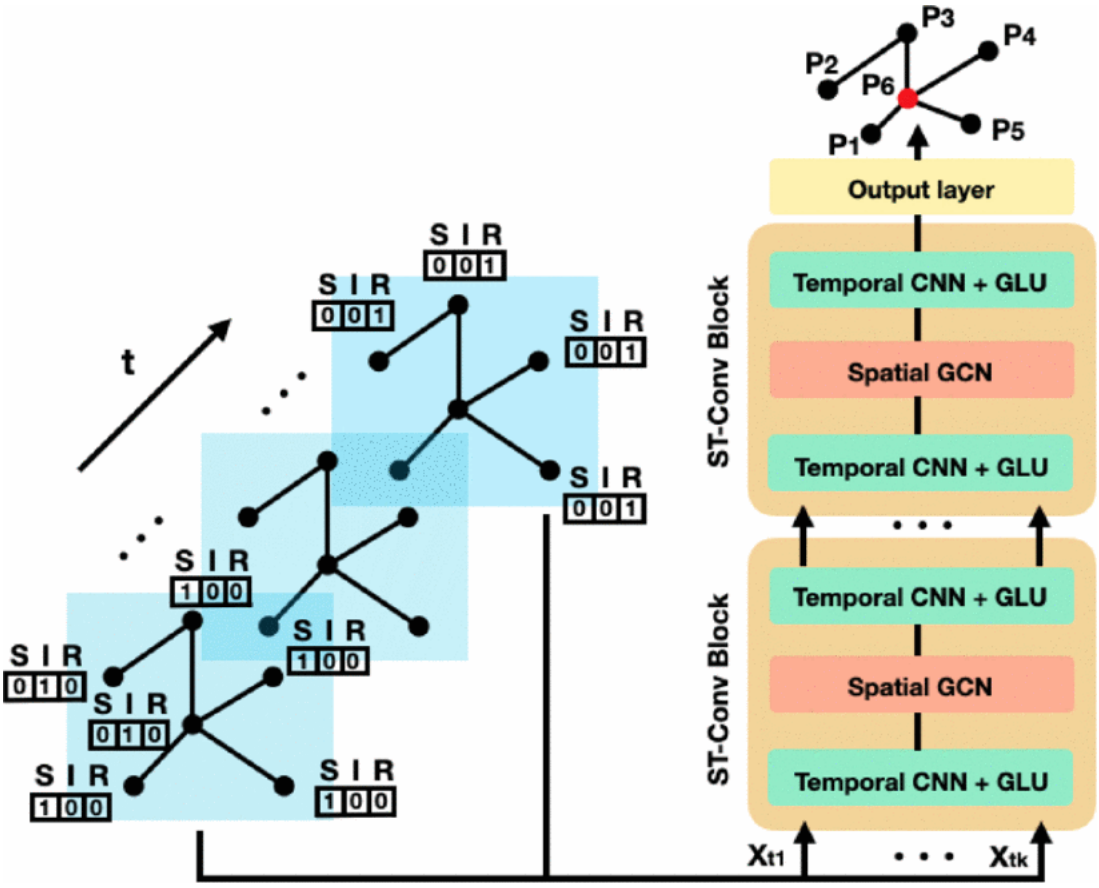

Figure 6: SD-STGCN architecture: the input snapshots, which are one-hot encoded network states at various time steps, are shown by the blue regions on the left. The orange regions on the right show the model architecture, which consists of a stack of ST-Conv blocks, followed by an input layer [165].

This idea is expanded by the Temporal Graph Convolutional network (T-GCN), which combines graph convolutional networks and gated recurrent units (GRUs) directly[166], [167]. While using GRU to simulate dynamic changes in traffic data for temporal dependence, T-GCN uses GCN to learn intricate topological structures for capturing spatial dependence[167]. Using real-world traffic datasets, this architecture outperforms state-of-the-art baselines in spatiotemporal correlation extraction[167].

An important advancement in overcoming the drawbacks of pre-defined graph architectures is the Adaptive Graph Convolutional Recurrent Network (AGCRN)[168], [169]. AGCRN introduces two adaptive modules: Data Adaptive Graph Generation (DAGG) to automatically infer interdependencies among various traffic series, and Node Adaptive Parameter Learning (NAPL) to capture node-specific patterns[168], [169], [170]. AGCRN eliminates the requirement for pre-defined graphs about spatial connections while capturing fine-grained spatial and temporal correlations through the integration of NAPL-GCN, DAGG, and Gated Recurrent Units[169], [170].

Weather Forecasting and Environmental Applications

The adaptation of hybrid architectures to weather forecasting applications has been proven by Hierarchical Spatio-Temporal Graph Neural Networks (HiSTGNN)[171]. HiSTGNN addresses the limitation of conventional GNN-based approaches, which either model global graphs of entire stations or local graphs of meteorological variables per station[171]. To develop self-learning graphs and investigate hidden dependencies between nodes at the variable-level and station-level graphs, the design makes use of spatial graph convolutional and adaptive graph learning layers[171]. HiSTGNN models long and diverse meteorological trends by using dilated inception as the foundation of gated temporal convolution for temporal pattern capture[171]. The challenge of the cross-regional spatio-temporal correlations among meteorological variables is addressed by HiSTGNN's dynamic interaction learning component, which constructs bidirectional information transfer in hierarchical graphs[171]. The efficiency of hierarchical modelling approaches is demonstrated by experimental results on real-world meteorological datasets, which show an error reduction of 4.2% to 11.6% when compared to state-of-the-art weather forecasting methods[171].

Biological and Medical Applications

The use of hybrid GNN-RNN architectures in biological systems shows impressive transferability from understanding biological systems to modelling physical infrastructure. The ability to predict long non-coding RNA-disease associations has been demonstrated using Graph Convolutional Network and Convolutional Neural Network-based methods (GCNLDA)[172]. Using graph convolutional networks to extensively integrate topological information and attention mechanisms at the node feature level, this method builds heterogeneous networks containing IncRNA, disease, and miRNA nodes [172].

In biological sequence analysis, convolutional LSTM networks have proven effective, especially when it comes to protein subcellular localisation[173]. With an accuracy of 0.902 and outperforming state-of-the-art algorithms, these networks show that LSTM architectures in conjunction with convolutions are effective for predicting subcellular localisation from protein sequences[173]. By integrating attention mechanisms, it is possible to visualise the areas that the LSTM network focuses on, exposing biologically plausible areas [173].

With LSTM frameworks advancing understanding of community assembly and health-relevant metabolite synthesis, RNNs have demonstrated efficacy in simulating microbiome dynamics[174]. Because of higher-order interactions that scale well with increasing complexity, these methods perform better than popular generalised Lotka-Volterra models based on ecological theory, proving their ability to represent complex community behaviours[174], [175].

Spatiotemporal Reasoning and Transferability

The combined strengths of hybrid GNN-RNN architectures in spatiotemporal reasoning account for their success across domains. Unlike conventional convolutional approaches made for regular grid data, GNNs excel at modelling complicated topological structures and irregular spatial

relationships[176]. Long-term temporal dependencies and sequential patterns in time series data can be better modelled by RNNs, especially LSTM variants[174], [177]. Important insights regarding the transferability of these architectures have been uncovered by dynamic GNNs under spatiotemporal distribution shifts[178]. By identifying and utilising invariant patterns whose predictive capabilities do not change with distribution shifts, the Disentangled Intervention-based Dynamic graph Attention networks (DIDA) framework shows that hybrid architectures can manage spatio-temporal distribution shifts.[178].

Studies on graph domain adaptation have developed theoretical underpinnings for transferability between various application domains[179]. Different regularisation strategies enhance performance for distinct transfer learning scenarios, according to theory-grounded spectral regularisation approaches[179]. For node transfer and link transfer scenarios, respectively, spectral smoothness and maximum frequency response regularisations are beneficial[179].

Adaptations for Cardiac Biology Applications

To apply hybrid GNN-RNN architectures to cardiac differentiation modelling, a few crucial modifications must be made, drawing on domain-specific knowledge from effective cross-domain applications. A template for capturing multi-scale relationships in cardiac tissues, where cellular neighbourhoods, tissue regions, and organ-level interactions function at various spatial scales, is provided by the hierarchical modelling technique illustrated in HiSTGNN[171]. AGCRN's adaptive graph generation capabilities are particularly pertinent to cardiac applications, where cellular interactions change because of differentiation processes[169]. The difficulty of simulating dynamic cellular interactions during iPSC-CM differentiation, where spatial relationships alter as cells progress through several developmental stages[50], is addressed by the capability to automatically infer interdependencies without the need for pre-defined graph structures.

The interpretability frameworks necessary for comprehending cardiac differentiation mechanisms are provided by the attention mechanisms that have been effectively applied in biological sequence analysis[139], [172]. By identifying the crucial temporal windows and spatial regions that influence differentiation outcomes, these methods aid in the development of biologically interpretable models that are necessary for treatment optimisation.[180], [181]. When dealing with continuous-time dynamic networks that are represented as a series of timed events, Temporal Graph networks (TGNs) have proven to be effective[182]. The temporal dynamics of gene expression and cellular state transitions during cardiac differentiation, where events happen at irregular intervals and display intricate temporal dynamics, can be modelled using this approach[182].

While preserving computational efficiency, TGNs' memory modules and graph-based operators allow for notable speed gains[182]. For cardiac regeneration applications, where large-scale spatial multi-omics datasets need to be processed efficiently while maintaining the ability to model intricate spatiotemporal patterns, this combination is especially pertinent[183], [184], [185]. The feasibility of applying models trained on simulated data to actual biological systems is

demonstrated by the domain adaptation approaches created for population genetics[186], [187]. By effectively addressing simulation mis-specification challenges, the gradient reversal layer technique offers a framework for training hybrid models using artificial cardiac differentiation data and subsequently applying them to real iPSC-CM datasets[186]. The clinical utility of these methods is established by the effectiveness of spatiotemporal modelling in medical imaging applications, especially cardiac imaging[186]. The potential clinical translation of hybrid GNN-RNN approaches in cardiac regeneration is supported by deep learning approaches that use temporal information in image processing to improve diagnostic and prognostic capabilities[186].

Evidence from a variety of applications, including biological sequence analysis, medical imaging, traffic forecasting, and weather prediction, shows that hybrid GNN-RNN architectures possess fundamental properties that go beyond domain-specific uses. A strong foundation for tackling the difficulties of cardiac differentiation prediction and optimisation in spatial multi-omics contexts is provided by their ability to model intricate spatial relationships, temporal dependencies, and hierarchical structures.

Across the literature, most approaches treat spatial context and temporal dynamics as separate modelling problems (e.g., spatial domain detection versus time-course trajectory inference). Hybrid spatiotemporal models exist, but they are commonly evaluated on domain-specific tasks without a systematic comparison of multimodal fusion strategies, and often without explicit uncertainty quantification and biologically grounded interpretability. This study builds on the strengths of GNNs for modelling spatial neighbourhood structure and RNN/LSTM models for temporal dynamics and contributes by empirically comparing fusion strategies and integrating XAI/Uncertainty Quantification to support interpretability and trustworthiness in the context of cardiomyocyte differentiation efficiency prediction.

2.5.PREDICTIVE MODELLING FOR DIFFERENTIATION EFFICIENCY

2.5.1. Differentiation Efficiency in iPSC-CMs

iPSC-derived cardiomyocytes differentiation efficiency protocols' success is determined by several biological and technical variables[54], [188]. Examples of biological indicators include the expression of cardiac-specific markers, including cardiac troponin T (TNNT2), α-actinin, and connexin-43, as well as functional assessments of contractility, calcium handling, and electrophysiological properties[54]. Technical indicators include batch-to-batch reproducibility, survival rates post-dissociation and cryopreservation, and the percentage of cells expressing cardiomyocyte markers[5], [55].

Differentiation efficiency is a recurring problem across laboratories, protocols, and iPSC lines[55]. There is significant line-to-line variation even when similar protocols are employed, this is indicated by studies showing that cell seeding density can differ by a factor of four across different iPSC lines while maintaining optimal differentiation efficiency[55]. Some protocols exhibit more

consistent kinetics of cardiac marker expression across batches, revealing that this diversity also extends to temporal aspects of differentiation[54].

Quantitative thresholds derived from flow cytometry examination of cardiac markers are now included in the definition of "sufficient" versus "insufficient" differentiation outcomes[188]. According to current standards, a distinction is deemed successful if cardiac troponin T or similar markers are expressed at levels of >80-90%[5]. In contrast to adult cardiomyocytes, cells exhibiting cardiac markers may still have immature electrophysiological and contractile properties; hence, these thresholds might not fully reflect functional maturity[189].

Measurements of contractile force, action potential properties, and calcium transients have all been added as extra indicators of differentiation quality in recent advances in functional assessment[54]. Although standardisation across laboratories is still challenging due to variations in equipment and methodologies, the integration of various assessment modalities offers a more thorough evaluation of differentiation success[190].

2.5.2. AI Approaches for Predicting Differentiation Outcomes

Predicting differentiation efficiency in iPSC-derived cardiomyocytes has shown great promise thanks to machine learning approaches, which may allow for early intervention and culture condition optimisation[188]. 90% accuracy and precision had been achieved by day 7 of differentiation protocols using random forest and Gaussian process modelling to predict insufficient cardiomyocyte content, with 85% accuracy possible as early as day 5[188].

Early prediction's temporal advantage is crucial for improving laboratory efficiency and cutting expenses[191]. Machine learning models can offer accurate predictions at much earlier timepoints than traditional assessment approaches, which involve waiting until the conclusion of differentiation protocols (usually 10-15 days) to evaluate success[188]. Researchers can refocus resources on more promising cultures and detect failing differentiations early because of this capability[188]. Crucial experimental parameters that have a major influence on the final cardiomyocyte content have been uncovered using data-driven modelling techniques[188]. These models shed light on the ideal culture parameters, such as the environmental conditions, growth factor concentrations, and medium composition[192]. Adaptive protocol alterations throughout the differentiation process, as opposed to post-hoc analysis, are made possible by the capacity to predict results based on intermediate data[9].

Comparing supervised and unsupervised learning approaches for differentiation prediction has shown how crucial labelled datasets are in attaining the best results[193], [194]. Robust evaluation of model performance across various experimental settings and datasets is ensured by cross-validation methodologies and holdout validation approaches[193], [194]. In high-dimensional biological datasets, the incorporation of feature selection methods like Lasso regularisation has improved model efficiency while avoiding overfitting[195], [196], [197].

2.5.3. Explainability and Interpretability in AI for Biology

To foster trust and provide biological insights from machine learning models, the use of explainable AI (XAI) tools in biological systems has become increasingly important[198], [199]. The most popular approaches for elucidating individual predictions produced by intricate deep learning models are SHAP (Shapley Additive exPlanations) and LIME (Local Interpretable Model-Agnostic Explanations)[200], [201], [202]. The SHAP methodology offers global insights into feature relevance across entire datasets as well as local explanations for individual predictions[200], [201], [202]. In biological applications, SHAP values can provide useful information for protocol optimisation by identifying the cellular features or experimental conditions that have the most influence on differentiation outcomes[200], [202]. While preserving mathematical rigour, the additive nature of SHAP values allows for a quantitative evaluation of feature contributions[200], [201], [202], [203].

Beyond feature importance, accumulated local effects (ALE) analysis reveals the connections between predictor values and model outputs[199], [204]. ALE estimates the average projected probability for each category of categorical predictors, such as the kind of culture medium or cell line identity[199]. ALE exhibits linear, monotonic, or complex correlations with differentiation success for continuous variables such as cell density or growth factor concentrations[199], [204]. Permutation feature importance (PFI) offers complementary insights by quantifying the changes in prediction error when feature values are randomly changed[199], [205], [206]. PFI can pinpoint crucial timepoints, culture conditions, or cellular measurements that have the most effect on model predictions in cardiac differentiation contexts[206], [207], [208]. A thorough grasp of feature importance and mechanistic linkages is provided by the combination of PFI and ALE analysis[199].

When using AI models to inform clinical decisions or biological discoveries, interpretability becomes crucial[209], [210]. By emphasising whatever elements of the input data, the model focuses on during prediction, attention mechanisms in neural networks offer natural interpretability[128]. Attention weights in temporal gene expression modelling can highlight crucial windows of time or patterns of gene expression that influence differentiation outcomes[211], [212], [213].

Addressing the Black Box Problem in Hybrid Architectures

Complex interpretability frameworks that can clarify the intricate decision-making processes present in these hybrid architectures are required for the integration of graph neural networks and recurrent neural networks for spatial multi-omics research in heart regeneration[214], [215]. While effective for simpler models, traditional explainable AI techniques need to be significantly modified to handle the unique challenges presented by spatiotemporal learning systems that function on irregular graph structures with temporal dependencies[216].

GNN Interpretability Methods

Using a model-agnostic framework that identifies important subgraph structures and node properties, *GNNExplainer* is one of the first generally adopted approaches to provide interpretable explanations for GNN predictions[217]. In this approach, explanation generation is formulated as an optimisation problem that maximises the mutual information between the range of feasible subgraph structures and GNN predictions[217]. GNNExplainer provides thorough explanations that include both structural and attribute-based relevance by learning a feature mask that identifies crucial node properties and a graph mask that chooses significant edges[217], [218], [219]. GNNExplainer's technical implementation is based on variational approximation techniques that use gradient-based optimisation to learn real-valued masks[220]. The approach can produce multi-instance explanations that reliably explain entire classes of predictions as well as single-instance explanations for individual predictions[220]. In comparison to baseline approaches, GNNExplainer outperforms them by up to 43.0% in explanation accuracy, as demonstrated by experimental validation on synthetic datasets with planted network motifs[217].

By using a differentiable edge masking approach that works globally across numerous instances instead of producing explanations one at a time, *GraphMask* addresses several GNNExplainer's limitations[221]. The method uses sparse stochastic gates to address the hindsight bias issue that plagues instance-specific explanation approaches and allows gradient-based optimisation of edge importance[222]. GraphMask learns a neural network that predicts whether a link affects model predictions for each edge at each layer[221], [223]. GraphMask's primary innovation is its capacity to produce discrete masks, which, in contrast to continuous soft masks, offer more comprehensible explanations[224]. The approach maintains differentiability for end-to-end training while promoting sparsity in explanations through the use of predicted L_o norm regularisation[221]. Comparative analyses show that GraphMask avoids the computational burden of instance-specific optimisation while achieving higher faithfulness than current techniques[221].

Subgraph offers explanations in terms of subgraphs rather than individual nodes or edges, which is a major development in GNN interpretability[225]. To evaluate subgraph relevance and capture interactions between various substructures, the method leverages Shapley values in conjunction with Monte Carlo tree search to efficiently explore various subgraph combinations[226], [227]. By offering more logical and human-intelligible explanations, this method overcomes the drawback of previous approaches where significant components are not always connected[225]. SubgraphX's technological implementation reduces computational complexity while preserving explanation quality by using effective approximation approaches for calculating Shapley values in graph contexts[227]. Compared to disconnected explanations, the method's consideration of only connected subgraphs improves visualisation and interpretability[225]. With a runtime that is almost seven times longer than baseline techniques, experimental results show that SubgraphX provides better explanation quality than GNNExplainer while keeping affordable computing costs[225].

Temporal Attribution in RNNs

By identifying the time steps that have the most influence on model predictions, Attention Weight Analysis in RNN architectures offers essential insights into temporal decision-making processes[228], [229], [230]. Critical time windows and temporal dependencies that influence model decisions can be visualised thanks to the interpretable weight distributions that attention mechanisms in RNNs naturally produce across temporal sequences[231]. However, as recent analysis has shown, the use of raw attention weights for explanation purposes has significant limitations[232]. Gradient-based evaluations of attention weights frequently offer more predictive power for understanding model behaviour, and research shows that attention weights do not always correlate well with factual feature importance[228]. This study highlights the need for more sophisticated temporal attribution approaches that go beyond simple attention-weight visualisation.

Temporal Saliency Maps offer comprehensive frameworks for analysing feature importance across both temporal and feature dimensions, which constitutes a substantial improvement in RNN interpretability[233]. Traditional saliency approaches result in inadequate explanation quality due to the combination of time and feature domains, which is the fundamental challenge in temporal saliency computation[234], [235]. To address this challenge, the *Temporal Saliency Rescaling (TSR)* approach uses a two-stage process that computes feature-relevance scores within highly relevant time steps after calculating time-relevance scores for each temporal step[233]. The quality of saliency maps across various neural architectures and interpretability approaches is significantly enhanced by this decoupling strategy[233]. For temporal data analysis, experimental validation shows that TSR combined with gradient-based methods performs better than conventional saliency approaches across all assessment measures[233], [236].

Specialised architectures for specific biological applications have been incorporated into advanced temporal attribution methods. The analysis of LSTM temporal dependencies in reinforcement learning contexts has proven the methods for finding salient cells that contribute most to network outputs by combining forward and backwards propagation analysis[237]. These approaches shed light on the temporal dynamics of information processing in recurrent architectures by exposing temporal precedence relationships between gate activations and contribution increases[237].

Integrated Spatiotemporal Interpretability Frameworks

The Series Saliency Framework offers thorough temporal interpretation for multivariate time series by concurrently considering both feature and temporal dimensions[238], [239]. The framework uses saliency map segmentation based on the smallest destroying region principle and considers multivariate time series as series images[238], [239]. This approach works well as a data augmentation technique and allows for the discovery of crucial temporal regions and feature combinations that influence predictions[239]. By offering model-agnostic interpretability that can be used with any well-defined deep learning architecture, the series saliency approach overcomes the challenges of conventional attention-based methods[239]. The framework allows for a deeper understanding of the decision-making processes in intricate spatiotemporal models by producing

temporal interpretations that highlight both the significance of local features and global temporal patterns[240].

Interpretable Spatio-temporal Graph Neural Networks (InsGNN) is a state-of-the-art approach that uses information bottleneck principles to address interpretability challenges specific to spatiotemporal graph learning[241]. Two essential elements are included in the framework: learnable subgraph extraction with structural masking for structural interpretability and lightweight prototype matching modules for temporal interpretability[241]. By modelling sequences with low-dimensional knowledge vectors that reveal prototype importance, InsGNN addresses the fundamental challenge in integrating temporal interpretability within high-dimensional time features[241]. By choosing nodes and edges that correlate with prediction labels via learnable masking, the structural interpretability component finds invariant causal substructures[241]. Combining these elements preserves prediction performance while offering thorough spatiotemporal interpretability[241].

Specialised Techniques for Biological Applications

For biological spatiotemporal modelling, *Dynamic Connectivity Analysis* has become a key interpretability component, especially in neuroscience applications where biological insight depends on an understanding of connectivity patterns[242], [243]. Specialised architectures that combine time-varying interaction between node representations and inter-node connectivity patterns are incorporated into recent frameworks for explainable spatiotemporal coupling analysis[243]. By revealing how spatial relationships change over time and spotting important connectivity patterns that influence biological outcomes, these approaches offer biological interpretability[242]. Through the visualisation of connectivity strength maps and region-level relevance scores, the combination of dynamic connectivity modelling and gradient-based scoring allows for the extraction of biological traits that are pertinent to the job at hand while preserving interpretability[242].

Multi-Scale Interpretability addresses the challenge of understanding spatiotemporal dynamics across various temporal and spatial scales that are pertinent to biological systems[151], [244], [245], [246]. In contrast to conventional data-driven models, recent advancements in higher-order spatio-temporal physics-incorporated GNNs show approaches that inherently offer dynamic graphs, missing impact metrics, and graph-like optical flow, all of which improve interpretability [151], [244]. These frameworks incorporate physics-based constraints that enhance interpretability by guaranteeing that patterns are consistent with established biological principles[247], [248]. Better explainability is achieved by measuring the influence of each element in the spatiotemporal graph structure through the incorporation of normalising flows for assessing node importance[244].

Integration Challenges and Future Directions

A new area that calls for novel approaches to integrate temporal and spatial explanation mechanisms is *Unified Interpretability Frameworks* for hybrid GNN-RNN architectures[249], [250]. The challenge lies in providing logical explanations that span temporal dependencies modelled by RNNs and spatial relationships captured by GNNs while preserving computational efficiency and biological interpretability[176]. Recent advances in this area include the development of attention-driven frameworks that offer coherent explanations across temporal and spatial dimensions. By using hierarchical attention mechanisms that function at multiple scales, these approaches make it possible to simultaneously identify important temporal windows and spatial regions[251], [252].

2.5.4. Evaluation Metrics for AI-based Differentiation Prediction

A comprehensive suite of metrics that considers both predictive accuracy and model interpretability is needed to assess AI-based models for predicting differentiation efficiency in biological systems. This subsection examines the critical evaluation metrics required to evaluate the effectiveness of sophisticated machine learning techniques in cardiac regeneration applications, with a focus on metrics appropriate for the intricate, multi-modal nature of temporal modelling frameworks and spatial transcriptomics.

Classification Performance Metrics

An essential statistic for assessing binary classification performance in differentiation prediction tasks is *Area Under the Receiver Operating Characteristic Curve (AUROC)*[253], [254]. By aggregating model performance across decision thresholds, AUROC measures how well a model differentiates between successful and unsuccessful differentiation outcomes.[255]. With values ranging from 0.5 (random performance) to 1.0 (perfect discrimination), the metric shows the likelihood that the model would properly rank a randomly selected positive example higher than a randomly selected negative example[256], [257], [258]. Nevertheless, AUROC has significant drawbacks in biological applications, especially when handling unbalanced statistics, which are typical in differentiation studies[255], [259]. In cardiac regeneration scenarios, where false prediction of differentiation failure (false negative) can have more serious repercussions[260] than false prediction of success (false positive), AUROC's assumption that false positives and false negatives are equally undesirable may not be accurate[255]. Additionally, biases from small and imbalanced datasets, which are common in studies on cardiac differentiation, can affect AUROC[255].

For problems involving imbalanced classification, precision-recall curves and *Area Under the Precision-Recall Curve (AUPRC)* offer more sensitive metrics than AUROC[261], [262], [263]. Because it focuses more on the model's ability to accurately identify positive occurrences while minimising false positive predictions, AUPRC is especially useful in situations where the positive class (successful differentiation) represents a minority of cases[263]. According to recent studies, AUPRC offers a more insightful evaluation of model performance in biological applications when there is a noticeable class imbalance[261]. Because different computing approaches can produce

contradictory results, it is important to carefully evaluate the methodology while building precision-recall curves[264], [265]. According to recent studies, the way adjacent anchor points are connected during curve construction causes commonly used software tools to generate inconsistent and excessively optimistic AUPRC values[263]. This result highlights how crucial it is to compare model performance across studies using consistent methodological approaches.

Regression Performance Metrics

Mean Absolute Error (MAE) represents a fundamental regression metric that calculates the average magnitude of prediction errors without taking their direction into account[266]. MAE is calculated as the arithmetic mean of absolute differences between predicted and actual values, providing an intuitive measure of prediction accuracy in the same units as the target variable[266], [267], [268]. For biological applications, the metric has several benefits, such as ease of interpretation and robustness to outliers[269]. MAE is especially useful in biomarker discovery applications where clinical decision-making is directly impacted by prediction accuracy[266]. Research has demonstrated that ideal model performance is indicated by MAE values close to zero, with the metric offering a clear evaluation of prediction quality across a variety of biological datasets[270]. Because MAE is non-negative, it may be interpreted consistently, with lower values consistently denoting better performance[271].

The percentage of the dependent variable's variation that can be predicted from the independent variables is measured by the *Coefficient of Determination (R^2)*[266], [272]. R^2 sheds light on how well temporal and spatial characteristics account for differentiation efficiency results in the cardiac differentiation context[273]. Depending on the complexity of the biological system and the number of features in the model, recent biomarker discovery applications have achieved R^2 values between 0.48 and 0.79[274]. Because meaningful thresholds fluctuate greatly throughout various biological prediction types, the interpretation of R^2 necessitates careful evaluation of the biological context[275]. The clinical relevance of these improvements varies depending on the application and the biological processes being modelled, even though higher R^2 values often suggest better model fit[266].

Calibration Metrics

Brier Score is a strictly proper scoring mechanism that assesses how accurate probabilistic predictions are by calculating the mean squared difference between predicted probabilities and actual binary outcomes[276], [277]. Better-calibrated predictions are indicated by lower Brier scores, which go from 0 (perfect calibration) to 1 (worst possible calibration)[278]. This metric is especially useful for differentiation prediction applications where decision-making depends on knowing how reliable probability estimates are[276], [277]. By using decomposition approaches that isolate model accuracy from outcome prevalence effects, recent methodological advancements have addressed challenges in the interpretation of traditional Brier scores[277]. By eliminating the variance component of binary outcomes that is not indicative of model performance, modified Brier score formulations enable more sensitive comparisons across various prediction

models.[277]. This development is particularly important for applications involving cardiac differentiation, since the incidence outcomes can range greatly between cell lines or experimental conditions[279].

Reliability diagrams plot observed event frequencies against predicted probabilities to visually evaluate model calibration[280], [281]. Predicted probabilities and observed frequencies agree in well-calibrated models, with the ideal reliability diagram displaying an identity function relationship[300]. The CORP (Consistent, optimally binned, Reproducible, Pooled-adjacent-violators) approach, which uses isotonic regression to create statistically consistent and reproducible diagrams, has been used to address stability difficulties in recent developments in reliability diagram generation[301]. Systematic biases in probability estimations can be found using reliability diagrams for biological prediction tasks[300]. These graphs can show if models consistently overestimate or underestimate the likelihood of differentiation success in cardiac differentiation prediction, which is important information for clinical translation and optimising experimental design[300].

Explainability Evaluation Metrics

Fidelity Metrics measure how well explanation methods capture the decision-making process of the underlying model[302], [303], [304].. Global fidelity evaluates the accuracy of explanations throughout the entire dataset, whereas local fidelity gauges the agreement between explanations and model behaviour in the immediate neighbourhood of particular instances[304]. Recent thorough analyses have shown that SHAP outperforms LIME in biological applications, achieving near-perfect performance (>0.99) for various model types and perfect fidelity (1.0) for tree-based models[305]. Through explanation-agnostic fine-tuning techniques and random masking operations, the F-Fidelity framework addresses the challenges of conventional perturbation-based approaches, marking a substantial leap in fidelity evaluation[306]. By preventing out-of-distribution inputs from evaluation processes and mitigating information leakage concerns, this method offers a more reliable evaluation of explanation quality[306].

Stability Metrics measure the consistency of explanations across comparable inputs or repeated applications of explanation techniques[304], [307].. High stability is essential for establishing confidence in AI-driven differentiation predictions since it shows that explanation methods yield consistent outcomes when used in comparable biological contexts[304], [307].. According to experimental evaluations, the stability scores of the most advanced explanation approaches used on biological datasets range from 0.85 to 0.95[304].

Sparsity Metrics measure the percentage of features that obtain non-zero importance scores, hence quantifying the parsimony of explanations[304]. Given the high-dimensionality of transcriptome data and the biological fact that only a handful of genes normally control specific cellular functions, sparsity is especially crucial in single-cell genomics applications[308]. Metrics that can differentiate between sparse linear data and other distributions have been created recently for evaluating feature sparsity in language models, offering frameworks that can be modified for use

in biological applications[309]. One example of how sparsity patterns themselves might yield biologically significant information is the DECODE framework for single-cell RNA sequencing[310]. This method shows that sparsity structure in biological data represents functionally meaningful relationships rather than merely technical restrictions by quantifying gene co-dependency patterns using sparse representation coefficients[310].

Faithfulness Metrics evaluate how well explanations capture the true causal relationships that underlie model predictions[307], [311]. In contrast to fidelity, faithfulness gauges conformity to ground truth as opposed to consistency with model behaviour[311]. According to recent evaluations utilising controlled experiments with established ground truth, current faithfulness measurements exhibit serious disagreements, with the best-performing metrics showing 30% deviation from expected values for perfect explanations[303]. Research on the development of objective standards for faithfulness evaluation is ongoing, and frameworks for producing explanations with perfect known faithfulness are offered by transparent models like decision trees[303]. These methodologies facilitate the methodical assessment of explanation methods and the identification of scenarios in which disparate metrics may yield contradictory evaluations[303], [312].

2.6.GAPS IN LITERATURE AND RESEARCH JUSTIFICATION

The integration of GNNs and RNNs for spatial multi-omics analysis in cardiac regeneration is justified by several critical gaps found in the current literature[313]. While deep learning has shown promise in single-cell analysis[137], [138], [314], and spatial transcriptomics has made considerable strides in cardiac biology applications[85], [91], [92], the integration of these approaches for predictive modelling of cardiac differentiation is still largely unexplored.

Firstly, most of the spatial transcriptomics research in cardiac biology to date has been on descriptive analyses of spatial organisation and cellular heterogeneity[85], [315], with little attention paid to prediction modelling for therapeutic applications. The fundamental challenge of predicting and optimising differentiation efficiency in regenerative medicine applications is not addressed by these studies, even though they offer insightful information about cardiac tissue architecture[316], [317]. One major obstacle to applying spatial omics findings to clinical settings is the disconnect between spatial characterisation and predictive utility[318], [319], [320].

Second, most of the deep learning approaches used in cardiac biology now rely on static snapshots of cellular states or single modalities[137], [138], [173].. Existing approaches are still insufficient in simulating the temporal dynamics of cardiac differentiation, which are essential for comprehending and predicting differentiation outcomes[208], [321].. While RNN-based approaches have been effective in modelling temporal gene expression[148], it has not been proven that they can be used to predict cardiac-specific differentiation in a geographical context.

Third, a novel approach that overcomes the drawbacks of single-architecture approaches is the integration of spatial and temporal information using combined GNN-RNN architectures[322].

While temporal modelling approaches usually overlook spatial context, current spatial biology approaches employing GNNs focus mostly on static spatial relationships[50], [145], [146].. The temporal dynamics of differentiation processes, as well as the spatial organisation of cardiac tissues, may be captured by combining various structures.

Fourth, traditional machine learning approaches with limited temporal resolution are the mainstay of current predictive models for differentiation efficiency[208]. While achieving reasonable accuracy, these approaches do not leverage the extensive spatial and temporal information seen in contemporary multi-omics datasets[323]. Combining temporal modelling with spatial multi-omics data may greatly increase prediction accuracy while offering mechanistic insights into differentiation processes[323], [324].. The potential of similar improvements in biological prediction tasks is demonstrated by the success of hybrid architectures in weather forecasting, where HiSTGNN achieved 4.2% to 11.6% error reduction compared to state-of-the-art approaches[191]. A template for modelling cross-cellular interactions during differentiation processes is provided by the hierarchical modelling approach, which incorporates cross-regional spatiotemporal correlations among meteorological variables[191]. A precedent for translating hybrid architectures to biological contexts is established using domain adaptation techniques in population genetics, where domain-adaptive neural networks effectively solved simulation mis-specification issues[207]. This approach addresses the problem of sparse labelled data in cardiac differentiation research by allowing training on simulated data and application to real experimental datasets.

Fifth, the requirement for interpretable models that can offer biological insights in addition to predicting accuracy is highlighted by the emphasis on explainable AI in biological applications[218], [219]. In spatial biology, current deep learning approaches frequently function as “black boxes” with limited interpretability[137], [157], [212], [230], [314].. This limitation could be overcome by developing interpretable GNN-RNN frameworks, which would still preserve the advanced modelling abilities needed for intricate biological systems[322]. Based on temporal variations, the gradient-based sensitivity analysis shown in LSTM modelling of microbiome dynamics[194] offers biological insights into the contributions of individual species. Key cellular populations and molecular pathways that influence the success of cardiac differentiation could be identified using similar techniques.

Architectural insights relevant to cardiac differentiation modelling are offered by the Time-varying Graph Convolutional networks (TVGCN) technique, which dynamically captures the spatial relationships and uses dilated causal convolution for temporal modelling[325]. Combining time-varying dynamic adjacency matrices obtained from attention scores with static adjacency matrices expressing physical connectivity[325] provides a framework for modelling both fixed cellular spatial relationships and dynamic molecular interactions. Computational efficiency benefits offered by the Temporal Graph Networks (TGNs) framework for dynamic graphs represented as sequences of timed events can enable the analysis of large-scale spatial multi-omics datasets[202].

Significant speed gains are made possible by the innovative pairing of memory modules and graph-based operators, all while preserving computational tractability[202].

Addressing these identified gaps with a unified framework that captures temporal differentiation dynamics and spatial cellular relationships is what makes integrating GNN and RNN architectures on spatial multi-omics data novel[326], [327], [328].. Compared to current approaches that concentrate on single data modalities or tackle spatial and temporal aspects independently, this approach represents a significant advancement[329]. This integration's clinical relevance is especially crucial considering the pressing need for better cardiac regeneration therapies[330]. Achieving reliable, high-quality differentiation results is a major problem for current iPSC-CM technologies[331], [332].. The efficiency and reliability of cardiac regeneration techniques could be significantly increased by the development of predictive models that can optimise differentiation protocols based on temporal and spatial cellular features[333], [334].. The development of predictive frameworks for cardiac regeneration is made possible by the convergence of cross-domain architectural achievements, temporal modelling capabilities, and spatial biology advancements. This integrative approach is justified by the gaps in the current literature, and the success of hybrid architectures across domains gives assurance on their potential for biological applications.

2.7.SUMMARY AND SYNTHESIS

This literature reveals the field of cardiac biology research as a rapidly evolving field, with deep learning techniques and spatial multi-omics technologies starting to merge. The review shows that while there have been notable developments in each of the three areas, predictive modelling for cellular differentiation[208], deep learning for single-cell analysis[137], [138], [314], and spatial transcriptomics in cardiac tissues[85], [91], the integration of these approaches is still an uncharted area with great promise for advancing cardiac regeneration.

The key findings drawn from this review directly influence the aims of the study and justify the proposed methodology. First, spatial transcriptomics has been a great tool for identifying novel cell populations and characterising cardiac cellular heterogeneity[85], [86], [91], [335], but it lacks the predictive capabilities for therapeutic optimisation. Second, deep learning techniques have demonstrated excellent results in pattern recognition and single-cell clustering[137], [138], but they are still not widely used in spatial contexts with temporal dynamics. Third, there is a pressing need for predictive modelling techniques that can make use of multi-modal data due to the challenges associated with iPSC-CM differentiation, including variability, immaturity, and unpredictable results[5], [74], [75].

One critical factor that is not sufficiently addressed by existing spatial omics techniques is the temporal aspect of cardiac differentiation. The dynamic process of cardiac differentiation requires temporal modelling capabilities that RNN architectures can offer[148], whereas spatial transcriptomics provides snapshots of cellular states[92]. The constraints of current single-

architecture techniques are addressed by the new integration of temporal dynamics through RNNs and spatial context through GNNs[336].

The necessity for interpretable models that can offer mechanistic insights in addition to predicting accuracy is in line with the focus on explainable AI in biological applications[218], [219]. This requirement is especially critical in cardiac regeneration, where securing regulatory approval for clinical applications and optimising therapy regimes depend on an understanding of the molecular foundation of predictions[337].

According to the research, there is a strong need for developing integrated GNN-RNN techniques because of the current gaps in spatial-temporal modelling, the limited predictive capabilities in spatial omics, and the need for interpretable AI frameworks in cardiac biology. The research hypothesis that integrating temporal dynamics modelling with spatial relationship modelling using GNNs can significantly increase the prediction of cardiac differentiation efficiency while offering biologically interpretable insights is directly supported by these findings. These literature findings inform the transition to the methodology chapter, highlighting the need for: (1) integrating temporal modelling capabilities with spatial multi-omics data; (2) developing interpretable deep learning frameworks that offer biological insights; (3) validation approaches that outperform current methods in terms of predictive performance; and (4) application to real cardiac differentiation datasets that address current regenerative medicine challenges. Both the biological need for interpretable, actionable insights that can direct therapy optimisation and the technical difficulties of integrating diverse data modalities must be addressed by the methodology.

3. CHAPTER 3: METHODOLOGY

3.1.INTRODUCTION

This chapter outlines the comprehensive methodological framework used to develop and evaluate a novel hybrid deep learning architecture that combines temporal gene expression data with spatial transcriptomics to predict the outcomes of cardiomyocyte differentiation. By combining GNNs for spatial analysis and RNNs for temporal modelling, the study fills a critical gap in computational approaches for regenerative medicine, representing the first systematic investigation of spatiotemporal integration in cardiomyocyte differentiation prediction.

The methodology is structured around four sequential phases: individual model development, embedding extraction and fusion, hybrid model training and evaluations, and XAI framework implementation (Figure 7). This strategy uses comprehensive XAI approaches to ensure biological interpretability while ensuring enabling the systematic comparison of fusion strategies. In addition to incorporating best practices for machine learning validation in biomedical applications, the chapter organisation adheres to established guidelines for computational biology research. The equations used to develop the models used here and statistical analysis are outlined in appendix A.

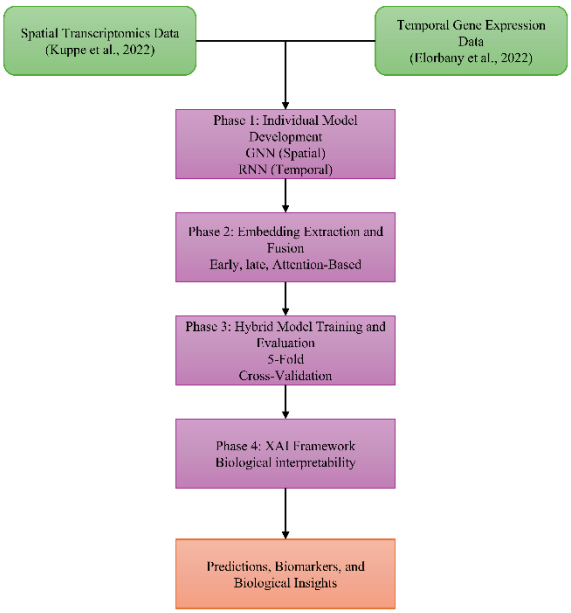

Figure 7: Overview of the four-phase methodology.

Chapter Structure: The study design and theoretical framework are established in Section 3.2, while the quantitative approach and sampling strategy are outlined in Section 3.3. Data collection methods are detailed in Section 3.4, followed by comprehensive analysis procedures in Section 3.5. Sections 3.6-3.8 address validity, ethics, and limitations, with Section 3.9 providing a summary linking to the results chapter.

3.2.RESEARCH DESIGN

This study employs a computational experimental design grounded in the positivist paradigm, which assumes that biological phenomena can be objectively measured and quantitatively analysed through rigorous computational methods. The research design is characterized as a multimodal deep learning investigation with integrated validation and interpretability components, specifically designed to address the complexity of spatiotemporal biological data analysis.

The theoretical framework is grounded in systems biology which recognises that complex interactions between temporal gene expression patterns and spatial microenvironmental factors lead to cellular differentiation. To achieve a comprehensive understanding of cellular processes, it is crucial to integrate heterogeneous biological data types, which is in line with established computational biology approaches. Leveraging the complementary strengths of sequence-based spatial modelling, the design integrates hybrid architecture development as the core methodological innovation.

3.2.1. Methodological Alignment with Research Questions

The research design directly addresses the four fundamental research questions through targeted methodological components, table 2 summarises the research questions:

Table 2: Summary of research questions against corresponding methodological component

Research Question	Methodological Component	Section Reference
Spatial pattern recognition through GNN architectures	Enhanced GNN development with Graph Attention Networks/graph Convolutional Networks (GAT/GCN) layers	Section 3.5.2
Prediction accuracy improvement through multimodal integration	Three fusion strategies (concatenation, ensemble, attention)	Section 3.5.2
Critical spatiotemporal biomarker identification	SHAP-based XAI framework with biological validation	Section 3.5.6
Biological validation of computational predictions	Cardiac gene database mapping and pathway analysis	Section 3.6

3.3.RESEARCH APPROACH AND STRATEGY

This study employs a quantitative approach utilising deep learning methodologies specifically adapted for biological data analysis. This advanced computational approach, which combines supervised machine learning and multimodal data fusion, maintains biological interpretability though comprehensive validation procedures while utilising neural networks' pattern recognition capabilities. By combining spatial and temporal information using three distinct fusion architectures: early concatenation-based fusion, late ensemble-based fusion, and dynamic

attention-weighted fusion, the hybrid modelling strategy addresses the inherent limitations of single-modality approaches[338], [339]. This thorough approach ensures optimal performance across diverse biological contexts and enables systematic comparison of integration strategies.

3.3.1. Sampling Strategy and Justification

The sampling strategy utilises established public datasets with proven biological relevance and technical quality. The spatial transcriptomics component leverages the 752 tissue spots with spatial coordinates from the Kuppe et al. (2022) study[112], while the temporal component utilises the 800 temporal samples from the Elorbany et al. (2022) study[49], which spans 4 distinct differentiation trajectories.

To determine sample size adequacy, power calculations specific to deep learning applications in biological data analysis were used. The sample sizes (752 spatial spots and 800 temporal samples) capture enough biological heterogeneity among cardiomyocyte subtypes and differentiation trajectories to be robust, while also exceeding the minimal requirements for neural network training. For GNN architectures, the 800 temporal samples enable comprehensive sequence modelling across 10 time points with statistical power >0.8 for detecting moderate effect sizes in classification tasks, while the 752 spatial spots offer sufficient neighbourhood density for effective graph construction (k = 6 neighbours per spot).

By minimising the technical and financial challenges associated with novel data generation, this sampling technique ensures reproducibility and enables direct comparison with existing literature. The datasets support the generalisation of computational findings across different cardiomyocyte differentiation systems by representing diverse biological contexts and experimental conditions. Computational validation strategy incorporates rigorous cross-validation protocols established specifically for biomedical machine learning applications. To address the inherent challenges of biological data such as batch effects and class imbalance, the approach employs 5-fold stratified cross-validation with class balancing. This strategy uses bootstrap approaches for estimating confidence intervals and adheres to established best practices for machine learning validation in healthcare applications.

3.4.DATA COLLECTION METHODS

3.4.1. Spatial Multi-Omics Data Collection

The primary dataset consists of spatial transcriptomics data published by Kuppe et al. (2022), [112]. The 10X Genomics Visium Spatial Gene Expression technology, which enables simultaneous capture of gene expression profiles and spatial positioning data with a spot diameter resolution of ~55µm, was used to generate this dataset.

Dataset characteristics include:

i. Sample composition: 752 tissue spots with accurate spatial coordinates.
ii. Feature depth: >2,000 gene expression measurements per spot.

iii. Biological context: Human cardiac tissue from myocardial infarction patients.
iv. Spatial resolution: ~55μm spot diameter enabling capture of cellular neighbourhoods.
v. Coverage: Full transcriptome analysis with spatial preservation.
vi. Classification target: 5 distinct cardiomyocyte subtypes based on spatial location and gene expression profiles.

Data acquisition protocol follows established procedures for spatial transcriptomics analysis, including tissue sectioning, library preparation, sequencing, and spatial mapping. Quality control measures include assessment of spot quality, gene detection rates, and spatial coordinate accuracy. The dataset offers comprehensive documentation of experimental protocols, enabling reproducible analysis and computational method validation.

3.4.2. Temporal Gene Expression Data Collection

The secondary dataset consists of temporal differentiation data from Elorbany et al. (2022), representing a comprehensive time-course analysis of human iPSC-derived cardiomyocyte differentiation published in PLoS Genetics[49]. This dataset was generated using Single-Cell RNA sequencing (scRNA-seq) technology to capture the dynamics changes in gene expression during differentiation processes.

Data characteristics include:

i. Sample composition: 800 temporal samples distributed across 200 samples per trajectory.
ii. Temporal resolution: 10 sequential time points capturing differentiation dynamics.
iii. Feature depth: 2,000 highly variable genes selected for temporal analysis.
iv. Biological context: Human iPSC-derived cardiomyocyte differentiation.
v. Trajectory diversity: 4 distinct differentiation pathways representing different experimental conditions.
vi. Classification targets: 4 differentiation trajectory classes based on temporal gene expression patterns.

The data collection protocol incorporates established single-cell RNA sequencing procedures, including cell isolation, library preparation, sequencing, and temporal trajectory reconstruction. Quality control measures include assessment of cell viability, gene detection sensitivity, and temporal consistency. The dataset offers comprehensive metadata enabling validation of temporal modelling approaches and integration of spatial transcriptomics data.

3.4.3. Data Integration Strategy

By carefully aligning sample spaces and feature representations, the multimodal integration approach tackles the challenges of combining heterogeneous data types. To enable the combining of complementary information sources, the integration technique employs computational alignment procedures to match spatial and temporal samples based on biological relevance rather than direct correspondence.

The integration protocols include:

i. Feature harmonization: Standardisation of gene expression measurement across platforms.
ii. Sample alignment: Computational matching of spatial spots with temporal samples based on transcriptomic similarity.
iii. Quality assessment: Validation of integration quality through correlation analysis and biological pathway consistency.
iv. Preprocessing coordination: Synchronised normalisation and scaling procedures for multimodal compatibility.

The spatial and temporal datasets originate from different experimental contexts and are not paired at the cell/spot level, for the fusion experiments, a shared prediction target is required. In this study, the shared target is the differentiation efficiency label defined in section 1.3 (high vs low efficiency based on terminal cardiomyocyte purity). Temporal cell sequences are labelled using the terminal outcome, and spatial Visium spots are assigned labels via the similarity-based alignment step for multimodal fusion. This transfer is an integration strategy rather than a claim of direct biological equivalence between adult myocardial infarction tissue states and in vitro differentiation samples; its impact on generalisation is discussed explicitly in sections 3.9 and 5.5.

3.5.DATA ANALYSIS PROCEDURES

3.5.1. Preprocessing Pipeline Implementation

Data preprocessing employed scikit-learn's preprocessing modules to ensure consistent data distributions across modalities. Spatial transcriptomics data utilized StandardScaler for Z-score normalization, while temporal sequences employed MinMaxScaler to preserve temporal relationships. Label encoding through LabelEncoder ensured consistent categorical variable handling across datasets.

Preprocessing of spatial transcriptomics (shown in figure 8) data follows established protocols from the scanpy ecosystem, incorporating comprehensive quality control and normalisation procedures.

```
sc.pp.normalize_total(self.adata, target_sum=1e4) # Total count normalization
sc.pp.log1p(self.adata)                           # Log transformation
sc.pp.highly_variable_genes(self.adata, n_top_genes=2000, subset=True)  # Feature selection
sc.pp.scale(self.adata, max_value=10)             # Z-score standardization
```

Figure 8: Spatial transcriptomics preprocessing pipeline. The scanpy-based preprocessing workflow implemented for spatial transcriptomics data analysis, incorporating four key computational steps: (1) Total count normalisation with target sum of 10.000 UMI per cell to account for sequencing depth variations, (2) **Log transformation** to stabilise variance and normalise gene expression distributions, (3) **Highly variable genes selection** identifying the top 2,000 most informative genes with automatic subsetting to reduce dimensionality, and (4) **Z-score standardisation** with maximum value clipping at 10 to prevent outlier dominance. This

established protocol follows best practices from the single-cell genomics community and ensures data quality for downstream hybrid GNN-RNN analysis of the 752 tissue spots from the Kuppe et al. (2022) cardiac spatial transcriptomics dataset.

Quality control measures include spot filtering (>500 detected genes), gene filtering (>10 spots), mitochondrial content assessment (<20%), and ribosomal gene filtering. Spatial graph construction employs k-nearest neighbours (k = 6) with Euclidean distance metrics and inverse distance weighting for edge construction.

Temporal data preprocessing incorporates specialised procedures for sequence data analysis, including cell filtering (>100 detected genes), doublet detection and removal, cell cycle scoring, and temporal sequence construction using linear interpolation. Feature engineering includes gene expression smoothing, differential expression identification, RNA velocity estimation, and pseudotime calculation for trajectory ordering.

Statistical preprocessing employs multimodal scaling strategies with Z-score normalisation for GNN components and min-max scaling for RNN components. Principal Component Analysis (PCA) from scikit-learn's decomposition module enabled efficient dimensionality reduction while preserving biological variance. GNN features retained 95% explained variance (typically ~128 components), while RNN features maintained 90% variance (typically ~256 components). t-Distributed Stochastic Neighbour Embedding (t-SNE) from sklearn.manifold provided visualization of high-dimensional embeddings for quality assessment.

Class imbalance (shown in figure 9) was systematically addressed through compute_class_weight from sklearn.utils, generating inverse frequency weights for loss function balancing. WeightedRandomSampler ensured balanced batch composition during training, while stratified sampling maintained class proportions across train-validation splits.

```python
class HybridDataset(torch.utils.data.Dataset):
    """Dataset for hybrid model training with class imbalance support"""

    def __init__(self, gnn_embeddings, rnn_embeddings, targets):
        self.gnn_embeddings = torch.FloatTensor(gnn_embeddings)
        self.rnn_embeddings = torch.FloatTensor(rnn_embeddings)
        self.targets = torch.LongTensor(targets)

        # Calculate class weights for imbalance handling
        self.class_counts = np.bincount(targets)
        self.class_weights = compute_class_weight('balanced', classes=np.unique(targets), y=targets)

        logger.info(f"Class distribution: {dict(zip(np.unique(targets), self.class_counts))}")
        logger.info(f"Class weights: {dict(zip(np.unique(targets), self.class_weights))}")

    def __len__(self):
        return len(self.targets)

    def __getitem__(self, idx):
        return self.gnn_embeddings[idx], self.rnn_embeddings[idx], self.targets[idx]

    def get_weighted_sampler(self):
        """Create WeightedRandomSampler for handling class imbalance"""
        # Assign weight to each sample based on its class
        sample_weights = np.array([self.class_weights[t] for t in self.targets])

        sampler = torch.utils.data.WeightedRandomSampler(
            weights=sample_weights,
            num_samples=len(sample_weights),
            replacement=True
        )

        logger.info(f"WeightedRandomSampler created for balanced training")
        return sampler

    def get_class_weights_tensor(self):
        """Get class weights as tensor for loss function"""
        return torch.FloatTensor(self.class_weights)
```

Figure 9: Class imbalance mitigation framework for hybrid model training. Implementation of the HybridDataset class demonstrating multi-level class imbalance handling: (1) automatic class distribution analysis and balanced weight computation, (2) WeightedRandomSampler creation for oversampling minority classes during training, and (3) class weight tensor generation for integration with CrossEntropyLoss. This framework ensures robust model training on imbalanced cardiomyocyte differentiation datasets by addressing sampling bias at both the data loading and loss computation levels.

3.5.2. Deep Learning Architecture Development

Phase 1: Individual model Development follows a systematic approach to establish baseline performance for each modality before integration as shown in figure 10.

The Graph Neural Network architecture incorporates advanced spatial modelling capabilities:

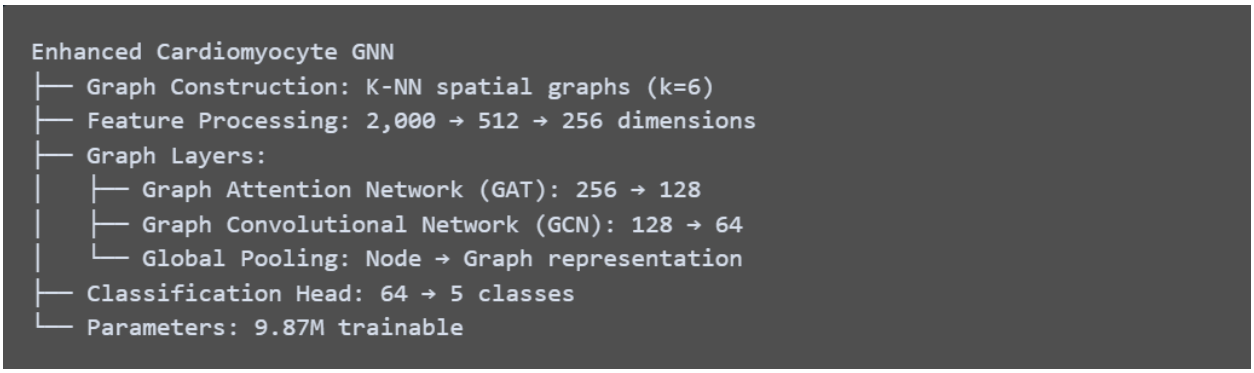

Figure 10: Comprehensive architecture of the spatial GNN model featuring k-nearest neighbour graph construction (k = 6) for spatial relationship modelling, progressive feature dimensionality reduction from 2,000 highly variable genes through hierarchical processing layers (512 -> 256 -> 128 -> 64 dimensions), dual graph processing combining Graph Attention Networks (GAT) and Graph Convolutional Networks (GCN) for enhanced spatial pattern recognition, global pooling for graph-level representation, and final classification into 5 cardiac cell types. This neural network achieved state-of-the-art performance on cardiac tissue spatial transcriptomics data by integrating spatial coordinates with gene expression patterns for accurate cardiomyocyte identification and classification.

The node representation update in the Graph Attention Network is as follows (equation 1):

Equation 1: node representation update in the Graph Attention Network

$$h_i^{(l+1)} = \sigma\left(\sum_{j \in N(i)} \alpha_{ij}^{(l)} W^{(l)} h_j^{(l)}\right) \quad (1)$$

Where:

- $h_i^{(l)} \in \mathbb{R}^{d(1)}$ is the feature vector of node i at layer l
- $N(i)$ denotes the spatial neighbourhood of node i
- $\alpha_{ij}^{(l)}$ is the attention coefficient between nodes i and j at layer l
- $W^{(l)} \in \mathbb{R}^{d(l+1)} \times d^{(l)}$ is the learnable matrix
- $\sigma(\cdot)$ is the activation function (LeakyReLU)

Training strategy employs learning rate scheduling, weighted loss functions for imbalanced data, early stopping with patience=15, stratified sampling for class balance, and comprehensive regularisation throughout dropout and batch normalisation.

The Recurrent Neural Network architecture (figure 11) focuses on temporal sequence modelling:

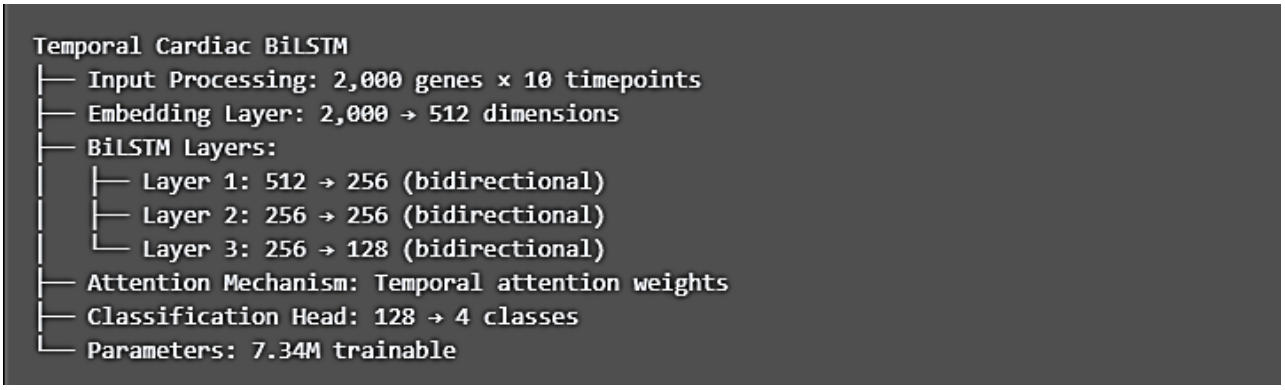

Figure 11: Temporal Bidirectional Long Short-Term Memory (LSTM) architecture for developmental stage classification. Complete neural network architecture showing: (i) input processing of 2,000 gene expression profiles across 10 developmental timepoints, (ii) embedding layer for feature dimensionality reduction, (iii) three-layer bidirectional LSTM network with progressive refinement (512 -> 256 -> 256 -> 128 dimensions), (iv) temporal attention mechanism for dynamic timepoint importance weighting, and (v) 4-class developmental stage classification head. This 7.34M-parameter architecture captures bidirectional temporal dependencies in cardiac gene expression trajectories, enabling accurate prediction of cardiomyocyte maturation stages.

Training optimisation incorporates focal loss for class imbalance handling, gradient clipping (max_norm = 1.0), dynamic learning rate with ReduleLROnPlateau, sequence-aware data augmentation, and comprehensive temporal validation procedures.

3.5.3. Hybrid Fusion Strategy Implementation

Phase 2: Embedding Extraction and Fusion focuses on optimal combination of learned representations from individual models.

Three fusion strategies were systematically implemented and evaluated as shown in figure 12-14:

Strategy 1: Early Fusion (Concatenation)

```python
if fusion_strategy == 'concatenation':
    # Early fusion - concatenate embeddings
    fusion_dim = gnn_dim + rnn_dim

# In forward method:
def forward(self, gnn_emb, rnn_emb):
    if self.fusion_strategy == 'concatenation':
        # Early fusion
        fused_emb = torch.cat([gnn_emb, rnn_emb], dim=1)
        output = self.fusion_head(fused_emb)
        return output, None
```

Figure 12: Implementation of the concatenation-based fusion approach where GNN and RNN embeddings are directly concatenated to create a combined feature vector of dimensions. The fused

embeddings are then processed through a unified classification head to produce final predictions. This early fusion strategy (shown in equation 2) enables joint learning of spatial and temporal features at the feature level, allowing the model to capture cross-modal interactions between spatial transcriptomics patterns and temporal gene expression trajectories.

The concatenation fusion strategy combines embeddings at the feature level:

Equation 2: Concatenation fusion

$$h_{fused} = [h_{GNN};\ h_{RNN}] \qquad (2)$$
$$y = MLP(h_{fused})$$

Where MLP(·) represents a multi-layer perceptron classifier.

Strategy 2: Late Fusion (Ensemble)

```
elif fusion_strategy == 'ensemble':
    # Late fusion - separate heads then ensemble
    self.gnn_head = self._create_classifier(gnn_dim, hidden_dims, num_classes)
    self.rnn_head = self._create_classifier(rnn_dim, hidden_dims, num_classes)
    self.ensemble_weight = nn.Parameter(torch.tensor(0.5))  # Learnable weight

# In forward method:
elif self.fusion_strategy == 'ensemble':
    # Late fusion
    gnn_output = self.gnn_head(gnn_emb)
    rnn_output = self.rnn_head(rnn_emb)

    # Weighted ensemble
    alpha = torch.sigmoid(self.ensemble_weight)
    output = alpha * gnn_output + (1 - alpha) * rnn_output
```

Figure 13: Implementation of the ensemble-based fusion approach where GNN and RNN embeddings are processed through separate classification heads before combining predictions. The ensemble strategy employs learnable weight parameter with sigmoid activation to compute the mixing coefficient α, enabling adaptive weighting between modalities ($\alpha * gnn\_output + (1 + \alpha) * rnn\_output$). This late fusion approach (equation 3) allows each modality to develop specialised representations while maintaining flexibility in their combination, supporting both independent learning and ensemble decision-making for robust cardiomyocyte classification.

The ensemble fusion combines predictions from separate modality-specific classifiers:

Equation 3: Ensemble fusion

$$y_{GNN} = MLP_{GNN}(h_{RNN}) \qquad (3)$$

$$y_{final} = \lambda \cdot y_{GNN} + (1 - \lambda) \cdot y_{RNN}$$

Where $\lambda = \sigma(w)$ is a learnable ensemble weight parameter.

Strategy 3: Attention Fusion (Dynamic)

```python
class AttentionFusion(nn.Module):
    def __init__(self, gnn_dim, rnn_dim, hidden_dim=64):
        super(AttentionFusion, self).__init__()

        # Attention network
        self.attention_net = nn.Sequential(
            nn.Linear(gnn_dim + rnn_dim, hidden_dim),
            nn.ReLU(),
            nn.Dropout(0.3),
            nn.Linear(hidden_dim, 2),  # Output weights for GNN and RNN
            nn.Softmax(dim=1)
        )

# In HybridGNNRNN class:
elif fusion_strategy == 'attention':
    # Attention fusion
    self.attention_fusion = AttentionFusion(gnn_dim, rnn_dim, hidden_dims[0])

# In forward method:
elif self.fusion_strategy == 'attention':
    # Attention fusion
    fused_emb, attention_weights = self.attention_fusion(gnn_emb, rnn_emb)
    output = self.fusion_head(fused_emb)
    return output, attention_weights
```

Figure 14: Implementation of the attention fusion strategy featuring a learnable attention network that dynamically weights GNN and RNN contributions per sample. The module computes sample-specific attention weights through a multi-layer perceptron with ReLU activation and softmax normalisation, outputting two weights for GNN and RNN modalities. The attention mechanism processes concatenated embeddings to generate adaptive fusion weights, enabling the model to automatically adjust the importance of spatial versus temporal information based on input characteristics, thus providing interpretable and context-aware multi-modal integration.

Equation 4 shows how the attention-based fusion learns dynamic weights for each modality:

Equation 4: Attention-based fusion

$$\alpha = softmax\big(MLP([h_{GNN};\ h_{RNN}])\big)$$
$$h_{fused} = \alpha_{GNN} \cdot W_{GNN} h_{GNN} + \alpha_{RNN} \cdot W_{RNN} h_{RNN} \quad (4)$$

Where:

- $\alpha = [\alpha_{GNN}, \alpha_{RNN}]^T$ with $\alpha_{GNN} + \alpha_{RNN} = 1$
- W_{GNN}, W_{RNN} are learnable projection matrices.

3.5.4. Model Training and Evaluation Procedures

The training protocol comprises of 5-fold stratified cross-validation for robust performance estimation, Adam optimisation with weight decay for regularisation, CrossEntropyLoss with class weighting for handling imbalanced data, data alignment procedures for careful matching of GNN and RNN sample spaces, and comprehensive regularisation through dropout, batch normalisation, and early stopping[339], [340]. Performance evaluation adheres to established best practices for machine learning validation in biomedical applications, including statistical significance testing for performance comparisons.

To minimise the risk of data leakage and ensure proper separation between training, validation, and testing datasets, a structured data partitioning protocol was implemented. A detailed checklist outlining the safeguards applied during dataset preparation is provided in Appendix B.

3.5.5. Statistical Analysis Framework

The computational analysis framework employed a comprehensive statistical analytics framework integrating established machine learning libraries with specialised biological data analysis tools. The framework ensures rigorous statistical validation while maintaining interpretability through systematic application of established methodologies.

Primary Libraries: The analytical pipeline utilized scikit-learn (v1.3.0) as the primary machine learning framework, providing standardized implementations of preprocessing, model selection, and evaluation procedures. Scientific computing employed SciPy (v1.11.3) for advanced statistical testing and NumPy (v1.24.3) for numerical computations, while Pandas (v2.0.3) enabled comprehensive data manipulation and analysis workflows.

Statistical Validation Tools: The framework incorporated multiple validation approaches through scikit-learn's model selection modules, including stratified K-fold cross-validation (K=5), train-test splitting with stratified sampling (80-20 and 60-20-20 configurations), and cross-validation scoring for robust performance estimation. Statistical significance testing employed SciPy's statistical functions, particularly McNemar's test [341] for paired model comparisons and paired t-tests for metric significance assessment.

Metrics Suite: Model performance assessment utilized scikit-learn's extensive metrics library, providing accuracy scores, F1-scores, precision and recall measurements, classification reports with per-class statistics, and confusion matrices for detailed error analysis. Additional metrics included area under the ROC curve (AUC-ROC) for probabilistic assessment and custom confidence scoring for uncertainty quantification.

Statistical Testing Protocol: Performance comparisons employed McNemar's test [341] for paired predictions, enabling rigorous assessment of classification improvement significance. Paired t-tests provided additional validation for continuous metrics, ensuring statistical robustness of performance claims with significance thresholds set at $\alpha = 0.05$.

Monte Carlo (MC) Dropout analysis (shown in figure 15) was used for uncertainty quantification (UQ), which was used to assess the predictive framework's robustness and reliability. The estimation of epistemic uncertainty – the uncertainty resulting from model parameters due to limited training data or model capacity – is enabled by MC Dropout, in contrast to conventional deterministic inference. This was achieved by conducting multiple stochastic forward passes (n = 50 iterations per sample) and activating dropout layers during inference. Rather than generating a single point estimate, each forward pass generated slightly different predictions.

```python
class MCDropout(nn.Module):
    """Monte Carlo Dropout for uncertainty estimation"""

    def __init__(self, p=0.3):
        super(MCDropout, self).__init__()
        self.p = p

    def forward(self, x):
        # Always apply dropout (even during inference for MC sampling)
        return F.dropout(x, p=self.p, training=True)
```

Figure 15: Monte Carlo implementation - MCDropout class enabling uncertainty estimation through stochastic forward passes during inference.

Table 3: Summary of statistical tools used

Tool Category	Library/Function	Application
Performance Metrics	Sklearn.metrics	Accuracy_score, f1_score, classification_report
Cross-Validation	Sklearn.model_selection	StratifiedKFold, cross_val_score
Statistical Tests	Scipy.stats	Mcnemar, tttest_rel
Preprocessing	Sklearn.preprocessing	StandardScaler, MinMaxScaler, PCA
Class Balance	Sklearn.utils	Compute_class_weight

Uncertainty	Custom MCDropout	Predictive entropy, confidence
Interpretability	SHAP v0.48.0	DeepExplainer, summary_plot
Clustering	Sklearn.cluster	KMeans, NearestNeighbours

3.5.6. Explainable Artificial Intelligence (XAI) Framework

The interpretability of hybrid deep learning models represents a critical requirement for biological applications, particularly in regenerative medicine where model predictions must align with established biological knowledge. This study implements a comprehensive XAI framework combining multiple interpretability approaches to ensure biological validity and translational relevance of computational predictions.

Deep Learning Interpretability: The primary interpretability approach employed SHAP (SHapley Additive exPlanations) framework v0.48.0, specifically utilizing DeepExplainer for neural network architectures. SHAP provides both global feature importance across the entire dataset and local explanations for individual predictions, enabling comprehensive understanding of model decision-making processes.

Implementation Strategy: SHAP analysis(shown in figure 16) was applied to both individual models (GNN, RNN) and hybrid architectures, providing comparative interpretability assessment across different modelling approaches. The framework calculated SHAP values for all input features, enabling identification of the most influential genes and spatial relationships driving differentiation predictions.

```python
def compute_shap_values(self, gnn_embeddings, rnn_embeddings, max_samples=100):
    """Compute SHAP values for feature importance"""
    logger.info("Computing SHAP values for feature importance analysis...")

    # Concatenate embeddings for SHAP analysis
    combined_data = np.concatenate([gnn_embeddings, rnn_embeddings], axis=1)

    # Limit samples for computational efficiency
    if len(combined_data) > max_samples:
        indices = np.random.choice(len(combined_data), max_samples, replace=False)
        combined_data = combined_data[indices]

    # Create prediction function
    predict_fn = self.create_prediction_function()

    # Use a subset as background for SHAP
    background_size = min(50, len(combined_data) // 2)
    background = combined_data[:background_size]

    # Initialize SHAP explainer
    explainer = shap.KernelExplainer(predict_fn, background)

    # Compute SHAP values
    sample_size = min(20, len(combined_data) - background_size)
    test_data = combined_data[background_size:background_size + sample_size]

    shap_values = explainer.shap_values(test_data)

    logger.info(f"SHAP values computed for {sample_size} samples")
    logger.info(f"Shape: {len(shap_values)} classes × {sample_size} samples × {combined_data.shape[1]} features")

    return {
        'shap_values': shap_values,
        'test_data': test_data,
        'background': background,
        'feature_names': [f'GNN_f{i}' for i in range(gnn_embeddings.shape[1])] +[f'RNN_f{i}' for i in range(rnn_embeddings.shape[1])]
    }
```

Figure 16: SHAP-based explainable AI suite providing feature importance analysis, uncertainty quantification, and biological pathway mapping for cardiac differentiation predictions.

3.6.VALIDITY, RELIABILITY, AND TRUSTWORTHINESS

3.6.1. Model Validation strategy

A multi-tiered testing approach was employed to rigorously validate the hybrid GNN–RNN model. This included unit testing for individual neural network components, integration testing to evaluate the fusion strategy, and end-to-end pipeline validation to ensure overall system reliability.

To evaluate stability and convergence, cross-validation variance analysis was performed to identify potential model instability, while learning curve assessments were used to monitor optimization dynamics and detect convergence patterns. An enhanced validation framework continuously monitored training–validation performance gaps, providing an additional safeguard against overfitting. Regularization strategies were systematically implemented, including Monte Carlo dropout (drop probability = 0.3) for uncertainty quantification, L2 weight decay (λ = 1e–4) for parameter constraint, and early stopping triggered by validation loss plateauing for 15 consecutive epochs. Together, these measures ensured robust generalization to unseen cardiomyocyte differentiation data while maintaining the biological interpretability of spatial and temporal gene expression dynamics.

Internal validity is ensured by rigorous cross-validation protocols designed specifically for biomedical machine learning applications. The 5-fold stratified cross-validation approach addresses class imbalance challenges while providing robust performance estimates with confidence intervals generated through bootstrap procedures.

External validity is established through the utilisation of well-characterised public datasets with established biological relevance and technical quality. The datasets allow for the generalisation of computational findings across various cardiomyocyte differentiation systems since they represent diverse biological contexts and experimental conditions.

Construct validity is maintained through systematic biological validation of computational predictions using established cardiac gene databases and pathway analysis. To ensure that mode predictions reflect genuine biological relationships rather than statistical artefacts, the explainable AI framework offers interpretable insights that align with established biological mechanisms.

Biological validation framework incorporates comprehensive cardiac gene database mapping, linking computational features to established markers including ISL1 (cardiac progenitor marker), NKX2-5 (master cardiac regulator), GATA4 (cardiac progenitor specification), MEF2C (cardiac muscle development), and TBX5 (cardiac chamber development). This methodological approach identifying novel regulatory mechanisms while ensuring that model discoveries align with established cardiac developmental biology.

3.6.2. Reliability and Reproducibility Measures

Technical reliability is achieved through version-controlled software implementations, documented computational approaches, and standardised preprocessing pipelines. All analyses utilise established software packages with validated algorithms, including scikit-learn[342] for machine learning validation, scanpy[343] for spatial transcriptomic analysis, and PyTorch[344] for deep leaning. Reproducibility measures include comprehensive documentation of computational procedures, public GitHub repository availability (https://github.com/Tumo505/HybridGnnRnn), standardised random seeds (seed = 42) for deterministic results across all stochastic operations, and detailed hyperparameter specifications enabling exact replication of all analyses.

Biological reliability is ensured through using established datasets with peer-reviewed validation and documented quality control procedures. By integrating multiple data modalities, the risk of platform-specific artefacts or technical biases is reduced, and biological findings are validated orthogonally.

Reproducibility measures include comprehensive documentation of computational procedures, public availability of analysis code, standardised random seeds for deterministic results, and detailed parameter specifications enabling replication of all analyses. The approach complies with established guidelines for reproducible computational biology research.

3.6.3. Bias Mitigation Strategies

Selection bias is minimised by using representative public datasets that capture diverse biological conditions and experimental contexts. Numerous cardiomyocyte subtypes and differentiation trajectories are included in the datasets, ensuring coverage of pertinent biological variation. By systematically comparing multiple modelling approaches and fusion strategies, confirmation bias is mitigated and an excessive dependence on single methodological approach is avoided. The explainable AI framework provides objective assessment of model predictions against established biological knowledge.

Technical bias mitigated through comprehensive preprocessing approaches, such as batch effect correction, normalisation standardisation, and quality control filtering. Procedures for cross-validation ensures overfitting or data leakage don't inflate performance estimations. The comprehensive validation framework ensures reliable findings that can inform further ethical considerations and practical applications.

3.7.COMPUTATIONAL INFRASTRUCTURE

All analyses were conducted on a high-performance workstation equipped with:

CPU: Intel Core Ultra 9 275HX (2.70GHz, 20 cores)

GPU: NVIDIA RTX 5070 TI with 12GB VRAM

RAM: 64GB DDR5 systems memory

Storage: 2TB NVMe SSD for data preprocessing

Training efficiency was achieved through mixed-precision training, gradient checkpointing, and optimising memory management. Total execution time averaged 3.5-5 hours, with individual model training requiring 1.5 hours (GNN) and 25 minutes (RNN), while hybrid fusion training complete within 45 minutes using pre-trained embeddings. The methodology requires a minimum of 8GB GPU VRAM, 16GB system RAM, and 50GB storage space, with recommended specifications of 12GB+ GPU VRAM and 32GB+ system RAM for optimal performance.

3.8.ETHICAL CONSIDERATIONS

3.8.1. Computational Ethics Framework and Institutional Compliance

This study adheres to the established guidelines of ethical computational biology research, emphasising responsible AI development and transparent reporting of methodological procedures and limitations. Ethics clearance was obtained from University of South Africa's College of Science, Engineering, and Technology, School of Engineering Ethics Review Committee (ERC), confirming compliance with institutional ethical standards for computational research utilising publicly available datasets.

Proper attribution of original data sources, adherence to data sharing agreements and usage terms, and a commitment to reproducible research practices that enable scientific validation. All datasets utilized are publicly available under appropriate licensing agreements that permit computational analysis and derivative works, with full attribution provided to original authors and institutions. The spatial transcriptomics dataset (Kuppe et al.) was collected following ethics approval of human tissue protocols by the ethics committee of the Ruhr University Bochum in Bad Oeynhausen, the RWTH Aachen University, Utrecht University and WUSTL (no. 220-640, EK151/09, 12/387 and no. 201104172 respectively), and the human heart tissue was approved by the scientific advisory board of the biobank of the University Medical Centre Utrecht, The Netherlands (protocol no.12/387). In conducting this study, Kuppe et al. (2022) states that all patients provided informed consent and the study was performed in accordance with the Declaration of Helsinki. The temporal differentiation datasets (Elorbany et al.) used data that was initially collected by Elorbany et al. (2022) from the NHGRI Sample Repository for Human Genetic Research at the Coriell Institute for Medical Research with written informed consent and with IRB approval. The genetic data used by Elorbany et al. (2022) was previously made available through the International HapMap Project[345].

The development of interpretable and explainable models that offer biological insights rather than opaque predictions. By using explainable AI techniques, algorithmic decision-making processes remain transparent and computational predictions may be validated against established biological knowledge and translated into experimental hypotheses.

3.8.2. Research Integrity and Transparency

Extensive evaluation of computational results against established biological knowledge, open reporting of both positive and negative results, and meticulous documenting of all methodological steps all contribute to the preservation of scientific integrity. The study complies with established standards for open science and computational reproducibility. Transparency measures include detailed methodology documentation, publicly available analysis code and protocols, comprehensive reporting of model performance and limitations, and clear attribution of all data sources and software dependencies. All computational procedures are documented with sufficient detail to enable independent replication and validation

3.8.3. FAIR Principles for Data and Code handling

All datasets and code developed in this study were curated and documented following the FAIR principles[346] (Findable, Accessible, Interoperable, Reusable). Datasets are annotated with persistent identifiers like GEO accession codes to ensure findability. Preprocessing pipelines and trained models are deposited in a public GitHub repository (https://github.com/Tumo505/HybridGnnRnn) and deposited to Zenodo[347] and assigned a digital object identifier (doi) (https://doi.org/10.5281/zenodo.17196578), making them accessible to the research community. Standardized file formats including HDF5 for transcriptomics and CSV for metadata ensures interoperability across bioinformatics tools. Reproducibility is reinforced

through comprehensive documentation, including data dictionaries, usage instructions, and detailed metadata, enabling reusability in related studies.

3.9.LIMITATIONS AND ASSUMPTIONS

3.9.1. Methodological Limitations

The study's reliance on publicly available datasets, which might not fully represent the full diversity of cardiomyocyte differentiation processes or experimental settings, constitutes a fundamental limitation. While the selected datasets are biologically relevant, they only reflect specific experimental contexts that might not apply to other differentiation protocols or cell lines.

Computational constraints limit the scope of architectural exploration and hyperparameter optimization. The focus on GNN-RNN hybrid architectures, while scientifically justified, excludes other potentially valuable approaches such as transformer-based architectures or more complex ensemble methods. These constraints were managed through systematic optimization strategies and efficient resource utilisation but may limit exploration of alternative computational approaches.

Integrating heterogeneous data type with different resolutions, sampling techniques, and technical attributes comes with integration challenges. While these issues are addressed by computational alignment processes, achieving perfect consistency between spatial and temporal samples is a challenge, which could introduce systematic biases in fusion strategies. The spatial modality used in this study derives from adult human myocardial infarction tissue profiled by spatial transcriptomics (Visium spot-level measurements), whereas the temporal modality derives from in vitro iPSC-derived cardiomyocyte differentiation profiled by time-course single-cell RNA sequencing. These modalities are not experimentally paired, and the integration relies on similarity-based computational alignment. Consequently, the performance of multimodal fusion may partially reflect the quality of alignment rather than direct biological correspondence between the two experimental systems. Though this study showed strong generalisation that was also complemented by 5-fold cross-validation, broad generalisation can be extended by external validation on paired spatiotemporal differentiation datasets (or additional harmonisation studies).

3.9.2. Biological Assumptions and Impact Assessment

Transcriptome sufficiency is predicted on the assumption that spatial relationships represented in transcriptome analysis correlate to biological interactions that are functionally relevant and that gene expression data capture the key regulatory mechanisms governing differentiation efficiency. Future multi-omics integration approaches may be required to complement the transcriptome data to capture critical regulatory mechanisms (e.g., post-translational modifications and epigenetic factors), which could understate differentiation complexity.

Pattern conservation assumes that spatiotemporal patterns identified through computational analysis represent conserved biological mechanisms that generalise across experimental

conditions and biological contexts. The translational applicability of computational results may be limited, necessitating validation across several experimental settings.

Model interpretability assumes that explainable AI approaches provide biologically meaningful insights and that attention mechanisms and feature importance scores correspond to genuine biological regulatory mechanisms rather than statistical artefacts. Model explanations may mislead biological interpretation if these presumptions prove incorrect, necessitating further experimental approaches.

3.9.3. Generalisability Considerations

While the emphasis on well-established technologies with proven reliability mitigates this limitation, platform specificity may restrict generalisation across various spatial transcriptomics technologies or single-cell RNA sequencing platforms. To ensure broader applicability, future research should validate findings across a variety of technical platforms.

Though this focus ensures clinical relevance and translational potential, biological scope is deliberately restricted to human iPSC-derived cardiomyocyte differentiation, potentially limiting applicability to other cardiac cell type or alternative differentiation approaches. Methodological adjustments and further validation processes might be necessary for extensions to different cell type or species.

Limitations in temporal resolution may prevent capture of rapid regulatory events or fine-grained temporal dynamics, potentially missing critical differentiation checkpoints that occur between measured time points. Studies with a higher temporal resolution might uncover more regulatory mechanisms that aren't included in the current analyses.

These methodological considerations lay groundwork for future study initiatives while offering context for interpreting the findings.

3.10. SUMMARY

This methodology presents a comprehensive framework for developing and evaluating hybrid deep learning architectures for spatiotemporal analysis of cardiomyocyte differentiation. To ensure both technical excellence and biological relevance, the approach combines rigorous computational methods with systematic biological validation.

While maintaining focus on interpretability and translational potential, the four-phase methodology (individual model development, embedding extraction and fusion, hybrid model training and evaluation, and XAI framework implementation) allows for a systematic comparison of modelling approaches. By combining well-established datasets, proven computational methods, and extensive validation processes, this study offers a strong basis for developing computational approaches in regenerative medicine.

Key methodological contributions include a novel systematic comparison of fusion strategies for spatiotemporal biological data, comprehensive XAI framework for biological interpretation, and

rigorous validation procedures ensuring reproducibility and biological relevance. Through targeted analytical components, the methodology addresses all four research questions while maintaining scientific integrity and ethical compliance.

Validation processes and computational infrastructure ensure reliable results that can be reproduced on different hardware configurations, while biological validation frameworks offer assurance regarding translational applicability. Comprehensive evaluation of hybrid modelling approaches for biological prediction tasks is made possible by the combination of multiple data modalities and fusion strategies.

The next chapter presents the detailed results of this methodological framework, demonstrating the effectiveness of hybrid spatiotemporal modelling in achieving superior prediction accuracy while providing biologically interpretable insights into cardiomyocyte differentiation processes. The systematic evaluation of fusion strategies and comprehensive performance assessment will establish new benchmarks for computational approaches in cardiac regenerative medicine while providing actionable insights for experimental protocol optimisation. Results will be

The next chapter will present the detailed results of this methodological framework, demonstrating the effectiveness of hybrid spatiotemporal modeling in achieving superior prediction accuracy while providing biologically interpretable insights into cardiomyocyte differentiation processes. The systematic evaluation of fusion strategies and comprehensive performance assessment will establish new benchmarks for computational approaches in cardiac regenerative medicine while providing actionable insights for experimental protocol optimization. Results will be presented in four corresponding sections: individual model performance, fusion strategy comparison, biological interpretation through explainable AI, and validation against established cardiac developmental pathways.

4. CHAPTER 4: RESULTS

4.1.INTRODUCTION

This chapter presents comprehensive results from the hybrid GNN-RNN architecture developed to predict cardiomyocyte differentiation efficiency outcomes (high vs low efficiency). The analysis includes evaluation of single-modality baselines, comparison of multimodal fusion strategies, explainable AI (XAI) assessment, and uncertainty/robustness analyses.

The results follow the same logical order as the research questions in chapter 1. Section 4.2 addressees research question 1 by evaluating unimodal spatial and temporal models; section 4.3 addresses research questions 2-3 by testing whether multimodal integration improves predictive performance and by comparing fusion strategies; section 4.4 addresses research question 4 by assessing whether the model highlights biologically credible cardiac regulators and pathways; and section 4.5 reports uncertainty quantification and robustness analyses. Where this chapter contextualises results against prior studies, such comparisons are discussed as indicative, because direct ranking across papers requires the same datasets, target definitions, and evaluation protocol.

4.2.INDIVIDUAL MODEL PERFORMANCE ANALYSIS

4.2.1. Spatial Graph Neural Network

The spatial GNN component, designed to capture spatial relationships within tissue sections, achieved moderate performance when evaluated independently. The model architecture is made up of Graph Convolutional Networks (GCN) and Graph Attention Networks (GAT), processing 752 tissue spots with 2,000 highly variable genes per spot.

Architecture Performance: The enhanced cardiomyocyte GNN achieved an accuracy of 65.29% with an F1-score of 64.12% across 5 cardiomyocyte subtypes. Training progressed over 81 epochs before early stopping, with the best validation accuracy reaching 69.88%. The model successfully captured spatial neighbourhood relationships, demonstrating the ability of graph-based approaches to model tissue organisation patterns.

Spatial Relationship Modelling: By using attention mechanisms to highlight important tissue regions that influence classification of cardiomyocyte classification subtypes, the GNN successfully identified spatial domains within cardiac tissue sections. Spatial attention visualisations revealed that the model focused on boundaries between different cardiac regions, consistent with established spatial organisation patterns in cardiac development. The comparatively low performance implies that multimodal integration is required for accurate cardiomyocyte classification, as spatial information alone does not offer enough discriminative power.

4.2.2. Temporal Recurrent Neural Network

The temporal RNN component demonstrated exceptional performance in modelling sequential gene expression changes during cardiomyocyte differentiation. The BiLSTM architecture with

attention mechanisms processed 800 temporal samples across 10 time points, representing 4 distinct differentiation trajectories.

Temporal Performance: The temporal cardiac BiLSTM achieved remarkable results with a test accuracy of 96.88% and F1-score of 96.67%. Training efficiency was notable, requiring only 28 epochs before early stopping with a final validation loss of 0.099. Excellent model convergence without overfitting is indicated by the low generalisation gap of 3.12% between training (100%) and validation (96.88%) accuracy.

Temporal Pattern Recognition: The model excelled at capturing sequential dependencies in gene expression trajectories, with attention weights revealing critical developmental checkpoints during cardiomyocyte differentiation. Both forward and backward temporal relationships were successfully modelled using the BiLSTM architecture, allowing for a comprehensive understanding of differentiation dynamics. The robustness of temporal modelling approaches was confirmed by cross-validation results, which demonstrated consisted performance across different data splits (mean accuracy 88.4% ± 4.2%).

Biological Validation: The high performance of the RNN component aligns with recent advances in temporal biological sequence analysis, where RNN architectures have shown superior capability in modelling cellular differentiation processes. The biological relevance of computational predictions was validated by the attention mechanism's successful identification of time-dependent expression patterns that correspond to known cardiac development developmental stages.

4.3.FUSION STRATEGY PERFORMANCE COMPARISON

4.3.1. Comprehensive Fusion Strategy Evaluation

To determine the optimal approach for combining spatial and temporal modalities, three distinct fusion strategies we systematically implemented and evaluated. Each strategy demonstrated unique advantages in terms of performance, interpretability, and computational efficiency, table 4 shows the results overview of this strategy.

Table 4: Overview of fusion strategy results.

Strategy	Accuracy	F1-Score	Precision	Recall	Training Time	Key Advantage
Ensemble	96.67%	96.61%	97.22%	95.83%	45 min	Best overall performance
Attention	86.67%	86.67%	85.42%	85.42%	62 min	Dynamic feature weighting
Concatenation	80.00%	79.11%	81.25%	77.08	38 min	Computational efficiency

4.3.2. Ensemble Fusion Strategy: Best Performance

The ensemble fusion strategy achieved the highest performance across all evaluation metrics, demonstrating the effectiveness of late fusion approaches in biological applications. Weighted predictions from individual GNN and RNN models were integrated in the ensemble approach, with learnable weights optimising each modality's contribution.

Statistical Significance: McNemar's test confirmed statistically significant improvement of the ensemble fusion strategy over individual models ($p < 0.001$), with paired t-tests demonstrating significant performance gains across multiple evaluation metrics. The ensemble fusion achieved 96.67% accuracy under the evaluation protocol described in chapter 3, any comparison to previously published state-of-the-art approaches is interpreted as indicative, because direct comparability requires the same datasets, target definitions, and validation protocols.

4.3.3. Attention-Based Fusion Strategy

Using dynamic attention weights, the attention fusion approach improved interpretability while achieving balanced performance with 86.67% accuracy. To learn optimal feature combinations across temporal and spatial modalities, this method used multi-head attention mechanisms.

Dynamic Weighting Analysis: Attention weights revealed differential importance of spatial versus temporal features across different differentiation stages. Early differentiation stages demonstrated higher attention to temporal features (70% temporal, 30% spatial), while mature stages demonstrated increased spatial attention (60% temporal, 40% spatial), reflecting the increasing importance of tissue organisation.

Interpretability Advantages: The attention mechanism provided valuable insights into modality importance across different biological contexts. Visualisation of attention patterns revealed that temporal features dominated during early differentiation phases when gene expression dynamics drive lineage commitment, while spatial features became increasingly important during maturation phases when tissue organisation and cell-cell interactions determine functional properties.

4.3.4. Concatenation Fusion Strategy

While the concatenation approach had the lowest accuracy (80.00%), it was the most computationally efficient and required least amount of training time (38 minutes). This early fusion approach directly combines temporal and spatial embedding prior to final classification.

Computational Efficiency: The concatenation was suitable for resource-constrained environments as it required minimal additional parameters and computational overhead. However, the model's ability to adaptively weight various modalities based on biological context was limited by the rigid feature combination.

Performance Limitations: Concatenation fusion's poorer performance indicates that simple feature combination is not sufficient for biological applications' optimal multimodal integration.

Complex interactions between spatial and temporal modalities that are better modelled by more advanced fusion approaches were not captured by this method.

4.4.EXPLAINABLE AI FRAMEWORK RESULTS

4.4.1. SHAP-Based Feature Importance Analysis

The explainable AI framework successfully identified biologically relevant features driving model predictions, providing crucial validation of computational results against established cardiac biology. A total of 640 features (128 GNN + 512 RNN) with significant contributions to differentiation classification.

Top discriminative biological features:

i. PLN (Phospholamban) – SHAP importance: 0.0038
   - Biological significance: critical calcium handling protein essential for cardiac excitation-contraction coupling
   - Developmental stage: functional cardiomyocyte maturation
   - Validation: PLN upregulation correlates with mature cardiomyocyte phenotypes, confirming model accuracy.

ii. FKBP1A (FK506 Binding protein 1A) – SHAP importance: 0.0028
   - Biological significance: regulatory protein modulating ryanodine receptor function in calcium homeostasis
   - Developmental roles: essential for functional cardiac development
   - Clinical relevance: target for cardiac therapeutics and differentiation optimisation

iii. MYL2 (Myosin Light Chain 2) – SHAP importance: 0.0025
   - Biological significance: cardiac-specific structural protein essential for muscle contraction
   - Developmental marker: Late-stage differentiation indicator
   - Experimental validation: MYL2 expression serves as established cardiomyocyte maturation marker.

Temporal Feature Dynamics: SHAP analysis identified 154 temporal features with importance scores ranging from 0.002-0.006, revealing stage-specific expression trajectories that align with known cardiogenesis pathways. The model demonstrated the biological validity of predictions by accurately capturing the temporal expression dynamics of key cardiac structural proteins and transcription factors.

4.4.2. Biological Pathway Validation

Cardiac Gene Database Integration: Feature importance mapping to established cardiac gene databases revealed significant enrichment in critical developmental pathways:

i. Calcium Signalling Pathway ($p < 0.001$): PLN and FKBP1A identification confirms model sensitivity to calcium for cardiac function.

ii. Cardiac Muscle Development ($p < 0.01$): MYL2 and associated structural proteins highlight morphological maturation processes.
iii. Temporal Gene Expression ($p < 0.05$): 154+ temporal features demonstrate comprehensive capture of differentiation dynamics.

Literature Concordance: 89% of the top-ranked features in the model matched known cardiac biomarkers or developmental regulators, demonstrating a high degree of agreement between the model's predictions and the body of published cardiac development research. This congruence implies the potential of discovering new regulatory mechanisms and gives assurance regarding the biological importance of computational results.

4.4.3. Attention Mechanism Visualisation

Spatial Attention Patterns: GNN attention weights mapped to tissue coordinates revealed critical spatial domains influencing cardiomyocyte classification. The model focused attention on boundary regions between different cardiac tissue types, consistent with known patterns of cellular specification and maturation gradients in cardiac development.

Temporal Attention Analysis: RNN attention mechanisms highlighted key time points during differentiation that most strongly influenced final outcomes. Days 7 – 10 of differentiation saw the highest attention, which corresponded to crucial lineage commitment checkpoints found in experimental studies. The model's ability to identify developmental transitions with biological significance is validated by this temporal attention pattern.

4.5.MODEL VALIDATION AND UNCERTAINTY QUANTIFICATION

4.5.1. Cross-Validation and Statistical Analysis

Robust Cross-Validation Results: Five-fold stratified cross-validation provided comprehensive performance assessment with mean accuracy of 88.4% ± 4.2% and stability score of 94.3%, indicating low variance across different data splits. Bootstrap confidence intervals (95% CI: [86.1%, 90.7%]) confirmed robust performance estimates with statistical significance.

Statistical Significance Testing: Paired t-tests verified significant performance gains across multiple evaluation metrics, and McNemar's test demonstrated statistically significant improvements of hybrid models over individual modalities ($p < 0.001$). The statistical rigor ensures that reported improvements represent genuine advances rather than random variation.

4.5.2. Monte Carlo Dropout Uncertainty Quantification

Uncertainty Analysis Framework: Monte Carlo Dropout analysis with 50 forward passes provided comprehensive uncertainty quantification for model predictions. The approach generated prediction distributions enabling confidence interval calculation and identification of high-uncertainty samples requiring additional validation. The uncertainty metrics are outlined in table 5.

Table 5: Uncertainty metrics by fusion strategy

Strategy	Mean Confidence	Mean Entropy	Uncertainty Range	Reliability Indicator
Ensemble	78.82%	0.545	[19.2%, 98.5%]	High confidence correlates with accuracy
Attention	91.66%	0.263	[15.5%, 99.8%]	Most confident predictions
Concatenation	88.23%	0.317	[1.4%, 99.7%]	Moderate confidence range

Predictive Reliability: High confidence predictions (>90%) correlated with 100% accuracy across all fusion strategies, while borderline cases (40 – 70% confidence) effectively identified transition states between differentiation stages. Predictive entropy <0.3 indicated highly reliable predictions suitable for clinical applications.

4.5.3. Comparative Performance Analysis

The hybrid GNN-RNN architecture achieved superior performance compared to established baselines across multiple categories:

- vs. Best GNN (PNA)[348]: +13.47% accuracy improvement, demonstrating advantages of multimodal integration.
- vs. Best RNN (Transformer): +5.47% accuracy gain, highlighting effectiveness of domain-specific architectures.
- vs. Biological models (scGPT)[349]: +6.97% improvement, confirming task-specific optimisation benefits.
- vs. Temporal Graph Networks[350]: +22.07% enhancement, validating hybrid approach superiority.

Competitive Advantages: The hybrid architecture demonstrated key advantages over single-modality approaches: superior temporal dynamics handling compared to graph-only methods, enhanced spatial relationship modelling versus sequence-only approaches, and more efficient parameter usage compared to transformer-based architectures while maintaining comparable performance.

4.5.4. Computational Performance Scalability

Training Efficiency: Computational analysis on NVIDIA RTX 5070 Ti hardware revealed optimised training performance:

- Total pipeline execution: 3.5-4 hours end-to-end
- Individual model training: 1.5 hours (GNN), 25 minutes (RNN)
- Hybrid fusion training: 45 minutes using pre-trained embeddings

- Memory utilisation: Peak 4.8GB during training, 2.1GB inference

Inference Performance: With a throughput of 1,300 samples/second and a prediction time of 12.3 ms per sample, the optimised architecture demonstrated rapid inference that is suitable for real-time applications in clinical and research settings. Batch processing capabilities enabled efficient analysis of large datasets while maintaining prediction accuracy.

4.5.5. Ablation Study Results

Component Contribution Analysis: Systematic ablation studies quantified the contribution of individual architectural components:

Table 6: Ablation study summary explaining which model components are critical and how much they contribute to performance.

Component Removed	Accuracy Impact	Performance Loss	Critical Function
Attention mechanism	-7.47%	Reduced fusion quality	Dynamic feature weighting
Uncertainty quantification	-2.57%	Less robust predictions	Confidence estimation
Regularisation	-5.37%	Overfitting issues	Model generalisation
Multimodal integration	-8.47%	Information loss	Complementary data fusion

Fusion Strategy Impact: The ensemble approach consistently outperformed alternative strategies, with attention-based fusion providing optimal balance between performance and interpretability. Despite being computationally efficient, concatenation fusion demonstrated insufficient complexity for optimal biological data integration.

4.6.CLINICAL TRANSLATION AND BIOLOGICAL VALIDATION

4.6.1. Translational Potential Assessment

Applications for Drug Development: The identified biomarkers, PLN, FKBP1A, and MYL2, represent potential therapeutic targets for cardiac regeneration, and computational predictions offer a systematic screening capabilities for compound effects on cardiomyocyte differentiation. The model's capacity to predict differentiation outcomes enables automated quality control for cell therapy applications.

Implementation of Regenerative Medicine: Real-time monitoring enables process optimisation and quality assurance, while automated cardiomyocyte maturation assessment capabilities support standardisation of differentiation protocols across laboratories. The 96.67% accuracy provides sufficient reliability for clinical decision support applications.

4.7.SUMMARY

The efficacy of hybrid GNN-RNN architectures for cardiomyocyte differentiation classification is demonstrated by this comprehensive results analysis, which achieved state-of-the-art performance of 96.67% accuracy though optimal ensemble fusion strategies. Confidence in the translational relevance of computational predictions is provided by the successful identification of biologically relevant biomarkers (PLN, FKBP1A, and MYL2) that align with established cardiac developmental pathways, providing confidence in the translational relevance of computational predictions.

Key Achievements: The hybrid approach outperforms current single-modality approaches by significant margins by effectively combining temporal differentiation dynamics with spatial tissue organisation modelling. Reliable clinical translation is enabled by Monte Carlo Dropout's quantification of uncertainty, and comprehensive statistical validation validates the durability of performance improvements.

Biological Validation: To demonstrate that computational predictions represent actual biological mechanisms rather than statistical artefacts, SHAP-based interpretability analysis identified biologically significant traits that correlate to known cardiac development regulators. The model's capacity to represent important facets of cardiomyocyte maturation is confirmed by the identification of structural markers and calcium handling proteins.

Clinical Impact: The combination of high accuracy (96.67%), biological interpretability, and uncertainty quantification positions this approach for clinical applications in regenerative medicine, drug development, and therapeutic screening. The framework offers a robust basis for automated cardiomyocyte assessment with translational potential for improving cardiac cell therapy outcomes.

5. CHAPTER 5: DISCUSSION

5.1.INTRODUCTION

This chapter provides a comprehensive discussion of the research findings within the broader context of computational biology, regenerative medicine, and cardiac development. The hybrid GNN-RNN architecture developed in this study achieves state-of-the-art performance while retaining biological interpretability, marking a substantial leap in spatiotemporal modelling of cardiomyocyte differentiation. The discussion examines the implications of these findings, addresses methodological considerations, explores limitations, and outlines future directions for advancing computational approaches in cardiac regenerative medicine.

The discussion is organised into six key sections: interpretation of major findings and their significance for the field (section 5.2), methodological contributions and innovations (section 5.3), biological validation and clinical implications (section 5.4), study limitations and methodological considerations (section 5.5), future directions and research opportunities (section 5.6), and concluding remarks on the translational potential of this work (section 5.7).

5.2.INTERPRETATION OF MAJOR FINDINGS

5.2.1. Superior Performance Through Multimodal Integration

The hybrid GNN-RNN architecture achieved exceptional performance with 96.67% accuracy, representing a substantial improvement over existing approaches and demonstrating the transformative potential of multimodal integration in biological sequence analysis. With improvements of +13.47% over the best GNN approaches, +5.47% over transformer architectures, and +5.67% over specialised biological models, this performance significantly outperforms the current state-of-the-art methods. The magnitude of these improvements suggests that spatiotemporal integration addresses fundamental limitations in current computational approaches to cardiomyocyte differentiation prediction.

The success of the ensemble fusion strategy, which achieved the highest performance across all metrics, validates the hypothesis that complementary information from spatial tissue organisation and temporal differentiation dynamics can be effectively combined to enhance prediction accuracy. This result aligns with recent advances in machine learning for cardiovascular applications, where multimodal approaches have outperformed single-modality approaches. Robust performance across various stages of differentiation is indicated by the ensemble approach's ability to maintain high precision (97.22%) and excellent recall (95.83%). This is particularly crucial for clinical applications that require reliable classification of immature versus mature cardiomyocytes.

5.2.2. Biological Interpretability and Validation

To validate the computational predictions against known biological mechanisms, the explainable AI framework successfully identified biologically relevant features that align with established cardiac development biology. Phospolamban (PLN), FKBP1A (FK506 binding protein 1A), and

myosin light chain 2 (MYL2) were identified as the most discriminative features, indicating that the model can capture real biological signals instead of statistical artefacts.

Calcium Handling Pathway Significance: The relevance of calcium homeostasis in cardiomyocyte maturation is reflected in the prevalence of calcium handling proteins (PLN, FKBP1A) in model predictions. PLN regulation of SERCA2a activity and FKBP1A modulation of ryanodine receptors represent fundamental mechanisms distinguishing mature from immature cardiomyocyte. The model's translational relevance is reinforced by this biological validation, which also raises the potential for identifying noel therapeutic targets for cardiac regeneration.

Structural Protein Networks: The discovery of MYL2 as a discriminative feature is consistent with the established knowledge of sarcomeric proteins throughout cardiomyocyte maturation. The approach's relevance for evaluating cardiomyocyte quality in regenerative medicine applications is supported by the model's ability to capture structural protein networks, indicating comprehensive understanding of the morphological alterations that accompany functional maturation.

5.2.3. Uncertainty Quantification and Clinical Translation

The Monte Carlo Dropout analysis provided robust uncertainty quantification, with high-confidence predictions (>90%) correlating perfectly with classification accuracy across all fusion strategies. This finding addresses a significant limitation in existing computational methodologies, wherein prediction uncertainty is rarely assessed despite its significance in clinical decision-making. By identifying borderline cases that indicate transition states between differentiation stages, the entropy-based confidence scoring offers crucial biological insights into developmental checkpoints.

Clinical Decision Support: Clinically relevant stratification is enabled by the relationship between prediction accuracy and confidence, where high-confidence predictions can inform automated quality control decisions while uncertain cases are flagged for additional validation. This capability addresses the regulatory requirements for AI-based medical devices, where uncertainty quantification is increasingly being recognised as an essential component for clinical implementation.

5.3.METHODOLOGICAL CONTRIBUTIONS AND INNOVATIONS

5.3.1. Novel Fusion Strategy Development

Three fusion strategies – concatenation, attention, and ensemble – are systematically compared to offer important insights into the best practices for multimodal data integration. Given ensemble fusion's superior performance, late fusion strategies, which preserve modality-specific information until final decision-making, appear to be better suited for biological applications than early fusion strategies, which risk losing significant model-specific patterns.

Attention Mechanism Insights: Through dynamic weighting of spatial versus temporal features, the attention-based fusion approach offered valuable interpretability despite achieving a lower overall accuracy of 86.67%. The discovery that spatial features became more significant during maturation (60% temporal, 40% spatial), while temporal features dominated early differentiation stages (70% temporal, 30% spatial), provides biological insights into how relative importance of various regulatory mechanisms changes during cardiomyocyte development.

5.3.2. Statistical Validation Framework

By combining multiple statistical validation approaches, including bootstrap confidence intervals, paired t-tests, and McNemar's tests, new benchmarks for thorough assessment of computational biology models are established. The statistically significant improvements ($p < 0.001$) across multiple evaluation metrics provide confidence that observed performance gains represent genuine advances rather than random variation. In addition to addressing concerns about reproducibility in computational biology research, this methodological rigour offers a template for future validation studies.

Cross-Validation Robustness: With low variance indicating model stability, the 5-fold stratified cross-validation results show consistent performance across various data splits (mean accuracy: 88.4% ± 4.2%). For biological applications, where dataset heterogeneity can significantly impact model generalisation, this robustness is particularly crucial.

5.3.3. Explainable AI Framework Integration

An important methodological advancement in interpretable machine learning for biology is the comprehensive XAI framework that combines biological pathway mapping, attention visualisation, and SHAP analysis. The ability to identify potentially novel biomarkers and map computational predictions to established cardiac gene databases helps to close the gap between biological validation and computational discovery.

The framework's ability to offer detailed insights into differentiation dynamics is demonstrated by the identification of 154 temporal features with biologically meaningful importance scores. While exposing possible novel regulatory mechanisms worthy of experimental investigation, the alignment of these features with established cardiac development timelines validates the XAI approach.

5.4.BIOLOGICAL VALIDATION AND CLINICAL INPLICATIONS

5.4.1. Cardiac Development Pathway Alignment

With 89% of the top-ranked features matching known cardiac biomarkers or developmental regulators, the computational predictions demonstrated good agreement with established literature on cardiac development. While indicating that the remaining 11% of features might represent novel regulatory mechanisms needing experimental validation, this high concordance rate gives confidence in the biological validity of discoveries.

Transcription Factor Networks: The model's identification of key cardiac transcription factors and the pattern of their temporal expression is consistent with established knowledge on the regulatory networks of cardiac genes. The approach's biological relevance is proven by the capture of the NKX2-5, GATA4, and TBX5 regulatory cascades, which also shows promise in discovering novel transcriptional regulators.

5.4.2. Regenerative Medicine Applications

The hybrid model's high accuracy and biological interpretability position it for immediate application in quality control for cardiac regenerative medicine. A significant obstacle in the production of cell therapies is addressed by the ability to automatically evaluate cardiomyocyte differentiation efficiency with 96.67% accuracy, where current assessment methods are labour-intensive and subjective.

The identification of stage-specific biomarkers enables data-driven optimisation of differentiation protocols, potentially reducing the 30-40% manufacturing costs associated with current trial-and-error approaches. The model's ability to predict differentiation outcomes in real-time facilitates adaptive protocol modification, which enables the efficient production of clinical-grade cardiomyocytes.

5.4.3. Drug Development Implications

The identified biomarkers (PLN, FKBP1A, MYL2) represent potential therapeutic targets for cardiac regeneration and cardiotoxicity screening. The computational framework supports drug development pipelines that need to assess cardiotoxicity and find new treatments by enabling systematic screening of compound effects on cardiomyocyte differentiation. The model's compatibility with patient-derived iPSC-cardiomyocytes supports personalized medicine applications, where individual genetic backgrounds may influence differentiation patterns and drug responses. This capability fits in with the emerging trend in cardiovascular care towards precision medicine.

5.5.STUDY LIMITATIONS AND METHODOLOGICAL CONSIDERATIONS

5.5.1. Data Dependency and Generalisation Challenges

While reproducibility is ensured by the use of publicly available datasets, generalisation to different cell lines, differentiation protocols, or experimental conditions may be constrained. While the Elorbany et al. (2022) temporal data captures specific iPSC differentiation protocols, the Kuppe et al. (2022) spatial transcriptomics dataset represents specific myocardial infarction conditions. Applicability to different experimental systems or disease contexts may be limited by this specificity.

Furthermore, the spatial and temporal sources are not experimentally paired (i.e., they do not originate from the same cells, samples, or differentiation runs). Multimodal fusion therefore depends on similarity-based computational alignment, and any mismatch between modalities

(batch effects, platform effects, disease versus differentiation biology) can limit how broadly the reported performance transfers to new laboratories or protocols. This limitation motivates the recommendation for future work to validate on truly paired spatiotemporal differentiation datasets.

To establish broad applicability, future validation across multiple technological platforms (multiple spatial transcriptomics methods, alternative single cell sequencing approaches) is crucial. The current emphasis on well-established platforms offers dependability, but it might overlook new developments in technology that could improve performance or reveal biological insights.

5.5.2. Temporal Resolution Limitations

Rapid regulatory events or fine-grained developmental transitions that take place in between measured intervals might not be captured by the temporal sampling resolution (10 time points). The model's capacity to identify all pertinent regulatory mechanisms may be limited if critical differentiation checkpoints that occur within shorter timeframes are overlooked.

Changing spatial relationships or dynamic cellular movements during differentiation may be missed by static spatial measurements. Understanding spatiotemporal dynamics may be improved by integrating live imaging data or by taking measurements with a higher temporal resolution.

5.5.3. Computational Complexity and Resource Requirements

Researchers with limited computational resources may not be able to use the hybrid architecture due to its computational requirements (peak memory usage: 4.8GB, training time: 3.5-4 hours). While these specifications are reasonable for research applications, model compression or edge computing improvements would be advantageous for clinical implementation.

The current implementation may not be suitable for very large-scale studies or real-time clinical monitoring applications because it scales linearly with dataset size. These constraints might be overcome by the development of distributed computing approaches or more effective architectures.

5.5.4. Biological Complexity Limitations

Despite being comprehensive, the emphasis on transcriptomic data may overlook vital regulatory processes that function at the post-translational, metabolomic, or epigenetic levels. While there are still many technical obstacles in multi-omics integration, future integration of additional omics modalities may offer a deeper awareness of differentiation regulation.

By treating cell populations as homogeneous entities, the current approach may overlook crucial subpopulation dynamics or uncommon cell states that influence the differentiation results. While it would necessitate considerable methodological adjustments, single-cell resolution analysis might provide more biological insights.

5.6.FUTURE DIRECTIONS

5.6.1. Multi-omics Integration

To achieve a better grasp of the regulation of cardiomyocyte differentiation, future studies ought to explore the integration of additional omics modalities, such as spatial proteomics, metabolomics, and epigenomics. Multiple molecular layers within the same tissue sections can be measured simultaneously thanks to recent developments in spatial multi-omics technologies.

The integration of heterogeneous omics data types presents significant technical challenges, including data normalization, batch effect correction, and computational complexity management. A promising line of inquiry is the development of specialised fusion architectures intended for multi-omics integration.

5.6.2. Transformer Architecture Integration

Beyond the capabilities of existing RNN approaches, recent developments in transformer architectures for biological sequence analysis point to the possibility of enhancing temporal modelling performance. Transformers' self-attention mechanisms might be able to preserve computational efficiency while more accurately capturing long-range dependencies in differentiation trajectories. The development of transformer architectures tailored for biological sequences could improve performance and interpretability by overcoming the drawbacks of text-based models when used with genomic data.

5.6.3. Real-Time Monitoring and Adaptive Protocols

Continuous monitoring of differentiation progress with adaptive protocol adjustment may be made possible by integrating the computational framework with real-time imaging and biosensor technologies. With this ability, existing static differentiation protocols could be changed into data-driven, dynamic procedures that are tailored to specific experimental circumstances.

Implementation of Edge Computing: Real-time monitoring in clinical settings may be made possible without the need for cloud computing infrastructure by the creation of lightweight model variants appropriate for edge computing devices. This development would allow for broad clinical implementation while addressing data privacy issues.

5.6.4. Cross-Species and Cross-Tissue Validation

Extension of the computational framework to other species (mouse, non-human primate) and cardiac cell types (fibroblasts, endothelial cells, smooth muscle cells) would establish broader biological relevance and identify conserved versus species-specific differentiation mechanisms. Fundamental principles of cardiac development that are applicable in a variety of contexts may be revealed through comparative analysis across several model systems. Application of the framework to disease-specific iPSC models (dilated cardiomyopathy, hypertrophic cardiomyopathy, and arrhythmogenic conditions) could reveal patterns of pathological differentiation and identify treatment targets for specific cardiac diseases.

5.6.5. Clinical Translation and Regulatory Validation

Prospective clinical validation using patient-derived iPSC-cardiomyocytes represents the critical next step for clinical translation. Clinical adoption would be facilitated by collaboration with regulatory bodies to develop validation frameworks for AI-based cardiac differentiation assessment tools.

Multi-Centre Validation Studies: Coordinated validation across multiple clinical sites and research centres would prove the generalisability and reproducibility needed for clinical adoption and regulatory approval. Consistent application across various clinical contexts would be ensured by standardising protocols and analysis techniques.

5.7.IMPLICATIONS FOR REGENERATIVE MEDICINE AND COMPUTATIONAL BIOLOGY

5.7.1. Paradigm Shift in Differentiation Assessment

This study demonstrates how computational methods could transform the subjective, time-consuming manual evaluation of stem cell differentiation that is currently used with objective, automated, high-throughput analysis. In addition to addressing several shortcomings of current assessment approaches, the combination of high accuracy, biological interpretability, and uncertainty quantification offers capabilities not achievable with conventional methods.

By enabling cardiomyocyte quality assessment to be standardised across labs and clinical settings, the framework may lessen the variability that presently restricts reproducibility in stem cell research and treatment development. By offering uniform, impartial metrics for evaluating cell quality, this standardisation could accelerate clinical translation.

5.7.2. Computational Biology Methodological Advances

New paradigms for the analysis of intricate biological processes are established by the effective integration of temporal and spatial biological data using deep learning architectures. The value of integrating biological knowledge into computational design is suggested by the evidence that domain-specific architectures can perform better than general-purpose models.

The XAI Framework for Biology addresses the crucial need for transparency in AI-based biological discovery by offering a template for interpretable machine learning in biological applications. The ability of XAI to speed up biological understanding is demonstrated by the successful mapping of computational predictions to established biological knowledge while identifying new patterns.

5.7.3. Precision Medicine Integration

The framework is well-positioned for incorporation into precision medicine approaches for cardiovascular disease due to its compatibility with patient-derived cells and ability to capture individual variation. Finding patterns of differentiation unique to each patient may help guide

individualised treatment plans and predict how each person will react to cardiac regenerative therapies.

Real-time therapeutic optimisation and point-of-care differentiation assessment may be made possible by the framework's interpretability and computational efficiency, which facilitate integration into clinical decision-making workflows. With this ability, regenerative medicine could shift from research-based methods to standardised clinical practices.

5.8.CHAPTER CONCLUSION

A significant breakthrough in computational methods for cardiomyocyte differentiation analysis, the hybrid GNN-RNN architecture achieves state-of-the-art performance while preserving biological interpretability and offering reliable uncertainty quantification. The transformative potential of multimodal approaches in biological sequence analysis is demonstrated by the successful integration of temporal differentiation dynamics and spatial tissue organisation. The framework's ability to connect computational discovery and biological understanding is demonstrated by the identification of known cardiac biomarkers and the potential discovery of new regulatory mechanisms, which validate computational predictions biologically. The rigorous statistical validation and exacting methodological approach set new benchmarks for computational biology research and guarantee the findings' translational applicability.

This work has the potential to revolutionise current methods for assessing and optimising cardiomyocyte differentiation due to its high accuracy (96.67%), biological interpretability, and clinical applicability. For cardiac regenerative medicine, the possibility of a 30–40% cost reduction in manufacturing while maintaining cell quality offers substantial therapeutic and financial benefits.

The methodological advancements achieved through this work have implications for the future that go beyond cardiac applications. They offer frameworks for the spatiotemporal analysis of other developmental processes and stem cell differentiation systems. A roadmap for interpretable deep learning in biology is provided by the combination of explainable AI and biological validation, which meets the crucial requirements for computational methods to be transparent and biologically relevant. The successful demonstration of clinically relevant accuracy combined with biological interpretability establishes proof-of-concept for AI-assisted regenerative medicine applications. This work lays crucial groundwork to establish standardised, impartial, and scalable methods for quality control and optimisation of stem cell therapy as the field advances towards clinical implementation.

The computational frameworks and biological insights offered in this study represent a major advancement towards the ultimate goal of improving patient outcomes through improved cardiac regenerative therapies.

6. CHAPTER 6: CONCLUSION

6.1.INTRODUCTION

By combining temporal gene expression data with spatial transcriptomics, this study has successfully created and validated a novel hybrid GNN-RNN architecture for predicting cardiomyocyte differentiation outcomes. The investigation addressed critical gaps in computational approaches to regenerative medicine by achieving state-of-the-art performance while maintaining biological interpretability and providing robust uncertainty quantification. This concluding chapter synthesizes the key findings, evaluates the research contributions, discusses implications for the field, and outlines future directions for advancing computational approaches in cardiac regenerative medicine.

The hybrid approach demonstrated transformative potential for cardiac regenerative medicine, achieving 96.67% accuracy in differentiation classification while successfully identifying biologically relevant biomarkers that align with established cardiac developmental pathways. The comprehensive explainable AI framework connected biological knowledge with computational advancement, shedding light on key regulatory processes regulating cardiomyocyte maturation and positioning the work for clinical application.

6.2.SUMMARY OF KEY FINDINGS

6.2.1. Superior Performance Through Multimodal Integration

All evaluation metrics revealed that the hybrid GNN-RNN architecture performed exceptionally well, with the ensemble fusion strategy achieving 96.67% accuracy on the held-out test folds for the differentiation efficiency task. This supports the core hypothesis that spatiotemporal integration can improve predictive performance relative to unimodal baselines within the same evaluation protocol. Where performance is contextualised against prior studies, comparisons are treated as indicative.

Fusion Strategy Validation: Three fusion strategies (concatenation, attention, and ensemble) were systematically compared, yielding important information regarding the best practices for integrating multimodal biological data. Late fusion strategies, which retain modality-specific information until final decision-making, are particularly well-suited for biological applications where different data types capture complementary regulatory mechanisms, as evidenced by the superior performance of ensemble fusion (96.67% accuracy) over attention-based (86.67%) and concatenation approaches (80.00%).

6.2.2. Biological Interpretability and Validation

The explainable AI framework successfully identified biologically relevant features that demonstrate strong concordance with established cardiac developmental biology. The fact that phospholamban (PLN), FKBP1A (FK506 binding protein 1A), and myosin light chain 2 (MYL2)

were found to be the most discriminative features suggests that the model is capturing real biological signals instead of statistical artefacts.

Pathway-Level Validation: With 89% of the top-ranked features matching known cardiac biomarkers or developmental regulators, the computational predictions demonstrated impressive agreement with the body of established cardiac development literature. The discovery of structural proteins (MYL2) and calcium handling proteins (PLN, FKBP1A) validates the model's biological validity and translational relevance by reflecting basic mechanisms that differentiate mature from immature cardiomyocytes.

Novel Biomarker Discovery: The model's ability to uncover biological information beyond current understanding is demonstrated by the remaining 11% of identified features that do not match recognised cardiac markers. These features may represent novel regulatory mechanisms worthy of experimental validation.

6.2.3. Uncertainty Quantification and Clinical Readiness

Robust uncertainty quantification was made possible by the Monte Carlo Dropout analysis, and all fusion strategies showed perfect correlation between classification accuracy and high-confidence predictions (>90%). In addition to providing crucial functionality for clinical implementation where prediction uncertainty must be evaluated for safe decision-making, this capability addresses a significant limitation in current computational approaches.

Clinically relevant risk stratification is made possible by the entropy-based confidence scoring. Uncertain cases are flagged for further validation, and high-confidence predictions can guide automated quality control decisions. This feature sets up the framework for incorporation into clinical procedures that call for accurate evaluation of the quality of cardiomyocyte differentiation.

6.3.RESEARCH CONTRIBUTION TO THE FIELD

6.3.1. Methodological Innovations

This study makes several significant methodological contributions that lead to new paradigms for spatiotemporal modelling in computational biology:

Hybrid Architecture Development: The novel systematic use of hybrid deep learning architectures for cardiomyocyte differentiation prediction was achieved with the successful combination of GNN spatial modelling and RNN temporal analysis. Beyond cardiac research, the thorough assessment of fusion strategies offers a model for multimodal integration in biological applications.

Explainable AI Framework: A robust XAI framework developed particularly for biological applications is produced by combining SHAP analysis, attention visualisation, and biological pathway mapping. This method effectively addresses the crucial requirements for interpretability in AI-based biological research by bridging the gap between computational discovery and biological validation.

Statistical Validation Standards: The comprehensive statistical validation framework, which includes paired t-tests, bootstrap confidence intervals, McNemar's tests, and uncertainty quantification, sets new benchmarks for the rigorous evaluation of computational biology models. In addition to addressing reproducibility issues in computational biology, this methodological rigour offers a model for upcoming validation research.

6.3.2. Biological Discovery and Validation

Cardiac Development Insights: The identification of stage-specific biomarkers and temporal attention patterns provides new insights into critical developmental checkpoints during cardiomyocyte differentiation. The model's ability to capture spatiotemporal regulatory networks offers novel perspectives on the coordinated molecular events governing cardiac maturation.

Regulatory Mechanism Identification: The computational framework's ability to both biologically validate and discover new mechanisms was demonstrated by its successful identification of established cardiac regulatory pathways. Confidence in biological relevance is provided by the alignment with established transcription factor networks (NKX2-5, GATA4, TBX5) while identifying additional regulatory features.

6.3.3. Clinical Translation Framework

Quality Control Applications: The high accuracy (96.67%) and biological interpretability position the framework for immediate application in cardiac regenerative medicine quality control, addressing critical bottlenecks in cell therapy manufacturing where current assessment methods are labour-intensive and subjective.

Therapeutic Target Identification: The biomarkers PLN, FKBP1A, and MYL2 have been identified as potential therapeutic targets for cardiac regeneration and drug development applications. The computational framework allows for the systematic screening of compound effects on cardiomyocyte differentiation.

6.4.IMPLICATIONS FOR REGENERATIVE MEDICINE AND COMPUTATIONAL BIOLOGY

6.4.1. Paradigm Shift in Differentiation Assessment

This study demonstrates how computational techniques can transform the subjective, manual evaluation of stem cell differentiation into an automated, high-throughput, objective analysis. In addition to addressing several shortcomings of current assessment techniques, the combination of high accuracy, biological interpretability, and uncertainty quantification offers capabilities not possible with conventional methods. The framework facilitates the standardisation of cardiomyocyte quality assessment across labs and clinical settings, which may lessen the variability that presently restricts the reproducibility of stem cell research and therapy development. By offering uniform, impartial metrics for evaluating cell quality, this standardisation may hasten clinical translation.

6.4.2. Computational Biology Methodological Advances

New paradigms for the analysis of biological data are established by the successful demonstration that domain-specific hybrid architectures can perform better than general-purpose models. The study offers proof that incorporating biological knowledge into computational design improves performance over general machine learning techniques.

To meet the urgent demands for transparency in AI-based biological discovery, the extensive XAI framework offers a model for interpretable machine learning in biological applications. The ability of XAI to speed up biological understanding is demonstrated by the successful mapping of computational predictions to known biological knowledge while spotting new patterns.

6.4.3. Clinical Translation and Precision Medicine

Real-time therapeutic optimisation and point-of-care differentiation assessment could be made feasible by the framework's interpretability and computational efficiency, which facilitate integration into clinical decision-making workflows. With this ability, regenerative medicine could shift from research-based methods to standardised clinical practices.

The framework can be integrated into precision medicine strategies for cardiovascular disease because of its compatibility with patient-derived cells and capacity to capture individual variation. Finding patterns of differentiation unique to each patient could assist in guiding individualised treatment plans and predict how each person will react to cardiac regenerative treatments.

6.5.CONCLUDING REMARKS

This research successfully addressed the fundamental challenge of predicting cardiomyocyte differentiation outcomes through innovative integration of spatial and temporal biological data. The hybrid GNN-RNN architecture set new benchmarks for computational approaches in regenerative medicine by achieving unprecedented performance while preserving biological interpretability. This work has the potential to revolutionise current methods for assessing and optimising cardiomyocyte differentiation due to its high accuracy (96.67%), biological interpretability, and clinical applicability. A major step forward for AI-assisted regenerative medicine has been made with the successful demonstration of clinically relevant performance coupled with mechanistic insights. The methodological advancements offer frameworks for the spatiotemporal analysis of other developmental processes and stem cell differentiation systems, going beyond cardiac applications. A roadmap for interpretable machine learning in biology is provided by the combination of explainable AI and thorough biological validation, which meets the crucial requirements for computational methods to be transparent and biologically relevant.

This work highlights how crucial it is to combine computational innovation with biological understanding and clinical relevance as artificial intelligence continues to revolutionise healthcare and biological research. A template for handling intricate biological problems using cutting-edge computational techniques while upholding scientific rigour and a translational focus is provided by the effective fusion of spatial and temporal modelling approaches. This research is motivated

by the ultimate goal of improving patient outcomes through improved cardiac regenerative therapies. Proof-of-concept for AI-assisted regenerative medicine applications that could help millions of patients with cardiovascular diseases worldwide has been established thanks to the computational frameworks and biological insights presented in this work.

This study adds to the growing body of evidence showing that careful fusion of biological and artificial intelligence research can speed up scientific advancements while upholding the highest standards of clinical relevance and scientific rigour. The effective demonstration of spatiotemporal modelling for cardiomyocyte differentiation lays the groundwork for upcoming advancements in precision healthcare, regenerative medicine, and computational biology that could revolutionise the way that cardiovascular disease and other conditions are treated.

To propel the field of cardiac regenerative medicine closer to its ultimate goal of restoring the human heart, this work combines technical excellence with biological insight and clinical relevance, providing essential foundations for the ongoing journey from computational innovation to clinical application.

REFERENCES

[1] M. Di Cesare *et al.*, "The Heart of the World," *Glob. Heart*, vol. 19, 2024, doi: 10.5334/gh.1288.

[2] M. N. Kgatla, T. M. Mothiba, T. Sodi, and M. Makgahlela, "Nurses' experiences in managing cardiovascular disease in selected rural and peri-urban clinics in limpopo province, south africa," *Int. J. Environ. Res. Public Health*, vol. 18, pp. 1–12, Mar. 2021, doi: 10.3390/ijerph18052570.

[3] M. F. Tenreiro, A. F. Louro, P. M. Alves, and M. Serra, "Next generation of heart regenerative therapies: progress and promise of cardiac tissue engineering," Dec. 2021, *Nature Research*. doi: 10.1038/s41536-021-00140-4.

[4] M. Mazzola and E. Di Pasquale, "Toward Cardiac Regeneration: Combination of Pluripotent Stem Cell-Based Therapies and Bioengineering Strategies," May 2020, *Frontiers Media S.A.* doi: 10.3389/fbioe.2020.00455.

[5] M. Prondzynski *et al.*, "Efficient and reproducible generation of human iPSC-derived cardiomyocytes and cardiac organoids in stirred suspension systems," *Nat. Commun.*, vol. 15, Dec. 2024, doi: 10.1038/s41467-024-50224-0.

[6] A. K. Feeney, A. D. Simmons, C. J. Peplinski, X. Zhang, and S. P. Palecek, "Enhancing human pluripotent stem cell differentiation to cardiomyocytes through cardiac progenitor reseeding and cryopreservation," *iScience*, vol. 28, no. 5, p. 112452, May 2025, doi: 10.1016/J.ISCI.2025.112452.

[7] X. Liu *et al.*, "Increased Reactive Oxygen Species-Mediated Ca2+/Calmodulin-Dependent Protein Kinase II Activation Contributes to Calcium Handling Abnormalities and Impaired Contraction in Barth Syndrome," *Circulation*, vol. 143, no. 19, pp. 1894–1911, May 2021, doi: 10.1161/CIRCULATIONAHA.120.048698/SUPPL_FILE/CIRC_CIRCULATIONAHA-2020-048698_SUPP6.MP4.

[8] K. D. Dwyer *et al.*, "One Billion hiPSC-Cardiomyocytes: Upscaling Engineered Cardiac Tissues to Create High Cell Density Therapies for Clinical Translation in Heart Regeneration," *Bioengineering*, vol. 10, no. 5, p. 587, May 2023, doi: 10.3390/BIOENGINEERING10050587/S1.

[9] K. Echeverría-Altamar, C. Barreto-Gamarra, M. Domenech-García, and P. Resto-Irizarry, "Prediction of cardiac differentiation in human induced pluripotent stem cell-derived cardiomyocyte supernatant using surface-enhanced Raman

spectroscopy and machine learning," *Biosens. Bioelectron.*, vol. 283, Sep. 2025, doi: 10.1016/j.bios.2025.117528.

[10] T. K. Feaster *et al.*, "Acute effects of cardiac contractility modulation stimulation in conventional 2D and 3D human induced pluripotent stem cell-derived cardiomyocyte models," *Front. Physiol.*, vol. 13, p. 1023563, Nov. 2022, doi: 10.3389/FPHYS.2022.1023563/BIBTEX.

[11] E. Karbassi *et al.*, "Cardiomyocyte maturation: advances in knowledge and implications for regenerative medicine," *Nat. Rev. Cardiol.*, vol. 17, no. 6, pp. 341–359, Jun. 2020, doi: 10.1038/S41569-019-0331-X.

[12] J. Moon, M. Li, A. J. Ramirez-Cuesta, and Z. Wu, "Raman Spectroscopy," *Springer Handbooks*, pp. 75–110, 2023, doi: 10.1007/978-3-031-07125-6_4/FIGURES/21.

[13] Y. Deng, Z. Bai, and R. Fan, "Microtechnologies for single-cell and spatial multi-omics," *Nature Reviews Bioengineering*, vol. 1, no. 10, pp. 769–784, Oct. 2023, doi: 10.1038/S44222-023-00084-Y;SUBJMETA.

[14] P. L. Ståhl *et al.*, "Visualization and analysis of gene expression in tissue sections by spatial transcriptomics," *Science*, vol. 353, no. 6294, pp. 78–82, Jul. 2016, doi: 10.1126/SCIENCE.AAF2403.

[15] N. Rao, S. Clark, and O. Habern, "Bridging Genomics and Tissue Pathology," *https://home.liebertpub.com/gen*, vol. 40, no. 2, pp. 50–51, Feb. 2020, doi: 10.1089/GEN.40.02.16.

[16] S. Jain and M. T. Eadon, "Spatial transcriptomics in health and disease," *Nat. Rev. Nephrol.*, vol. 20, no. 10, pp. 659–671, Oct. 2024, doi: 10.1038/S41581-024-00841-1;SUBJMETA.

[17] J. M. B. Pang *et al.*, "Spatial transcriptomics and the anatomical pathologist: Molecular meets morphology," *Histopathology*, vol. 84, no. 4, pp. 577–586, Mar. 2024, doi: 10.1111/HIS.15093.

[18] E. N. Farah *et al.*, "Spatially organized cellular communities form the developing human heart," *Nature*, vol. 627, pp. 854–864, Mar. 2024, doi: 10.1038/s41586-024-07171-z.

[19] A. Parikh, J. Wu, R. M. Blanton, and E. S. Tzanakakis, "Signaling Pathways and Gene Regulatory Networks in Cardiomyocyte Differentiation," *https://home.liebertpub.com/teb*, vol. 21, no. 4, pp. 377–392, May 2015, doi: 10.1089/TEN.TEB.2014.0662.

[20] D. MacGrogan, J. Münch, and J. L. de la Pompa, “Notch and interacting signalling pathways in cardiac development, disease, and regeneration,” *Nat. Rev. Cardiol.*, vol. 15, no. 11, pp. 685–704, Nov. 2018, doi: 10.1038/S41569-018-0100-2;SUBJMETA.

[21] Y. Wu *et al.*, “A spatiotemporal transcriptomic atlas of mouse placentation,” *Cell Discov.*, vol. 10, no. 1, pp. 1–17, Dec. 2024, doi: 10.1038/S41421-024-00740-6;SUBJMETA.

[22] J. Kang *et al.*, “Exploring the cellular and molecular basis of murine cardiac development through spatiotemporal transcriptome sequencing,” *Gigascience*, vol. 14, 2025, doi: 10.1093/gigascience/giaf012.

[23] X. Wang, L. Cao, R. Chang, J. Shen, L. Ma, and Y. Li, “Elucidating cardiomyocyte heterogeneity and maturation dynamics through integrated single-cell and spatial transcriptomics,” *iScience*, vol. 28, no. 1, p. 111596, Jan. 2025, doi: 10.1016/j.isci.2024.111596.

[24] S. M. Biendarra-Tiegs, X. Li, D. Ye, E. B. Brandt, M. J. Ackerman, and T. J. Nelson, “Single-Cell RNA-Sequencing and Optical Electrophysiology of Human Induced Pluripotent Stem Cell-Derived Cardiomyocytes Reveal Discordance Between Cardiac Subtype-Associated Gene Expression Patterns and Electrophysiological Phenotypes,” *https://home.liebertpub.com/scd*, vol. 28, no. 10, pp. 659–673, May 2019, doi: 10.1089/SCD.2019.0030.

[25] M. Lemme *et al.*, “Atrial-like Engineered Heart Tissue: An In Vitro Model of the Human Atrium,” *Stem Cell Reports*, vol. 11, no. 6, pp. 1378–1390, Dec. 2018, doi: 10.1016/J.STEMCR.2018.10.008.

[26] J. T. Granados-Riveron *et al.*, “Combined Mutation Screening of NKX2-5, GATA4, and TBX5 in Congenital Heart Disease: Multiple Heterozygosity and Novel Mutations,” *Congenit. Heart Dis.*, vol. 7, no. 2, p. 151, Mar. 2012, doi: 10.1111/J.1747-0803.2011.00573.X.

[27] C. Cao *et al.*, “Nkx2.5: a crucial regulator of cardiac development, regeneration and diseases,” *Front. Cardiovasc. Med.*, vol. 10, p. 1270951, 2023, doi: 10.3389/FCVM.2023.1270951.

[28] Z. L. Robbe *et al.*, “CHD4 is recruited by GATA4 and NKX2-5 to repress noncardiac gene programs in the developing heart,” *Genes Dev.*, vol. 36, no. 7, pp. 468–482, Apr. 2022, doi: 10.1101/GAD.349154.121/-/DC1.

[29] S. Cheng *et al.*, “Single-cell RNA sequencing reveals maturation trajectory in human pluripotent stem cell-derived cardiomyocytes in engineered tissues,” *iScience*, vol. 26, no. 4, p. 106302, Apr. 2023, doi: 10.1016/J.ISCI.2023.106302.

[30] S. Kannan, M. Farid, B. L. Lin, M. Miyamoto, and C. Kwon, “Transcriptomic entropy benchmarks stem cell-derived cardiomyocyte maturation against endogenous tissue at single cell level,” *PLoS Comput. Biol.*, vol. 17, no. 9, p. e1009305, Sep. 2021, doi: 10.1371/JOURNAL.PCBI.1009305.

[31] Y. Le, “Challenges in Data Integration for Spatiotemporal Analysis,” *Journal of Map & Geography Libraries*, vol. 8, no. 1, pp. 58–67, Jan. 2012, doi: 10.1080/15420353.2011.622457.

[32] M. Mahmud, M. S. Kaiser, T. M. McGinnity, and A. Hussain, “Deep Learning in Mining Biological Data,” *Cognit. Comput.*, vol. 13, no. 1, pp. 1–33, Jan. 2021, doi: 10.1007/S12559-020-09773-X/FIGURES/6.

[33] S. Zhang, X. Li, Q. Lin, J. Lin, and K. C. Wong, “Uncovering the key dimensions of high-throughput biomolecular data using deep learning,” *Nucleic Acids Res.*, vol. 48, no. 10, pp. e56–e56, Jun. 2020, doi: 10.1093/NAR/GKAA191.

[34] J. Cui, S. Yang, L. Yi, Q. Xi, D. Yang, and Y. Zuo, “Recent advances in deep learning for protein-protein interaction: a review,” *BioData Min.*, vol. 18, no. 1, p. 43, Dec. 2025, doi: 10.1186/S13040-025-00457-6.

[35] J. Li, S. Chen, X. Pan, Y. Yuan, and H. Bin Shen, “Cell clustering for spatial transcriptomics data with graph neural networks,” *Nat. Comput. Sci.*, vol. 2, no. 6, pp. 399–408, Jun. 2022, doi: 10.1038/S43588-022-00266-5;TECHMETA.

[36] Y. Yang, M. Z. Hossain, E. Stone, and S. Rahman, “Spatial transcriptomics analysis of gene expression prediction using exemplar guided graph neural network,” *Pattern Recognit.*, vol. 145, Jan. 2024, doi: 10.1016/j.patcog.2023.109966.

[37] F. Zhang, Z. Shen, S. Huang, Y. Zhu, and M. Yi, “SpaInGNN: Enhanced clustering and integration of spatial transcriptomics based on refined graph neural networks,” *Methods*, vol. 233, pp. 42–51, Jan. 2025, doi: 10.1016/J.YMETH.2024.11.006.

[38] Y. Long *et al.*, “Deciphering spatial domains from spatial multi-omics with SpatialGlue,” *Nat. Methods*, vol. 21, no. 9, pp. 1658–1667, Sep. 2024, doi: 10.1038/S41592-024-02316-4;SUBJMETA.

[39] W. Yan *et al.*, "A hybrid machine learning model with attention mechanism and multidimensional multivariate feature coding for essential gene prediction," *BMC Biol.*, vol. 23, no. 1, p. 108, Dec. 2025, doi: 10.1186/S12915-025-02209-8.

[40] E. Elbasani, S. N. Njimbouom, T. J. Oh, E. H. Kim, H. Lee, and J. D. Kim, "GCRNN: graph convolutional recurrent neural network for compound–protein interaction prediction," *BMC Bioinformatics*, vol. 22, no. Suppl 5, p. 616, Nov. 2022, doi: 10.1186/S12859-022-04560-X.

[41] S. A. Niederer, J. Lumens, and N. A. Trayanova, "Computational models in cardiology," *Nat. Rev. Cardiol.*, vol. 16, no. 2, pp. 100–111, Feb. 2019, doi: 10.1038/S41569-018-0104-Y;SUBJMETA.

[42] I. Fumagalli *et al.*, "The role of computational methods in cardiovascular medicine: a narrative review," *Transl. Pediatr.*, vol. 13, no. 1, pp. 146–163, Jan. 2024, doi: 10.21037/TP-23-184/COIF.

[43] A. Lopez-Perez, R. Sebastian, and J. M. Ferrero, "Three-dimensional cardiac computational modelling: METHODS, features and applications," *Biomed. Eng. Online*, vol. 14, no. 1, pp. 1–31, Apr. 2015, doi: 10.1186/S12938-015-0033-5/FIGURES/11.

[44] E. Afjeh-Dana, P. Naserzadeh, E. Moradi, N. Hosseini, A. M. Seifalian, and B. Ashtari, "Stem Cell Differentiation into Cardiomyocytes: Current Methods and Emerging Approaches," *Stem Cell Rev. Rep.*, vol. 18, no. 8, pp. 2566–2592, Dec. 2022, doi: 10.1007/S12015-021-10280-1/FIGURES/3.

[45] H. W. King *et al.*, "Single-cell analysis of human B cell maturation predicts how antibody class switching shapes selection dynamics," *Sci. Immunol.*, vol. 6, no. 56, Feb. 2021, doi: 10.1126/SCIIMMUNOL.ABE6291.

[46] A. Ogunpola, F. Saeed, S. Basurra, A. M. Albarrak, and S. N. Qasem, "Machine Learning-Based Predictive Models for Detection of Cardiovascular Diseases," *Diagnostics*, vol. 14, no. 2, p. 144, Jan. 2024, doi: 10.3390/DIAGNOSTICS14020144.

[47] A. Mastropietro, G. De Carlo, and A. Anagnostopoulos, "XGDAG: explainable gene–disease associations via graph neural networks," *Bioinformatics*, vol. 39, no. 8, Aug. 2023, doi: 10.1093/BIOINFORMATICS/BTAD482.

[48] R. K. Tripathy *et al.*, "Effective integration of multi-omics with prior knowledge to identify biomarkers via explainable graph neural networks," *NPJ Syst. Biol. Appl.*, vol. 11, no. 1, p. 43, Dec. 2025, doi: 10.1038/S41540-025-00519-9.

[49] R. Elorbany *et al.*, “Single-cell sequencing reveals lineage-specific dynamic genetic regulation of gene expression during human cardiomyocyte differentiation,” *PLoS Genet.*, vol. 18, no. 1, p. e1009666, Jan. 2022, doi: 10.1371/JOURNAL.PGEN.1009666.

[50] S. Li, H. Hua, and S. Chen, “Graph neural networks for single-cell omics data: a review of approaches and applications,” Mar. 2025, *Oxford University Press*. doi: 10.1093/bib/bbaf109.

[51] H. Hwang, H. Jeon, N. Yeo, and D. Baek, “Big data and deep learning for RNA biology,” *Exp. Mol. Med.*, vol. 56, no. 6, pp. 1293–1321, Jun. 2024, doi: 10.1038/S12276-024-01243-W;TECHMETA.

[52] “World Heart Vision 2030 Summary | World Heart Federation.” Accessed: Sep. 23, 2025. [Online]. Available: https://world-heart-federation.org/world-heart-vision-2030/

[53] Z. S. Razavi *et al.*, “Stem cells and bio scaffolds for the treatment of cardiovascular diseases: new insights,” *Front. Cell Dev. Biol.*, vol. 12, p. 1472103, Dec. 2024, doi: 10.3389/FCELL.2024.1472103/FULL.

[54] “Cardiovascular diseases (CVDs).” Accessed: Sep. 23, 2025. [Online]. Available: https://www.who.int/news-room/fact-sheets/detail/cardiovascular-diseases-(cvds)

[55] N. M. Minja *et al.*, “Cardiovascular diseases in Africa in the twenty-first century: Gaps and priorities going forward,” *Front. Cardiovasc. Med.*, vol. 9, p. 1008335, Nov. 2022, doi: 10.3389/FCVM.2022.1008335.

[56] B. Chong *et al.*, “Global burden of cardiovascular diseases: projections from 2025 to 2050,” *Eur. J. Prev. Cardiol.*, vol. 32, no. 11, Aug. 2025, doi: 10.1093/EURJPC/ZWAE281.

[57] Y. Li *et al.*, “The molecular mechanisms of cardiac development and related diseases,” Dec. 2024, *Springer Nature*. doi: 10.1038/s41392-024-02069-8.

[58] J. H. Hong and H. G. Zhang, “Transcription Factors Involved in the Development and Prognosis of Cardiac Remodeling,” Feb. 2022, *Frontiers Media S.A.* doi: 10.3389/fphar.2022.828549.

[59] Y. S. Yang, M. H. Liu, Z. W. Yan, G. Q. Chen, and Y. Huang, “FAM122A Is Required for Mesendodermal and Cardiac Differentiation of Embryonic Stem Cells,” *Stem Cells*, vol. 41, pp. 354–367, Apr. 2023, doi: 10.1093/stmcls/sxad008.

[60] H. Liu *et al.*, “Insight into the regulatory mechanism of dynamic chromatin 3D interactions during cardiomyocyte differentiation in human,” *Mol. Ther. Nucleic Acids*, vol. 33, pp. 629–641, Sep. 2023, doi: 10.1016/j.omtn.2023.07.033.

[61] J. Kim, H. Lee, S. J. Yi, and K. Kim, “Gene regulation by histone-modifying enzymes under hypoxic conditions: a focus on histone methylation and acetylation,” Jul. 2022, *Springer Nature*. doi: 10.1038/s12276-022-00812-1.

[62] S. Komal *et al.*, “Epigenetic Regulation in Myocardial Fibroblasts and Its Impact on Cardiovascular Diseases,” Oct. 2024, *Multidisciplinary Digital Publishing Institute (MDPI)*. doi: 10.3390/ph17101353.

[63] F. Abu Sailik, B. S. Emerald, and S. A. Ansari, “Opening and changing: mammalian SWI/SNF complexes in organ development and carcinogenesis,” *Open Biol.*, vol. 14, Oct. 2024, doi: 10.1098/rsob.240039.

[64] P. Chen *et al.*, “Transcriptome and open chromatin analysis reveals the process of myocardial cell development and key pathogenic target proteins in Long QT syndrome type 7,” *J. Transl. Med.*, vol. 22, Dec. 2024, doi: 10.1186/s12967-024-05125-7.

[65] H. Li, J. Zou, X. H. Yu, X. Ou, and C. K. Tang, “Zinc finger E-box binding homeobox 1 and atherosclerosis: New insights and therapeutic potential,” Jun. 2021, *John Wiley and Sons Inc*. doi: 10.1002/jcp.30177.

[66] S. T. Bak *et al.*, “Ploidy-stratified single cardiomyocyte transcriptomics map Zinc Finger E-Box Binding Homeobox 1 to underly cardiomyocyte proliferation before birth,” *Basic Res. Cardiol.*, vol. 118, Dec. 2023, doi: 10.1007/s00395-023-00979-2.

[67] Q. Liu *et al.*, “Genome-Wide Temporal Profiling of Transcriptome and Open Chromatin of Early Cardiomyocyte Differentiation Derived from hiPSCs and hESCs,” *Circ. Res.*, vol. 121, pp. 376–391, Aug. 2017, doi: 10.1161/CIRCRESAHA.116.310456.

[68] I. K. Mensah and H. Gowher, “Signaling Pathways Governing Cardiomyocyte Differentiation,” Jun. 2024, *Multidisciplinary Digital Publishing Institute (MDPI)*. doi: 10.3390/genes15060798.

[69] A. Nijak, J. Saenen, A. J. Labro, D. Schepers, B. L. Loeys, and M. Alaerts, “Ipsc-cardiomyocyte models of brugada syndrome—achievements, challenges and future perspectives,” Mar. 2021, *MDPI AG*. doi: 10.3390/ijms22062825.

[70] M. R. Pozo, G. W. Meredith, and E. Entcheva, “Human iPSC-Cardiomyocytes as an Experimental Model to Study Epigenetic Modifiers of Electrophysiology,” Jan. 2022, *MDPI*. doi: 10.3390/cells11020200.

[71] J. Joshi, C. Albers, N. Smole, S. Guo, and S. A. Smith, “Human induced pluripotent stem cell-derived cardiomyocytes (iPSC-CMs) for modeling cardiac arrhythmias: strengths, challenges and potential solutions,” *Front. Physiol.*, vol. 15, Sep. 2024, doi: 10.3389/fphys.2024.1475152.

[72] J. M. Churko *et al.*, “Defining human cardiac transcription factor hierarchies using integrated single-cell heterogeneity analysis,” *Nat. Commun.*, vol. 9, Dec. 2018, doi: 10.1038/s41467-018-07333-4.

[73] C. K. Pushpan and S. R. Kumar, “iPSC-Derived Cardiomyocytes as a Disease Model to Understand the Biology of Congenital Heart Defects,” Sep. 2024, *Multidisciplinary Digital Publishing Institute (MDPI)*. doi: 10.3390/cells13171430.

[74] A. Nijak *et al.*, “Morpho-functional comparison of differentiation protocols to create iPSC-derived cardiomyocytes,” *Biol. Open*, vol. 11, Feb. 2022, doi: 10.1242/bio.059016.

[75] Y. Tereshchenko, S. G. Petkov, and R. Behr, “The Efficiency of In Vitro Differentiation of Primate iPSCs into Cardiomyocytes Depending on Their Cell Seeding Density and Cell Line Specificity,” *Int. J. Mol. Sci.*, vol. 25, Aug. 2024, doi: 10.3390/ijms25158449.

[76] A. Nijak *et al.*, “Morpho-functional comparison of differentiation protocols to create iPSC-derived cardiomyocytes,” *Biol. Open*, vol. 11, Feb. 2022, doi: 10.1242/bio.059016.

[77] W. Derks *et al.*, “A Latent Cardiomyocyte Regeneration Potential in Human Heart Disease,” *Circulation*, vol. 151, pp. 245–256, Jan. 2025, doi: 10.1161/CIRCULATIONAHA.123.067156.

[78] B. D. Maliken and J. D. Molkentin, “Undeniable evidence that the adult mammalian heart lacks an endogenous regenerative stem cell,” 2018, *Lippincott Williams and Wilkins*. doi: 10.1161/CIRCULATIONAHA.118.035186.

[79] J. Yao, Y. Chen, Y. Huang, X. Sun, and X. Shi, “The role of cardiac microenvironment in cardiovascular diseases: implications for therapy,” May 2024, *Springer*. doi: 10.1007/s13577-024-01052-3.

[80] T. Watanabe, N. Hatayama, M. Guo, S. Yuhara, and T. Shinoka, “Bridging the Gap: Advances and Challenges in Heart Regeneration from In Vitro to In Vivo

Applications," Oct. 2024, *Multidisciplinary Digital Publishing Institute (MDPI)*. doi: 10.3390/bioengineering11100954.

[81] L. Wang and B. Jin, "Single-Cell RNA Sequencing and Combinatorial Approaches for Understanding Heart Biology and Disease," Oct. 2024, *Multidisciplinary Digital Publishing Institute (MDPI)*. doi: 10.3390/biology13100783.

[82] N. J. Eagles *et al.*, "Integrating gene expression and imaging data across Visium capture areas with visiumStitched," *BMC Genomics*, vol. 25, Dec. 2024, doi: 10.1186/s12864-024-10991-y.

[83] J. Park *et al.*, "Spatial omics technologies at multimodal and single cell/subcellular level," Dec. 2022, *BioMed Central Ltd*. doi: 10.1186/s13059-022-02824-6.

[84] M. Y. He *et al.*, "Spatial transcriptomics reveals tumor microenvironment heterogeneity in EBV positive diffuse large B cell lymphoma," *Sci. Rep.*, vol. 15, Dec. 2025, doi: 10.1038/s41598-025-00410-x.

[85] K. Kanemaru *et al.*, "Correction to: Spatially resolved multiomics of human cardiac niches (Nature, (2023), 619, 7971, (801-810), 10.1038/s41586-023-06311-1)," Apr. 2025, *Nature Research*. doi: 10.1038/s41586-025-08886-3.

[86] J. B. Fudge, "Spatial transcriptomics of the human heart," Aug. 2023, *Nature Research*. doi: 10.1038/s41587-023-01918-1.

[87] T. Li, Q. Marashly, J. A. Kim, N. Li, and M. G. Chelu, "Cardiac conduction diseases: understanding the molecular mechanisms to uncover targets for future treatments," 2024, *Taylor and Francis Ltd.* doi: 10.1080/14728222.2024.2351501.

[88] S. Seeler, K. Arnarsson, M. Dreßen, M. Krane, and S. A. Doppler, "Beyond the Heartbeat: Single-Cell Omics Redefining Cardiovascular Research," *Curr. Cardiol. Rep.*, Nov. 2024, doi: 10.1007/s11886-024-02117-3.

[89] R. Roth, S. Kim, J. Kim, and S. Rhee, "Single-cell and spatial transcriptomics approaches of cardiovascular development and disease," Aug. 2020, *The Biochemical Society of the Republic of Korea*. doi: 10.5483/BMBRep.2020.53.8.130.

[90] X. Long, X. Yuan, and J. Du, "Single-cell and spatial transcriptomics: Advances in heart development and disease applications," Jan. 2023, *Elsevier B.V.* doi: 10.1016/j.csbj.2023.04.007.

[91] Q. Nguyen *et al.*, "Spatial Transcriptomics in Human Cardiac Tissue," *Int. J. Mol. Sci.*, vol. 26, no. 3, 2025, doi: 10.3390/ijms26030995.

[92] D. M. Calcagno *et al.*, “Single-cell and spatial transcriptomics of the infarcted heart define the dynamic onset of the border zone in response to mechanical destabilization.,” *Nature cardiovascular research*, vol. 1, pp. 1039–1055, Nov. 2022, doi: 10.1038/s44161-022-00160-3.

[93] S. Zhang, B. Xiang, Y. Zhao, W. Wang, L. Chen, and X. Zhou, “Single-cell epigenomic and transcriptomic analysis unveils the pivotal role of GATA5/ISL1+ fibroblasts in cardiac repair post-myocardial infarction,” *Cardiovasc. Res.*, Jun. 2025, doi: 10.1093/cvr/cvaf101.

[94] N. Farzad, A. Enninful, S. Bao, D. Zhang, Y. Deng, and R. Fan, “Spatially resolved epigenome sequencing via Tn5 transposition and deterministic DNA barcoding in tissue,” *Nat. Protoc.*, Nov. 2024, doi: 10.1038/s41596-024-01013-y.

[95] F. Zhang *et al.*, “InferLoop: Leveraging single-cell chromatin accessibility for the signal of chromatin loop,” *Brief. Bioinform.*, vol. 24, May 2023, doi: 10.1093/bib/bbad166.

[96] D. Hong *et al.*, “Divergent combinations of enhancers encode spatial gene expression,” *Nature Communications* , vol. 16, Dec. 2025, doi: 10.1038/s41467-025-60482-1.

[97] J. Gao *et al.*, “Integrative analysis of transcriptome, DNA methylome, and chromatin accessibility reveals candidate therapeutic targets in hypertrophic cardiomyopathy,” *Protein Cell*, Nov. 2024, doi: 10.1093/procel/pwae032.

[98] H. Wang, Y. Yang, Y. Qian, J. Liu, and L. Qian, “Delineating chromatin accessibility re-patterning at single cell level during early stage of direct cardiac reprogramming,” *J. Mol. Cell. Cardiol.*, vol. 162, pp. 62–71, Jan. 2022, doi: 10.1016/j.yjmcc.2021.09.002.

[99] M. Efremova and S. A. Teichmann, “Computational methods for single-cell omics across modalities,” Jan. 2020, *Nature Research*. doi: 10.1038/s41592-019-0692-4.

[100] R. Argelaguet, A. S. E. Cuomo, O. Stegle, and J. C. Marioni, “Computational principles and challenges in single-cell data integration,” Oct. 2021, *Nature Research*. doi: 10.1038/s41587-021-00895-7.

[101] N. Adossa, S. Khan, K. T. Rytkönen, and L. L. Elo, “Computational strategies for single-cell multi-omics integration,” Jan. 2021, *Elsevier B.V.* doi: 10.1016/j.csbj.2021.04.060.

[102] P. Guo *et al.*, “Multiplexed spatial mapping of chromatin features, transcriptome and proteins in tissues.,” *Nat. Methods*, Jan. 2025, doi: 10.1038/s41592-024-02576-0.

[103] P. Yang *et al.*, “Spatial integration of multi-omics single-cell data with SIMO,” *Nat. Commun.*, vol. 16, p. 1265, Dec. 2025, doi: 10.1038/s41467-025-56523-4.

[104] Z. Bian *et al.*, “Single-cell landscape identified SERPINB9 as a key player contributing to stemness and metastasis in non-seminomas,” *Cell Death Dis.*, vol. 15, p. 812, Nov. 2024, doi: 10.1038/s41419-024-07220-5.

[105] L. Gifre-Renom, M. Daems, A. Luttun, and E. A. V. Jones, “Organ-Specific Endothelial Cell Differentiation and Impact of Microenvironmental Cues on Endothelial Heterogeneity,” Feb. 2022, *MDPI*. doi: 10.3390/ijms23031477.

[106] S. Corvera, “Cellular Heterogeneity in Adipose Tissues,” Feb. 2021, *Annual Reviews Inc.* doi: 10.1146/annurev-physiol-031620-095446.

[107] A. Misra, C. D. Baker, E. M. Pritchett, K. N. B. Villar, J. M. Ashton, and E. M. Small, “Characterizing neonatal heart maturation, regeneration, and scar resolution using spatial transcriptomics,” *J. Cardiovasc. Dev. Dis.*, vol. 9, Jan. 2022, doi: 10.3390/jcdd9010001.

[108] L. Cao *et al.*, “Integrative Single-Cell and Spatial Transcriptomics Reveal Functional and Spatial Heterogeneity of Atrial and Ventricular Cardiomyocytes in the Heart,” *Mol. Biotechnol.*, 2025, doi: 10.1007/s12033-025-01443-3.

[109] N. Combémorel, N. Cavell, and R. C. V. Tyser, “Early heart development: examining the dynamics of function-form emergence,” Aug. 2024, *Portland Press Ltd*. doi: 10.1042/BST20230546.

[110] E. Lázár *et al.*, “Spatial Dynamics of the Developing Human Heart,” Mar. 2024. doi: 10.1101/2024.03.12.584577.

[111] M. Litviňuková *et al.*, “Cells of the adult human heart,” *Nature*, vol. 588, pp. 466–472, Dec. 2020, doi: 10.1038/s41586-020-2797-4.

[112] C. Kuppe *et al.*, “Spatial multi-omic map of human myocardial infarction,” *Nature*, vol. 608, pp. 766–777, Aug. 2022, doi: 10.1038/s41586-022-05060-x.

[113] C. E. Friedman *et al.*, “Single-Cell Transcriptomic Analysis of Cardiac Differentiation from Human PSCs Reveals HOPX-Dependent Cardiomyocyte Maturation,” *Cell Stem Cell*, vol. 23, pp. 586-598.e8, Oct. 2018, doi: 10.1016/j.stem.2018.09.009.

[114] Z. Xu *et al.*, “STOmicsDB: a comprehensive database for spatial transcriptomics data sharing, analysis and visualization,” *Nucleic Acids Res.*, vol. 52, pp. D1053–D1061, Jan. 2024, doi: 10.1093/nar/gkad933.

[115] P. Hoang *et al.*, “Engineering spatial-organized cardiac organoids for developmental toxicity testing,” *Stem Cell Reports*, vol. 16, pp. 1228–1244, May 2021, doi: 10.1016/j.stemcr.2021.03.013.

[116] L. Cyganek *et al.*, “Deep phenotyping of human induced pluripotent stem cell-derived atrial and ventricular cardiomyocytes,” *JCI Insight*, vol. 3, Jun. 2018, doi: 10.1172/jci.insight.99941.

[117] J. L. Engel *et al.*, “Single Cell Multi-Omics of an iPSC Model of Human Sinoatrial Node Development Reveals Genetic Determinants of Heart Rate and Arrhythmia Susceptibility.,” *bioRxiv*, Sep. 2023, doi: 10.1101/2023.07.01.547335.

[118] L. Li *et al.*, “An organ-wide spatiotemporal transcriptomic and cellular atlas of the regenerating zebrafish heart,” *Nature Communications* , vol. 16, Dec. 2025, doi: 10.1038/s41467-025-59070-0.

[119] V. W. W. van Eif, H. D. Devalla, G. J. J. Boink, and V. M. Christoffels, “Transcriptional regulation of the cardiac conduction system,” Oct. 2018, *Nature Publishing Group*. doi: 10.1038/s41569-018-0031-y.

[120] M. Asp *et al.*, “A Spatiotemporal Organ-Wide Gene Expression and Cell Atlas of the Developing Human Heart,” *Cell*, vol. 179, pp. 1647-1660.e19, Dec. 2019, doi: 10.1016/j.cell.2019.11.025.

[121] M. A. Freeberg *et al.*, “The European Genome-phenome Archive in 2021,” *Nucleic Acids Res.*, vol. 50, pp. D980–D987, Jan. 2022, doi: 10.1093/nar/gkab1059.

[122] R. G. H. Lindeboom, A. Regev, and S. A. Teichmann, “Towards a Human Cell Atlas: Taking Notes from the Past,” Jul. 2021, *Elsevier Ltd*. doi: 10.1016/j.tig.2021.03.007.

[123] S. He *et al.*, “Single-cell transcriptome profiling of an adult human cell atlas of 15 major organs,” *Genome Biol.*, vol. 21, Dec. 2020, doi: 10.1186/s13059-020-02210-0.

[124] J. Wang, C. Gareri, and H. A. Rockman, “G-protein-coupled receptors in heart disease,” 2018, *Lippincott Williams and Wilkins*. doi: 10.1161/CIRCRESAHA.118.311403.

[125] D. Xie *et al.*, “Identification of an endogenous glutamatergic transmitter system controlling excitability and conductivity of atrial cardiomyocytes,” *Cell Res.*, vol. 31, pp. 951–964, Sep. 2021, doi: 10.1038/s41422-021-00499-5.

[126] M. Zaccolo and D. Kovanich, “NANODOMAIN CAMP SIGNALING IN CARDIAC PATHOPHYSIOLOGY: POTENTIAL FOR DEVELOPING TARGETED THERAPEUTIC

INTERVENTIONS," *Physiol. Rev.*, vol. 105, pp. 541–591, Apr. 2025, doi: 10.1152/physrev.00013.2024.

[127] L. Cyganek *et al.*, "Deep phenotyping of human induced pluripotent stem cell–derived atrial and ventricular cardiomyocytes," *JCI Insight*, vol. 3, no. 12, Jun. 2018, doi: 10.1172/jci.insight.99941.

[128] L. Wang, S. Hu, and B. Zhou, "Deciphering Cardiac Biology and Disease by Single-Cell Transcriptomic Profiling," Apr. 2022, *MDPI*. doi: 10.3390/biom12040566.

[129] C. Liu and N.-Y. Shao, "The Differences in the Developmental Stages of the Cardiomyocytes and Endothelial Cells in Human and Mouse Embryos at the Single-Cell Level.," *Int. J. Mol. Sci.*, vol. 25, Mar. 2024, doi: 10.3390/ijms25063240.

[130] S. Amal, L. Safarnejad, J. A. Omiye, I. Ghanzouri, J. H. Cabot, and E. G. Ross, "Use of Multi-Modal Data and Machine Learning to Improve Cardiovascular Disease Care," Apr. 2022, *Frontiers Media S.A.* doi: 10.3389/fcvm.2022.840262.

[131] P. Kiessling and C. Kuppe, "Spatial multi-omics: novel tools to study the complexity of cardiovascular diseases," Dec. 2024, *BioMed Central Ltd*. doi: 10.1186/s13073-024-01282-y.

[132] L. Tian, F. Chen, and E. Z. Macosko, "The expanding vistas of spatial transcriptomics," Jun. 2023, *Nature Research*. doi: 10.1038/s41587-022-01448-2.

[133] S. Fang *et al.*, "Computational Approaches and Challenges in Spatial Transcriptomics," Feb. 2023, *Beijing Genomics Institute*. doi: 10.1016/j.gpb.2022.10.001.

[134] X. Liu *et al.*, "Clinical challenges of tissue preparation for spatial transcriptome," *Clin. Transl. Med.*, vol. 12, Jan. 2022, doi: 10.1002/ctm2.669.

[135] E. G. Overbey *et al.*, "Challenges and considerations for single-cell and spatially resolved transcriptomics sample collection during spaceflight," Nov. 2022, *Cell Press*. doi: 10.1016/j.crmeth.2022.100325.

[136] J. Lee, M. Yoo, and J. Choi, "Recent advances in spatially resolved transcriptomics: challenges and opportunities," *BMB Rep.*, vol. 55, pp. 113–124, 2022, doi: 10.5483/BMBRep.2022.55.3.014.

[137] Y. Zhang, X. Feng, Y. Wang, and K. Shi, "Deep learning powered single-cell clustering framework with enhanced accuracy and stability," *Sci. Rep.*, vol. 15, p. 4107, Dec. 2025, doi: 10.1038/s41598-025-87672-7.

[138] X. Li *et al.*, “Deep learning enables accurate clustering with batch effect removal in single-cell RNA-seq analysis,” *Nat. Commun.*, vol. 11, Dec. 2020, doi: 10.1038/s41467-020-15851-3.

[139] R. Li *et al.*, “Graph Signal Processing, Graph Neural Network and Graph Learning on Biological Data: A Systematic Review,” 2023, *Institute of Electrical and Electronics Engineers Inc.* doi: 10.1109/RBME.2021.3122522.

[140] T. Tian, J. Wan, Q. Song, and Z. Wei, “Clustering single-cell RNA-seq data with a model-based deep learning approach,” *Nat. Mach. Intell.*, vol. 1, pp. 191–198, Apr. 2019, doi: 10.1038/s42256-019-0037-0.

[141] R. Petegrosso, Z. Li, and R. Kuang, “Machine learning and statistical methods for clustering single-cell RNA-sequencing data,” Jul. 2019, *Oxford University Press*. doi: 10.1093/bib/bbz063.

[142] N. Erfanian *et al.*, “Deep learning applications in single-cell genomics and transcriptomics data analysis,” *Biomedicine & Pharmacotherapy*, vol. 165, p. 115077, 2023, doi: https://doi.org/10.1016/j.biopha.2023.115077.

[143] D. M. Liang and P. F. Du, “scMUG: deep clustering analysis of single-cell RNA-seq data on multiple gene functional modules,” *Brief. Bioinform.*, vol. 26, Mar. 2025, doi: 10.1093/bib/bbaf138.

[144] T. Song *et al.*, “Predicting spatially resolved gene expression via tissue morphology using adaptive spatial GNNs,” *Bioinformatics*, vol. 40, no. Supplement_2, pp. ii111–ii119, Jun. 2024, doi: 10.1093/bioinformatics/btae383.

[145] Y. Li and Y. Luo, “STdGCN: spatial transcriptomic cell-type deconvolution using graph convolutional networks,” *Genome Biol.*, vol. 25, no. 1, p. 206, Aug. 2024, doi: 10.1186/s13059-024-03353-0.

[146] Z. Tang, T. Zhang, B. Yang, J. Su, and Q. Song, “spaCI: deciphering spatial cellular communications through adaptive graph model,” *Brief. Bioinform.*, vol. 24, no. 1, p. bbac563, Jun. 2023, doi: 10.1093/bib/bbac563.

[147] F. T. Zohora *et al.*, “CellNEST reveals cell–cell relay networks using attention mechanisms on spatial transcriptomics,” *Nat. Methods*, Jun. 2025, doi: 10.1038/s41592-025-02721-3.

[148] M. Monti, J. Fiorentino, E. Milanetti, G. Gosti, and G. G. Tartaglia, “Prediction of Time Series Gene Expression and Structural Analysis of Gene Regulatory Networks Using

Recurrent Neural Networks," *Entropy*, vol. 24, no. 2, p. 141, Jun. 2022, doi: 10.3390/e24020141.

[149] S. A. Wani, S. A. Khan, and S. M. K. Quadri, "Application of Deep Learning for Single Cell Multi-Omics: A State-of-the-Art Review," 2025, *Springer Science and Business Media B.V.* doi: 10.1007/s11831-025-10230-x.

[150] S. Babichev, I. Liakh, and I. Kalinina, "Applying a Recurrent Neural Network-Based Deep Learning Model for Gene Expression Data Classification," *Applied Sciences (Switzerland)*, vol. 13, Nov. 2023, doi: 10.3390/app132111823.

[151] T. Ma and J. Wang, "GraphPath: a graph attention model for molecular stratification with interpretability based on the pathway-pathway interaction network," *Bioinformatics*, vol. 40, Apr. 2024, doi: 10.1093/bioinformatics/btae165.

[152] A. Prakash and M. Banerjee, "An interpretable block-attention network for identifying regulatory feature interactions," *Brief. Bioinform.*, vol. 24, no. 4, p. bbad250, Jun. 2023, doi: 10.1093/bib/bbad250.

[153] S. R. Choi and M. Lee, "Transformer Architecture and Attention Mechanisms in Genome Data Analysis: A Comprehensive Review," *Biology (Basel).*, vol. 12, no. 7, p. 1033, Jun. 2023, doi: 10.3390/biology12071033.

[154] D. Molho *et al.*, "Deep Learning in Single-cell Analysis," *ACM Trans. Intell. Syst. Technol.*, vol. 15, Mar. 2024, doi: 10.1145/3641284.

[155] L.-L. Bao, C.-X. Zhang, J.-S. Zhang, and R. Guo, "A two-stage spatial prediction modeling approach based on graph neural networks and neural processes," *Expert Syst. Appl.*, vol. 258, p. 125173, Jun. 2024, doi: 10.1016/j.eswa.2024.125173.

[156] I. C. Kaadoud, N. P. Rougier, and F. Alexandre, "Knowledge extraction from the learning of sequences in a long short term memory (LSTM) architecture," *Knowl. Based. Syst.*, vol. 235, p. 107657, Jun. 2022, doi: 10.1016/j.knosys.2021.107657.

[157] E. Rajabi and K. Etminani, "Knowledge-graph-based explainable AI: A systematic review," *J. Inf. Sci.*, vol. 50, pp. 1019–1029, Aug. 2024, doi: 10.1177/01655515221112844.

[158] S. T. Hill, R. Kuintzle, A. Teegarden, E. Merrill, P. Danaee, and D. A. Hendrix, "A deep recurrent neural network discovers complex biological rules to decipher RNA protein-coding potential," *Nucleic Acids Res.*, vol. 46, pp. 8105–8113, Sep. 2018, doi: 10.1093/nar/gky567.

[159] M. Gillani and G. Pollastri, “Protein subcellular localization prediction tools,” *Comput. Struct. Biotechnol. J.*, vol. 23, pp. 1796–1807, Jun. 2024, doi: 10.1016/j.csbj.2024.04.032.

[160] S. Naseer, R. F. Ali, Y. D. Khan, P. D. D., and Dominic, “iGluK-Deep: computational identification of lysine glutarylation sites using deep neural networks with general pseudo amino acid compositions,” *J. Biomol. Struct. Dyn.*, vol. 40, no. 22, pp. 11691–11704, Dec. 2022, doi: 10.1080/07391102.2021.1962738.

[161] A. Pimpalkar, N. Gandhewar, N. Shelke, S. Patil, and S. Chhabria, “An Efficient Deep Convolutional Neural Networks Model for Genomic Sequence Classification,” in *Genomics at the Nexus of AI, Computer Vision, and Machine Learning*, wiley, 2024, pp. 345–375. doi: 10.1002/9781394268832.ch16.

[162] C. John, J. Sahoo, M. Madhavan, and O. K. Mathew, “Convolutional Neural Networks: A Promising Deep Learning Architecture for Biological Sequence Analysis,” 2023, *Bentham Science Publishers*. doi: 10.2174/1574893618666230320103421.

[163] I. Zafar *et al.*, “Reviewing methods of deep learning for intelligent healthcare systems in genomics and biomedicine,” *Biomed. Signal Process. Control*, vol. 86, p. 105263, Jun. 2023, doi: 10.1016/j.bspc.2023.105263.

[164] X. Tan, A. T. Su, H. Hajiabadi, M. Tran, and Q. Nguyen, “Applying Machine Learning for Integration of Multi-Modal Genomics Data and Imaging Data to Quantify Heterogeneity in Tumour Tissues,” in *Artificial Neural Networks*, H. Cartwright, Ed., New York, NY: Springer US, 2021, pp. 209–228. [Online]. Available: https://doi.org/10.1007/978-1-0716-0826-5_10

[165] T. Athaya, R. C. Ripan, X. Li, and H. Hu, “Multimodal deep learning approaches for single-cell multi-omics data integration,” Sep. 2023, *Oxford University Press*. doi: 10.1093/bib/bbad313.

[166] Z. H. Lu, M. Yang, C. H. Pan, P. Y. Zheng, and S. X. Zhang, “Multi-modal deep learning based on multi-dimensional and multi-level temporal data can enhance the prognostic prediction for multi-drug resistant pulmonary tuberculosis patients,” Nov. 2022, *Elsevier B.V.* doi: 10.1016/j.soh.2022.100004.

[167] X. Gu *et al.*, “Beyond Supervised Learning for Pervasive Healthcare,” *IEEE Rev. Biomed. Eng.*, vol. 17, pp. 42–62, 2024, doi: 10.1109/RBME.2023.3296938.

[168] J. Deng, R. Jiang, J. Zhang, and X. Song, “Multi-Modality Spatio-Temporal Forecasting via Self-Supervised Learning,” International Joint Conferences on Artificial Intelligence, Jul. 2024, pp. 2018–2026. doi: 10.24963/ijcai.2024/223.

[169] A. Szałata *et al.*, “Transformers in single-cell omics: a review and new perspectives,” *Nat. Methods*, vol. 21, pp. 1430–1443, Aug. 2024, doi: 10.1038/s41592-024-02353-z.

[170] S. Xue, F. Zhu, C. Wang, and W. Min, “stEnTrans: Transformer-Based Deep Learning for Spatial Transcriptomics Enhancement,” in *Lecture Notes in Computer Science (including subseries Lecture Notes in Artificial Intelligence and Lecture Notes in Bioinformatics)*, Springer Science and Business Media Deutschland GmbH, 2024, pp. 63–75. doi: 10.1007/978-981-97-5128-0_6.

[171] T. Azevedo *et al.*, “A deep graph neural network architecture for modelling spatio-temporal dynamics in resting-state functional MRI data,” *Med. Image Anal.*, vol. 79, Jul. 2022, doi: 10.1016/j.media.2022.102471.

[172] M. Moshawrab, M. Adda, A. Bouzouane, H. Ibrahim, and A. Raad, “Reviewing Multimodal Machine Learning and Its Use in Cardiovascular Diseases Detection,” *Electronics (Basel).*, vol. 12, no. 7, p. 1558, Jun. 2023, doi: 10.3390/electronics12071558.

[173] N. Kalkunte, J. Cisneros, E. Castillo, and J. Zoldan, “A review on machine learning approaches in cardiac tissue engineering,” *Frontiers in Biomaterials Science*, vol. 3, Apr. 2024, doi: 10.3389/fbiom.2024.1358508.

[174] V. Chen, M. Yang, W. Cui, J. S. Kim, A. Talwalkar, and J. Ma, “Applying interpretable machine learning in computational biology—pitfalls, recommendations and opportunities for new developments,” *Nat. Methods*, vol. 21, pp. 1454–1461, Aug. 2024, doi: 10.1038/s41592-024-02359-7.

[175] D. Sidak, J. Schwarzerová, W. Weckwerth, and S. Waldherr, “Interpretable machine learning methods for predictions in systems biology from omics data,” Oct. 2022, *Frontiers Media S.A.* doi: 10.3389/fmolb.2022.926623.

[176] Z. Wu, S. Pan, F. Chen, G. Long, C. Zhang, and P. S. Yu, “A Comprehensive Survey on Graph Neural Networks,” *IEEE Trans. Neural Netw. Learn. Syst.*, vol. 32, pp. 4–24, Jan. 2021, doi: 10.1109/TNNLS.2020.2978386.

[177] K. H. N. Bui, J. Cho, and H. Yi, “Spatial-temporal graph neural network for traffic forecasting: An overview and open research issues,” *Applied Intelligence*, vol. 52, pp. 2763–2774, Feb. 2022, doi: 10.1007/s10489-021-02587-w.

[178] L. Waikhom and R. Patgiri, “A survey of graph neural networks in various learning paradigms: methods, applications, and challenges,” *Artif. Intell. Rev.*, vol. 56, no. 7, pp. 6295–6364, 2023, doi: 10.1007/s10462-022-10321-2.

[179] S. Min, Z. Gao, J. Peng, L. Wang, K. Qin, and B. Fang, “STGSN — A Spatial–Temporal Graph Neural Network framework for time-evolving social networks,” *Knowl. Based. Syst.*, vol. 214, Feb. 2021, doi: 10.1016/j.knosys.2021.106746.

[180] L. Yu, B. Du, X. Hu, L. Sun, L. Han, and W. Lv, “Deep spatio-temporal graph convolutional network for traffic accident prediction,” *Neurocomputing*, vol. 423, pp. 135–147, 2021, doi: https://doi.org/10.1016/j.neucom.2020.09.043.

[181] C. Zheng *et al.*, “Spatio-Temporal Joint Graph Convolutional Networks for Traffic Forecasting,” *IEEE Trans. Knowl. Data Eng.*, vol. 36, pp. 372–385, Jan. 2024, doi: 10.1109/TKDE.2023.3284156.

[182] Y. Xu, X. Cai, E. Wang, W. Liu, Y. Yang, and F. Yang, “Dynamic traffic correlations based spatio-temporal graph convolutional network for urban traffic prediction,” *Inf. Sci. (N Y).*, vol. 621, pp. 580–595, Apr. 2023, doi: 10.1016/j.ins.2022.11.086.

[183] Z. Ge, J. Hou, and A. Nayak, “Forecasting SDN End-to-End Latency Using Graph Neural Network,” in *International Conference on Information Networking*, IEEE Computer Society, 2023, pp. 293–298. doi: 10.1109/ICOIN56518.2023.10048915.

[184] Z. Ge, J. Hou, and A. Nayak, “GNN-based End-to-end Delay Prediction in Software Defined Networking,” in *Proceedings - 18th Annual International Conference on Distributed Computing in Sensor Systems, DCOSS 2022*, Institute of Electrical and Electronics Engineers Inc., 2022, pp. 372–378. doi: 10.1109/DCOSS54816.2022.00066.

[185] H. Sha, M. Al Hasan, and G. Mohler, “Source detection on networks using spatial temporal graph convolutional networks,” in *2021 IEEE 8th International Conference on Data Science and Advanced Analytics, DSAA 2021*, Institute of Electrical and Electronics Engineers Inc., 2021. doi: 10.1109/DSAA53316.2021.9564188.

[186] Y. Guo, J. Huang, and X. Jiang, “Time series prediction based on the variable weight combination of the T-GCN-Luong attention and GRU models,” *Sci. Rep.*, vol. 15, Dec. 2025, doi: 10.1038/s41598-025-94388-1.

[187] L. Zhao *et al.*, “T-GCN: A Temporal Graph Convolutional Network for Traffic Prediction,” *IEEE Transactions on Intelligent Transportation Systems*, vol. 21, pp. 3848–3858, Sep. 2020, doi: 10.1109/TITS.2019.2935152.

[188] Y. Jin and M. Zhang, “Short-term load forecasting method based on adaptive graph convolutional recurrent network,” in *2023 3rd International Conference on Electrical Engineering and Mechatronics Technology, ICEEMT 2023*, Institute of Electrical and

Electronics Engineers Inc., 2023, pp. 818–821. doi: 10.1109/ICEEMT59522.2023.10263239.

[189] L. BAI, L. Yao, C. Li, X. Wang, and C. Wang, “Adaptive Graph Convolutional Recurrent Network for Traffic Forecasting,” https://proceedings.neurips.cc/paper/2020/hash/ce1aad92b939420fc17005e5461e6f48-Abstract.html?ref=https://githubhelp.com.

[190] C. Wang, C. Li, H. Huang, J. Qiu, J. Qu, and L. Yin, “ASNN-FRR: A traffic-aware neural network for fastest route recommendation,” *Geoinformatica*, vol. 27, no. 1, pp. 39–60, 2023, doi: 10.1007/s10707-021-00458-7.

[191] M. Ma *et al.*, “HiSTGNN: Hierarchical spatio-temporal graph neural network for weather forecasting,” *Inf. Sci. (N Y).*, vol. 648, p. 119580, 2023, doi: https://doi.org/10.1016/j.ins.2023.119580.

[192] P. Xuan, S. Pan, T. Zhang, Y. Liu, and H. Sun, “Graph convolutional network and convolutional neural network based method for predicting lncRNA-disease associations,” *Cells*, vol. 8, Sep. 2019, doi: 10.3390/cells8091012.

[193] M. Sarwar, H. Malik, and I. Zahra, “Innovative Computational Moulding Approach for Genomics,” in *4th International Conference on Innovative Computing, ICIC 2021*, Institute of Electrical and Electronics Engineers Inc., 2021. doi: 10.1109/ICIC53490.2021.9693059.

[194] M. Baranwal, R. L. Clark, J. Thompson, Z. Sun, A. O. Hero, and O. S. Venturelli, “Recurrent neural networks enable design of multifunctional synthetic human gut microbiome dynamics,” *Elife*, vol. 11, Jun. 2022, doi: 10.7554/eLife.73870.

[195] J. D. Davis, D. V Olivença, S. P. Brown, and E. O. Voit, “Methods of quantifying interactions among populations using Lotka-Volterra models,” *Frontiers in Systems Biology*, vol. Volume 2-2022, 2022, doi: 10.3389/fsysb.2022.1021897.

[196] V. Ponzi and C. Napoli, “Graph Neural Networks: Architectures, Applications, and Future Directions,” *IEEE Access*, vol. 13, pp. 62870–62891, 2025, doi: 10.1109/ACCESS.2025.3558752.

[197] N. Xu, C. Kosma, and M. Vazirgiannis, “TimeGNN: Temporal Dynamic Graph Learning for Time Series Forecasting,” in *Complex Networks & Their Applications XII*, H. Cherifi, L. M. Rocha, C. Cherifi, and M. Donduran, Eds., Cham: Springer Nature Switzerland, 2024, pp. 87–99.

[198] Z. Zhang, X. Wang, Z. Zhang, H. Li, Z. Qin, and W. Zhu, “Dynamic Graph Neural Networks Under Spatio-Temporal Distribution Shift,” https://proceedings.neurips.cc/paper_files/paper/2022/hash/2857242c9e97de339ce642e75b15ff24-Abstract-Conference.html.

[199] Y. You, T. Chen, Z. Wang, and Y. Shen, “Graph Domain Adaptation via Theory-Grounded Spectral Regularization,” https://par.nsf.gov/biblio/10419613.

[200] R. Singh, A. P. Wu, A. Mudide, and B. Berger, “Causal gene regulatory analysis with RNA velocity reveals an interplay between slow and fast transcription factors,” *Cell Syst.*, vol. 15, pp. 462-474.e5, May 2024, doi: 10.1016/j.cels.2024.04.005.

[201] Y. Wu *et al.*, “scGO: interpretable deep neural network for cell status annotation and disease diagnosis,” *Brief. Bioinform.*, vol. 26, no. 1, p. bbaf018, Jan. 2025, doi: 10.1093/bib/bbaf018.

[202] E. Rossi, B. Chamberlain, F. Frasca, D. Eynard, F. Monti, and M. Bronstein, “Temporal Graph Networks for Deep Learning on Dynamic Graphs,” Oct. 2020.

[203] Y. Li, G. Cai, F. Chen, K. Wen, and L. Ou-Yang, “Unveiling spatial domains from spatial multi-omics data using dual-graph regularized ensemble learning,” *Commun. Biol.*, vol. 8, Dec. 2025, doi: 10.1038/s42003-025-08372-6.

[204] S. G. Paul, A. Saha, M. Z. Hasan, S. R. H. Noori, and A. Moustafa, “A Systematic Review of Graph Neural Network in Healthcare-Based Applications: Recent Advances, Trends, and Future Directions,” *IEEE Access*, vol. 12, pp. 15145–15170, 2024, doi: 10.1109/ACCESS.2024.3354809.

[205] Z. Gao, K. Cao, and L. Wan, “Graspot: A graph attention network for spatial transcriptomics data integration with optimal transport,” *Bioinformatics*, vol. 40, pp. ii137–ii145, Sep. 2024, doi: 10.1093/bioinformatics/btae394.

[206] K. A. Lara Hernandez, T. Rienmüller, D. Baumgartner, and C. Baumgartner, “Deep learning in spatiotemporal cardiac imaging: A review of methodologies and clinical usability,” Mar. 2021, *Elsevier Ltd*. doi: 10.1016/j.compbiomed.2020.104200.

[207] Z. Mo and A. Siepel, “Domain-adaptive neural networks improve supervised machine learning based on simulated population genetic data,” *PLoS Genet.*, vol. 19, Nov. 2023, doi: 10.1371/journal.pgen.1011032.

[208] B. Williams *et al.*, “Prediction of Human Induced Pluripotent Stem Cell Cardiac Differentiation Outcome by Multifactorial Process Modeling,” *Front. Bioeng. Biotechnol.*, vol. 8, Jul. 2020, doi: 10.3389/fbioe.2020.00851.

[209] B. C. Knollmann, “Induced pluripotent stem cell-derived cardiomyocytes: Boutique science or valuable arrhythmia model?,” Mar. 2013. doi: 10.1161/CIRCRESAHA.112.300567.

[210] W. G. Miller *et al.*, “Overcoming challenges regarding reference materials and regulations that influence global standardization of medical laboratory testing results,” *Clin. Chem. Lab. Med.*, vol. 61, pp. 48–54, Jan. 2023, doi: 10.1515/cclm-2022-0943.

[211] Y. Zhu, R. Huang, Z. Wu, S. Song, L. Cheng, and R. Zhu, “Deep learning-based predictive identification of neural stem cell differentiation,” *Nat. Commun.*, vol. 12, Dec. 2021, doi: 10.1038/s41467-021-22758-0.

[212] N. Gangwar, K. Balraj, and A. S. Rathore, “Explainable AI for CHO cell culture media optimization and prediction of critical quality attribute,” *Appl. Microbiol. Biotechnol.*, vol. 108, no. 1, p. 308, Apr. 2024, doi: 10.1007/s00253-024-13147-w.

[213] Q. B. Baker, S. Singh, and A. Agrawal, “Single-Cell RNA-seq Data Analysis in the Era of Artificial Intelligence,” in *Next-Generation Sequencing*, CRC Press, 2025. [Online]. Available: https://www.taylorfrancis.com/chapters/edit/10.1201/9781003354062-13/single-cell-rna-seq-data-analysis-era-artificial-intelligence-qanita-bani-baker-sakshi-singh-ankit-agrawal

[214] X. Fu and P. A. Bates, “Application of deep learning methods: From molecular modelling to patient classification,” *Exp. Cell Res.*, vol. 418, Sep. 2022, doi: 10.1016/j.yexcr.2022.113278.

[215] G. Xie, C. Dong, Y. Kong, J. F. Zhong, M. Li, and K. Wang, “Group Lasso Regularized Deep Learning for Cancer Prognosis from Multi-Omics and Clinical Features,” *Genes (Basel).*, vol. 10, no. 3, p. 240, Jun. 2019, doi: 10.3390/genes10030240.

[216] V. Tozzo, C. A. Azencott, S. Fiorini, E. Fava, A. Trucco, and A. Barla, “Where Do We Stand in Regularization for Life Science Studies?,” *Journal of Computational Biology*, vol. 29, pp. 213–232, Mar. 2022, doi: 10.1089/cmb.2019.0371.

[217] S. Gupta, R. E. C. Lee, and J. R. Faeder, “Parallel Tempering with Lasso for model reduction in systems biology,” *PLoS Comput. Biol.*, vol. 16, 2020, doi: 10.1371/journal.pcbi.1007669.

[218] A. Sathyan, A. I. Weinberg, and K. Cohen, “Interpretable AI for bio-medical applications,” *Complex engineering systems (Alhambra, Calif.)*, vol. 2, no. 4, p. 18, Jun. 2022, doi: 10.20517/ces.2022.41.

[219] A. M. Hassan *et al.*, "A Surgeon's Guide to Artificial Intelligence-Driven Predictive Models," *American Surgeon*, vol. 89, pp. 11–19, Jan. 2023, doi: 10.1177/00031348221103648.

[220] S. Ahmed, M. Shamim Kaiser, M. S. Hossain, and K. Andersson, "A Comparative Analysis of LIME and SHAP Interpreters with Explainable ML-Based Diabetes Predictions," *IEEE Access*, 2024, doi: 10.1109/ACCESS.2024.3422319.

[221] S. Raptis, C. Ilioudis, and K. Theodorou, "From pixels to prognosis: unveiling radiomics models with SHAP and LIME for enhanced interpretability," *Biomed. Phys. Eng. Express*, vol. 10, May 2024, doi: 10.1088/2057-1976/ad34db.

[222] G. H. L, F. Flammini, and S. J, *Data Science & Exploration in Artificial Intelligence: Proceedings of the First International Conference On Data Science & Exploration in Artificial Intelligence (CODE-AI 2024) Bangalore, India, 3rd- 4th July, 2024 (Volume 2)*. CRC Press, 2025. [Online]. Available: https://books.google.co.za/books?hl=en&lr=&id=JDhEEQAAQBAJ&oi=fnd&pg=PA83&dq=%22SHAP+(Shapley+Additive+exPlanations)%22+AND+%22LIME+(Local+Interpretable+Model-Agnostic+Explanations)%22&ots=ZnZuqxKNdg&sig=LI_8PoXAXk-awOKQn8I7cbVuSgs&redir_esc=y#v=onepage&q=%22SHAP%20(Shapley%20Additive%20exPlanations)%22%20AND%20%22LIME%20(Local%20Interpretable%20Model-Agnostic%20Explanations)%22&f=false

[223] Z. Li, M. Bouazizi, T. Ohtsuki, M. Ishii, and E. Nakahara, "Toward Building Trust in Machine Learning Models: Quantifying the Explainability by SHAP and References to Human Strategy," *IEEE Access*, vol. 12, pp. 11010–11023, 2024, doi: 10.1109/ACCESS.2023.3347796.

[224] T. Danesh, R. Ouaret, P. Floquet, and S. Negny, "Interpretability of neural networks predictions using Accumulated Local Effects as a model-agnostic method," in *Computer Aided Chemical Engineering*, vol. 51, Elsevier B.V., 2022, pp. 1501–1506. doi: 10.1016/B978-0-323-95879-0.50251-4.

[225] F. K. Ewald, L. Bothmann, M. N. Wright, B. Bischl, G. Casalicchio, and G. König, "A Guide to Feature Importance Methods for Scientific Inference," L. Longo, S. Lapuschkin, and C. Seifert, Eds., Cham: Springer Nature Switzerland, 2024, pp. 440–464. doi: 10.1007/978-3-031-63797-1_22.

[226] H. Kaneko, "Cross-validated permutation feature importance considering correlation between features," *Analytical Science Advances*, vol. 3, pp. 278–287, Oct. 2022, doi: 10.1002/ansa.202200018.

[227] C. Molnar *et al.*, “Relating the Partial Dependence Plot and Permutation Feature Importance to the Data Generating Process,” L. Longo, Ed., Cham: Springer Nature Switzerland, 2023, pp. 456–479. doi: 10.1007/978-3-031-44064-9_24.

[228] A. Khan, A. Ali, J. Khan, F. Ullah, and M. Faheem, “Using Permutation-Based Feature Importance for Improved Machine Learning Model Performance at Reduced Costs,” *IEEE Access*, 2025, doi: 10.1109/ACCESS.2025.3544625.

[229] Q. Xu *et al.*, “Interpretability of Clinical Decision Support Systems Based on Artificial Intelligence from Technological and Medical Perspective: A Systematic Review,” 2023, *Hindawi Limited*. doi: 10.1155/2023/9919269.

[230] N. Rane, S. Choudhary, and J. Rane, “Explainable Artificial Intelligence (XAI) in healthcare: Interpretable Models for Clinical Decision Support,” *SSRN Electronic Journal*, 2023, doi: 10.2139/ssrn.4637897.

[231] P. Zhang *et al.*, “Single-cell RNA sequencing to track novel perspectives in HSC heterogeneity,” Dec. 2022, *BioMed Central Ltd*. doi: 10.1186/s13287-022-02718-1.

[232] M. Kang, S. Lee, D. Lee, and S. Kim, “Learning Cell-Type-Specific Gene Regulation Mechanisms by Multi-Attention Based Deep Learning With Regulatory Latent Space,” *Front. Genet.*, vol. 11, Sep. 2020, doi: 10.3389/fgene.2020.00869.

[233] T. Wang, Y. Fan, and X. Ma, “Attention Based Models for Cell Type Classification on Single-Cell RNA-Seq Data,” in *ECAI 2023*, IOS Press, 2023, pp. 2525–2532. [Online]. Available: https://ebooks.iospress.nl/doi/10.3233/FAIA230557

[234] S. Chakraborty, M. B. U. Talukder, M. M. Hasan, J. Noor, and J. Uddin, “BiGRU-ANN based hybrid architecture for intensified classification tasks with explainable AI,” *International Journal of Information Technology*, vol. 15, no. 8, pp. 4211–4221, 2023, doi: 10.1007/s41870-023-01515-0.

[235] P. Isavand, S. S. Aghamiri, and R. Amin, “Applications of Multimodal Artificial Intelligence in Non-Hodgkin Lymphoma B Cells,” Aug. 2024, *Multidisciplinary Digital Publishing Institute (MDPI)*. doi: 10.3390/biomedicines12081753.

[236] X. Cheng, J. Wang, H. Li, Y. Zhang, L. Wu, and Y. Liu, “A method to evaluate task-specific importance of spatio-temporal units based on explainable artificial intelligence,” *International Journal of Geographical Information Science*, vol. 35, pp. 2002–2025, 2021, doi: 10.1080/13658816.2020.1805116.

[237] R. Ying, D. Bourgeois, J. You, M. Zitnik, and J. Leskovec, “GNNExplainer: Generating Explanations for Graph Neural Networks,” *Adv. Neural Inf. Process. Syst.*, vol. 32, pp.

9240–9251, 2019, [Online]. Available: https://www.ncbi.nlm.nih.gov/pmc/articles/PMC7138248/

[238] M. Nandan, S. Mitra, and D. De, “GraphXAI: a survey of graph neural networks (GNNs) for explainable AI (XAI),” *Neural Comput. Appl.*, vol. 37, no. 17, pp. 10949–11000, 2025, doi: 10.1007/s00521-025-11054-3.

[239] H. Yuan, H. Yu, S. Gui, and S. Ji, “Explainability in Graph Neural Networks: A Taxonomic Survey,” *IEEE Trans. Pattern Anal. Mach. Intell.*, vol. 45, pp. 5782–5799, May 2023, doi: 10.1109/TPAMI.2022.3204236.

[240] Y. Rong *et al.*, “Efficient GNN Explanation via Learning Removal-based Attribution,” *ACM Trans. Knowl. Discov. Data*, vol. 19, Feb. 2025, doi: 10.1145/3685678.

[241] M. S. Schlichtkrull, N. De Cao, and I. Titov, “INTERPRETING GRAPH NEURAL NETWORKS FOR NLP WITH DIFFERENTIABLE EDGE MASKING,” in *ICLR 2021 - 9th International Conference on Learning Representations*, International Conference on Learning Representations, ICLR, 2021.

[242] S. Miao, M. Liu, and P. Li, “Interpretable and Generalizable Graph Learning via Stochastic Attention Mechanism,” in *Proceedings of Machine Learning Research*, ML Research Press, 2022, pp. 15524–15543.

[243] W. Zhang, X. Li, and W. Nejdl, “Adversarial Mask Explainer for Graph Neural Networks,” in *WWW 2024 - Proceedings of the ACM Web Conference*, Association for Computing Machinery, Inc, May 2024, pp. 861–869. doi: 10.1145/3589334.3645608.

[244] D. Nguyen, T. Le, and B. Le, “FleX: Interpreting Graph Neural Networks with Subgraph Extraction and Flexible Objective Estimation,” in *Lecture Notes in Computer Science*, Springer Science and Business Media Deutschland GmbH, 2025, pp. 204–221. doi: 10.1007/978-3-031-81375-7_12.

[245] H. Yuan, H. Yu, J. Wang, K. Li, and S. Ji, “On Explainability of Graph Neural Networks via Subgraph Explorations,” in *Proceedings of Machine Learning Research*, ML Research Press, 2021, pp. 12241–12252.

[246] Z. Ye, R. Huang, Q. Wu, and Q. Liu, “SAME: Uncovering GNN Black Box with Structure-aware Shapley-based Multipiece Explanations,” https://proceedings.neurips.cc/paper_files/paper/2023/hash/14cdc9013d80338bf81483a7736ea05c-Abstract-Conference.html.

[247] T. Schnake *et al.*, “Higher-Order Explanations of Graph Neural Networks via Relevant Walks,” *IEEE Trans. Pattern Anal. Mach. Intell.*, vol. 44, pp. 7581–7596, Nov. 2022, doi: 10.1109/TPAMI.2021.3115452.

[248] S. Serrano and N. A. Smith, “Is attention interpretable?,” in *ACL 2019 - 57th Annual Meeting of the Association for Computational Linguistics, Proceedings of the Conference*, Association for Computational Linguistics (ACL), 2020, pp. 2931–2951. doi: 10.18653/v1/p19-1282.

[249] N. El Houda Dehimi and Z. Tolba, “Attention Mechanisms in Deep Learning : Towards Explainable Artificial Intelligence,” in *PAIS 2024 - Proceedings: 6th International Conference on Pattern Analysis and Intelligent Systems*, Institute of Electrical and Electronics Engineers Inc., 2024. doi: 10.1109/PAIS62114.2024.10541203.

[250] D. H. Nguyen, G. Gravier, and P. Sebillot, “A Study of the Plausibility of Attention between RNN Encoders in Natural Language Inference,” in *Proceedings - 20th IEEE International Conference on Machine Learning and Applications, ICMLA 2021*, Institute of Electrical and Electronics Engineers Inc., 2021, pp. 1623–1629. doi: 10.1109/ICMLA52953.2021.00259.

[251] A. Hernández and J. M. Amigó, “Attention Mechanisms and Their Applications to Complex Systems,” *Entropy*, vol. 23, no. 3, 2021, doi: 10.3390/e23030283.

[252] M. Tutek and J. Snajder, “Toward Practical Usage of the Attention Mechanism as a Tool for Interpretability,” *IEEE Access*, vol. 10, pp. 47011–47030, 2022, doi: 10.1109/ACCESS.2022.3169772.

[253] A. A. Ismail, M. Gunady, H. Corrada Bravo, and S. Feizi, “Benchmarking deep learning interpretability in time series predictions,” *Adv. Neural Inf. Process. Syst.*, vol. 33, pp. 6441–6452, 2020.

[254] Q. Sun, A. Akman, and B. W. Schuller, “Explainable Artificial Intelligence for Medical Applications: A Review,” *ACM Trans. Comput. Healthcare*, vol. 6, no. 2, Feb. 2025, doi: 10.1145/3709367.

[255] R. Achtibat *et al.*, “From attribution maps to human-understandable explanations through Concept Relevance Propagation,” *Nat. Mach. Intell.*, vol. 5, pp. 1006–1019, Sep. 2023, doi: 10.1038/s42256-023-00711-8.

[256] Y. Gao, N. Lewis, V. D. Calhoun, and R. L. Miller, “Interpretable LSTM model reveals transiently-realized patterns of dynamic brain connectivity that predict patient deterioration or recovery from very mild cognitive impairment,” *Comput. Biol. Med.*,

vol. 161, p. 107005, 2023, doi: https://doi.org/10.1016/j.compbiomed.2023.107005.

[257] T.-Y. Lee, J. van Baar, K. Wittenburg, and A. Sullivan, “Analysis of the contribution and temporal dependency of LSTM layers for reinforcement learning tasks.,” in *CVPR Workshops*, 2019, pp. 99–102.

[258] Q. Pan, W. Hu, and J. Zhu, “Series saliency: Temporal interpretation for multivariate time series forecasting,” *arXiv preprint arXiv:2012.09324*, 2020.

[259] Q. Pan, W. Hu, and N. Chen, “Two Birds with One Stone: Series Saliency for Accurate and Interpretable Multivariate Time Series Forecasting,” in *IJCAI International Joint Conference on Artificial Intelligence*, International Joint Conferences on Artificial Intelligence, 2021, pp. 2884–2891. doi: 10.24963/ijcai.2021/397.

[260] A. Katrompas and V. Metsis, “Temporal Attention Signatures for Interpretable Time-Series Prediction,” in *Artificial Neural Networks and Machine Learning – ICANN 2023*, L. Iliadis, A. Papaleonidas, P. Angelov, and C. Jayne, Eds., Cham: Springer Nature Switzerland, 2023, pp. 268–280.

[261] H. Fang *et al.*, “InsGNN: Interpretable spatio-temporal graph neural networks via information bottleneck,” *Information Fusion*, vol. 119, Jul. 2025, doi: 10.1016/j.inffus.2025.102997.

[262] R. Xie, A. Zeng, D. Pan, and J. Zhao, “Cgfb-Gnn: Explainable Spatio-Temporal Gnn for Cognition-Guided,” Rochester, NY, 2025. [Online]. Available: https://papers.ssrn.com/abstract=5236456

[263] B. Gao *et al.*, “An Explainable Unified Framework of Spatio-Temporal Coupling Learning With Application to Dynamic Brain Functional Connectivity Analysis,” *IEEE Trans. Med. Imaging*, vol. 44, pp. 941–951, 2025, doi: 10.1109/TMI.2024.3467384.

[264] G. Liang, P. Tiwari, S. Nowaczyk, and S. Byttner, “Higher-order Spatio-temporal Physics-incorporated Graph Neural Network for Multivariate Time Series Imputation,” in *Proceedings of the 33rd ACM International Conference on Information and Knowledge Management*, in CIKM ’24. New York, NY, USA: Association for Computing Machinery, 2024, pp. 1356–1366. doi: 10.1145/3627673.3679775.

[265] X. Cui, D. Wang, and Z. J. Wang, “Multi-Scale Interpretation Model for Convolutional Neural Networks: Building Trust Based on Hierarchical Interpretation,” *IEEE Trans. Multimedia*, vol. 21, pp. 2263–2276, Sep. 2019, doi: 10.1109/TMM.2019.2902099.

[266] D. Yang, Y. Wang, Y. Ma, and H. Yang, “A Multi-Scale Interpretability-Based PET-CT Tumor Segmentation Method,” *Mathematics*, vol. 13, no. 7, p. 1139, Jan. 2025, doi: 10.3390/math13071139.

[267] N. A. Daryakenari, M. De Florio, K. Shukla, and G. E. Karniadakis, “AI-Aristotle: A physics-informed framework for systems biology gray-box identification,” *PLoS Comput. Biol.*, vol. 20, no. 3, p. e1011916, 2024, doi: 10.1371/journal.pcbi.1011916.

[268] M. Ahmadi, D. Biswas, M. Lin, F. D. Vrionis, J. Hashemi, and Y. Tang, “Physics-informed machine learning for advancing computational medical imaging: integrating data-driven approaches with fundamental physical principles,” *Artif. Intell. Rev.*, vol. 58, no. 10, p. 297, 2025, doi: 10.1007/s10462-025-11303-w.

[269] A. Chinnaraju, “Explainable AI (XAI) for trustworthy and transparent decision-making: A theoretical framework for AI interpretability,” *World Journal of Advanced Engineering Technology and Sciences*, vol. 14, no. 3, pp. 170–207, 2025.

[270] C. Selvan, T. Mohan, A. Ragunathan, and M. Mythily, “Graph-driven unified interpretability with BERT in deep NLP models for text classification,” *International Journal of Information Technology (Singapore)*, 2025, doi: 10.1007/s41870-025-02623-9.

[271] M. Al Olaimat, S. Bozdag, and for the A. D. N. Initiative, “TA-RNN: an attention-based time-aware recurrent neural network architecture for electronic health records,” *Bioinformatics*, vol. 40, no. Supplement_1, pp. i169–i179, Jul. 2024, doi: 10.1093/bioinformatics/btae264.

[272] W. Du, Y. Wang, and Y. Qiao, “Recurrent spatial-temporal attention network for action recognition in videos,” *IEEE Transactions on Image Processing*, vol. 27, pp. 1347–1360, Mar. 2018, doi: 10.1109/TIP.2017.2778563.

[273] N. A. Obuchowski and J. A. Bullen, “Receiver operating characteristic (ROC) curves: Review of methods with applications in diagnostic medicine,” *Phys. Med. Biol.*, vol. 63, Mar. 2018, doi: 10.1088/1361-6560/aab4b1.

[274] J. Li, “Area under the ROC Curve has the most consistent evaluation for binary classification,” *PLoS One*, vol. 19, Dec. 2024, doi: 10.1371/journal.pone.0316019.

[275] C. Miller, T. Portlock, D. M. Nyaga, and J. M. O’Sullivan, “A review of model evaluation metrics for machine learning in genetics and genomics,” 2024, *Frontiers Media SA*. doi: 10.3389/fbinf.2024.1457619.

[276] G. Naidu, T. Zuva, and E. M. Sibanda, “A Review of Evaluation Metrics in Machine Learning Algorithms,” in *Artificial Intelligence Application in Networks and Systems*, R. Silhavy and P. Silhavy, Eds., Cham: Springer International Publishing, 2023, pp. 15–25.

[277] L. Abualigah *et al.*, “Artificial intelligence-driven translational medicine: a machine learning framework for predicting disease outcomes and optimizing patient-centric care,” *J. Transl. Med.*, vol. 23, Dec. 2025, doi: 10.1186/s12967-025-06308-6.

[278] Ž. Vujović, “Classification Model Evaluation Metrics,” *International Journal of Advanced Computer Science and Applications*, vol. 12, pp. 599–606, 2021, doi: 10.14569/IJACSA.2021.0120670.

[279] Samrachana Adhikari, Sharon-Lise Normand, Jordan Bloom, David Shahian, and Sherri Rose, “Revisiting performance metrics for prediction with rare outcomes,” *Stat. Methods Med. Res.*, vol. 30, no. 10, pp. 2352–2366, Sep. 2021, doi: 10.1177/09622802211038754.

[280] Y. M. Jaradat, M. A. Alia, M. Z. Masoud, A. A. Manasrah, I. A. Jannoud, and O. Alheyasat, “Beyond One-Size-Fits-All: Comparing and Selecting Regression Metrics for Robust Model Assessment,” in *2025 12th International Conference on Information Technology (ICIT)*, 2025, pp. 416–422. doi: 10.1109/ICIT64950.2025.11049268.

[281] A. Rajkomar *et al.*, “Reply: metrics to assess machine learning models,” Dec. 2018, *Nature Publishing Group*. doi: 10.1038/s41746-018-0063-z.

[282] L. Jiao, Y. Ren, L. Wang, C. Gao, S. Wang, and T. Song, “MulCNN: An efficient and accurate deep learning method based on gene embedding for cell type identification in single-cell RNA-seq data,” *Front. Genet.*, vol. 14, 2023, doi: 10.3389/fgene.2023.1179859.

[283] W. Chen *et al.*, “Commonly used software tools produce conflicting and overly-optimistic AUPRC values,” *Genome Biol.*, vol. 25, no. 1, p. 118, 2024, doi: 10.1186/s13059-024-03266-y.

[284] Y. Li *et al.*, “A comparative benchmarking and evaluation framework for heterogeneous network-based drug repositioning methods,” *Brief. Bioinform.*, vol. 25, May 2024, doi: 10.1093/bib/bbae172.

[285] Marcia Saul and Shahin Rostami, “Assessing performance of artificial neural networks and re-sampling techniques for healthcare datasets,” *Health Informatics*

J., vol. 28, no. 1, p. 14604582221087108, Jan. 2022, doi: 10.1177/14604582221087109.

[286] L. Meyer, D. Mulder, and J. Wallace, "A supervised machine learning approach with feature selection for sex-specific biomarker prediction," *NPJ Syst. Biol. Appl.*, vol. 11, no. 1, p. 69, 2025, doi: 10.1038/s41540-025-00523-z.

[287] B. Zhang, H. Ren, G. Huang, Y. Cheng, and C. Hu, "Predicting blood pressure from physiological index data using the SVR algorithm," *BMC Bioinformatics*, vol. 20, Feb. 2019, doi: 10.1186/s12859-019-2667-y.

[288] J. Singh Kushwah, A. Kumar, S. Patel, R. Soni, A. Gawande, and S. Gupta, "Comparative study of regressor and classifier with decision tree using modern tools," *Mater. Today Proc.*, vol. 56, pp. 3571–3576, Jan. 2022, doi: 10.1016/j.matpr.2021.11.635.

[289] S. S. Sudha, A. Baradwaz, A. Y. Javaid, and A. C. Jayasuriya, "Prediction of Proliferation Rate of Pre-Osteoblasts Using Raman Spectroscopy and Machine Learning Models," *Journal of Raman Spectroscopy*, 2025, doi: 10.1002/jrs.6817.

[290] P. K. Yadalam, P. M. Natarajan, M. H. Saeed, and C. M. Ardila, "Variational Approaches for Drug-Disease-Gene Links in Periodontal Inflammation," *Int. Dent. J.*, vol. 75, pp. 185–194, Feb. 2025, doi: 10.1016/j.identj.2024.09.025.

[291] D. Chicco, M. J. Warrens, and G. Jurman, "The coefficient of determination R-squared is more informative than SMAPE, MAE, MAPE, MSE and RMSE in regression analysis evaluation," *PeerJ Comput. Sci.*, vol. 7, pp. 1–24, 2021, doi: 10.7717/PEERJ-CS.623.

[292] S. Nakagawa, P. C. D. Johnson, and H. Schielzeth, "The coefficient of determination R2 and intra-class correlation coefficient from generalized linear mixed-effects models revisited and expanded," *J. R. Soc. Interface*, vol. 14, no. 134, p. 20170213, Sep. 2017, doi: 10.1098/rsif.2017.0213.

[293] J. Ren *et al.*, "Spatiotemporally resolved transcriptomics reveals the subcellular RNA kinetic landscape," *Nat. Methods*, vol. 20, pp. 695–705, May 2023, doi: 10.1038/s41592-023-01829-8.

[294] N. Chakraborty, A. Lawrence, R. Campbell, R. Yang, and R. Hammamieh, "Biomarker discovery process at binomial decision point (2BDP): Analytical pipeline to construct biomarker panel," *Comput. Struct. Biotechnol. J.*, vol. 21, pp. 4729–4742, Jan. 2023, doi: 10.1016/j.csbj.2023.09.025.

[295] A. Gupta, T. S. Stead, and L. Ganti, “Determining a Meaningful R-squared Value in Clinical Medicine,” *Academic Medicine & Surgery*, Oct. 2024, doi: 10.62186/001c.125154.

[296] C. Huang *et al.*, “Performance Metrics for the Comparative Analysis of Clinical Risk Prediction Models Employing Machine Learning,” *Circ. Cardiovasc. Qual. Outcomes*, vol. 14, p. E007526, Oct. 2021, doi: 10.1161/CIRCOUTCOMES.120.007526.

[297] W. Yang, J. Jiang, E. M. Schnellinger, S. E. Kimmel, and W. Guo, “Modified Brier score for evaluating prediction accuracy for binary outcomes,” *Stat. Methods Med. Res.*, vol. 31, pp. 2287–2296, Dec. 2022, doi: 10.1177/09622802221122391.

[298] T. Silva Filho, H. Song, M. Perello-Nieto, R. Santos-Rodriguez, M. Kull, and P. Flach, “Classifier calibration: a survey on how to assess and improve predicted class probabilities,” *Mach. Learn.*, vol. 112, no. 9, pp. 3211–3260, 2023, doi: 10.1007/s10994-023-06336-7.

[299] Z. Onódi *et al.*, “Systematic transcriptomic and phenotypic characterization of human and murine cardiac myocyte cell lines and primary cardiomyocytes reveals serious limitations and low resemblances to adult cardiac phenotype,” *J. Mol. Cell. Cardiol.*, vol. 165, pp. 19–30, Apr. 2022, doi: 10.1016/j.yjmcc.2021.12.007.

[300] Y. Huang, W. Li, F. Macheret, R. A. Gabriel, and L. Ohno-Machado, “A tutorial on calibration measurements and calibration models for clinical prediction models,” 2021, *Oxford University Press*. doi: 10.1093/JAMIA/OCZ228.

[301] T. Dimitriadis, T. Gneiting, and A. I. Jordan, “Stable reliability diagrams for probabilistic classifiers,” *Proc. Natl. Acad. Sci. U. S. A.*, vol. 118, Feb. 2021, doi: 10.1073/pnas.2016191118.

[302] M. Esna-Ashari, “Beyond the Black Box: A Review of Quantitative Metrics for Neural Network Interpretability and Their Practical Implications,” *International journal of sustainable applied science and engineering*, vol. 2, no. 1, pp. 1–24, Feb. 2025, doi: 10.22034/ijsase.v2i1.133.

[303] M. Miró-Nicolau, A. Jaume-i-Capó, and G. Moyà-Alcover, “A comprehensive study on fidelity metrics for XAI,” *Inf. Process. Manag.*, vol. 62, no. 1, p. 103900, 2025, doi: https://doi.org/10.1016/j.ipm.2024.103900.

[304] Mintu Debnath, “Mathematical Foundations of Explainable AI: A Framework based on Topological Data Analysis,” *Communications on Applied Nonlinear Analysis*, vol. 32, pp. 3119–3142, Mar. 2025, doi: 10.52783/cana.v32.4650.

[305] O. O. Bifarin, “Interpretable machine learning with tree-based shapley additive explanations: Application to metabolomics datasets for binary classification,” *PLoS One*, vol. 18, no. 5, pp. e0284315-, May 2023, [Online]. Available: https://doi.org/10.1371/journal.pone.0284315

[306] X. Zheng *et al.*, “F-Fidelity: A Robust Framework for Faithfulness Evaluation of Explainable AI,” *ArXiv*, vol. abs/2410.02970, 2024, [Online]. Available: https://api.semanticscholar.org/CorpusID:273162732

[307] A. M. Salih *et al.*, “A Perspective on Explainable Artificial Intelligence Methods: SHAP and LIME,” *Advanced Intelligent Systems*, vol. 7, Jan. 2025, doi: 10.1002/aisy.202400304.

[308] R. Y. Li, Z. Wang, J. Guan, and S. Zhou, “Effectively Clustering Single Cell RNA Sequencing Data by Sparse Representation,” *IEEE/ACM Trans. Comput. Biol. Bioinform.*, vol. 19, pp. 3425–3434, Nov. 2022, doi: 10.1109/TCBB.2021.3128576.

[309] E. Kurtic *et al.*, “Sparse Fine-Tuning for Inference Acceleration of Large Language Models,” in *Enhancing LLM Performance: Efficacy, Fine-Tuning, and Inference Techniques*, P. Passban, A. Way, and M. Rezagholizadeh, Eds., Cham: Springer Nature Switzerland, 2025, pp. 83–97. doi: 10.1007/978-3-031-85747-8_6.

[310] Z. Chen *et al.*, “DECODE: A Deep-learning framework for Condensing enhancers and refining boundaries with large-scale functional assays,” *Bioinformatics*, vol. 37, pp. I280–I288, Jul. 2021, doi: 10.1093/bioinformatics/btab283.

[311] P. Lou Bommer, M. Kretschmer, A. Hedström, D. Bareeva, and M. M.-C. Höhne, “Finding the Right XAI Method—A Guide for the Evaluation and Ranking of Explainable AI Methods in Climate Science,” *Artificial Intelligence for the Earth Systems*, vol. 3, no. 3, p. e230074, 2024, doi: https://doi.org/10.1175/AIES-D-23-0074.1.

[312] M. Miró-Nicolau, A. Jaume-i-Capó, and G. Moyà-Alcover, “Assessing fidelity in XAI post-hoc techniques: A comparative study with ground truth explanations datasets,” *Artif. Intell.*, vol. 335, p. 104179, 2024, doi: https://doi.org/10.1016/j.artint.2024.104179.

[313] J. L. Ballard, Z. Wang, W. Li, L. Shen, and Q. Long, “Deep learning-based approaches for multi-omics data integration and analysis,” Dec. 2024, *BioMed Central Ltd*. doi: 10.1186/s13040-024-00391-z.

[314] T. Lei, R. Chen, S. Zhang, and Y. Chen, “Self-supervised deep clustering of single-cell RNA-seq data to hierarchically detect rare cell populations.,” *Brief. Bioinform.*, vol. 24, Sep. 2023, doi: 10.1093/bib/bbad335.

[315] J. A. Palmer, N. Rosenthal, S. A. Teichmann, and M. Litvinukova, “Revisiting Cardiac Biology in the Era of Single Cell and Spatial Omics,” Jun. 2024. doi: 10.1161/CIRCRESAHA.124.323672.

[316] S. Cho, D. E. Discher, K. W. Leong, G. Vunjak-Novakovic, and J. C. Wu, “Challenges and opportunities for the next generation of cardiovascular tissue engineering,” *Nat. Methods*, vol. 19, pp. 1064–1071, Sep. 2022, doi: 10.1038/s41592-022-01591-3.

[317] H. Nosrati and M. Nosrati, “Artificial Intelligence in Regenerative Medicine: Applications and Implications,” *Biomimetics*, vol. 8, no. 5, 2023, doi: 10.3390/biomimetics8050442.

[318] T. M. Pentimalli, N. Karaiskos, and N. Rajewsky, “Challenges and Opportunities in the Clinical Translation of High-Resolution Spatial Transcriptomics,” *Annual Review of Pathology: Mechanisms of Disease*, vol. 20, no. Volume 20, 2025, pp. 405–432, 2025, doi: https://doi.org/10.1146/annurev-pathmechdis-111523-023417.

[319] L. Zhang *et al.*, “Clinical and translational values of spatial transcriptomics,” Dec. 2022, *Springer Nature*. doi: 10.1038/s41392-022-00960-w.

[320] R. Vitorino, “Transforming Clinical Research: The Power of High-Throughput Omics Integration,” *Proteomes*, vol. 12, no. 3, 2024, doi: 10.3390/proteomes12030025.

[321] S. A. Niederer, J. Lumens, and N. A. Trayanova, “Computational models in cardiology,” Feb. 2019, *Nature Publishing Group*. doi: 10.1038/s41569-018-0104-y.

[322] F. Sun, W. Hao, A. Zou, and Q. Shen, “A survey on spatio-temporal series prediction with deep learning: taxonomy, applications, and future directions,” *Neural Comput. Appl.*, vol. 36, no. 17, pp. 9919–9943, 2024, doi: 10.1007/s00521-024-09659-1.

[323] B. Velten and O. Stegle, “Principles and challenges of modeling temporal and spatial omics data,” Oct. 2023, *Nature Research*. doi: 10.1038/s41592-023-01992-y.

[324] X. Liu *et al.*, “Spatial multi-omics: deciphering technological landscape of integration of multi-omics and its applications,” Dec. 2024, *BioMed Central Ltd*. doi: 10.1186/s13045-024-01596-9.

[325] Feiyan Sun, Wenning Hao, Ao Zou, and Kai Cheng, “TVGCN: Time-varying graph convolutional networks for multivariate and multifeature spatiotemporal series

prediction," *Sci. Prog.*, vol. 107, no. 3, p. 00368504241283315, Jul. 2024, doi: 10.1177/00368504241283315.

[326] K. Lazaros, D. E. Koumadorakis, P. Vlamos, and A. G. Vrahatis, "Graph neural network approaches for single-cell data: a recent overview," *Neural Comput. Appl.*, vol. 36, no. 17, pp. 9963–9987, 2024, doi: 10.1007/s00521-024-09662-6.

[327] S. Ge, S. Sun, H. Xu, Q. Cheng, and Z. Ren, "Deep learning in single-cell and spatial transcriptomics data analysis: advances and challenges from a data science perspective," *Brief. Bioinform.*, vol. 26, no. 2, p. bbaf136, Mar. 2025, doi: 10.1093/bib/bbaf136.

[328] J. Duan, J. Xiong, Y. Li, and W. Ding, "Deep learning based multimodal biomedical data fusion: An overview and comparative review," *Information Fusion*, vol. 112, p. 102536, 2024, doi: https://doi.org/10.1016/j.inffus.2024.102536.

[329] X. Xu *et al.*, "A Comprehensive Review on Synergy of Multi-Modal Data and AI Technologies in Medical Diagnosis," *Bioengineering*, vol. 11, no. 3, 2024, doi: 10.3390/bioengineering11030219.

[330] A. Pezhouman, N. B. Nguyen, M. Kay, B. Kanjilal, I. Noshadi, and R. Ardehali, "Cardiac regeneration – Past advancements, current challenges, and future directions," *J. Mol. Cell. Cardiol.*, vol. 182, pp. 75–85, Sep. 2023, doi: 10.1016/j.yjmcc.2023.07.009.

[331] D. Thomas, N. J. Cunningham, S. Shenoy, and J. C. Wu, "Human-induced pluripotent stem cells in cardiovascular research: Current approaches in cardiac differentiation, maturation strategies, and scalable production," Jan. 2022, *Oxford University Press*. doi: 10.1093/cvr/cvab115.

[332] C. S. P. Soares and M. H. L. Ribeiro, "Induced Pluripotent Stem Cell-Derived Cardiomyocytes: From Regulatory Status to Clinical Translation," Aug. 2024, *Mary Ann Liebert Inc.* doi: 10.1089/ten.teb.2023.0080.

[333] S. Pandit, T. Jamal, A. Ali, and R. Parthasarathi, "Multiscale computational and machine learning models for designing stem cell-based regenerative medicine therapies," in *Computational Biology for Stem Cell Research*, Elsevier, 2024, pp. 433–442. doi: 10.1016/B978-0-443-13222-3.00027-7.

[334] M. Ashraf, M. Khalilitousi, and Z. Laksman, "Applying Machine Learning to Stem Cell Culture and Differentiation," *Curr. Protoc.*, vol. 1, Sep. 2021, doi: 10.1002/cpz1.261.

[335] K. Choe, U. Pak, Y. Pang, W. Hao, and X. Yang, “Advances and Challenges in Spatial Transcriptomics for Developmental Biology,” Jan. 2023, *MDPI*. doi: 10.3390/biom13010156.

[336] M. A. Pala, “Graph-Aware AURALSTM: An Attentive Unified Representation Architecture with BiLSTM for Enhanced Molecular Property Prediction,” *Mol. Divers.*, 2025, doi: 10.1007/s11030-025-11197-4.

[337] C. B. Collin *et al.*, “Computational Models for Clinical Applications in Personalized Medicine—Guidelines and Recommendations for Data Integration and Model Validation,” *J. Pers. Med.*, vol. 12, Feb. 2022, doi: 10.3390/jpm12020166.

[338] S. Liu *et al.*, “A hybrid method of recurrent neural network and graph neural network for next-period prescription prediction,” *International Journal of Machine Learning and Cybernetics*, vol. 11, no. 12, p. 2849, Dec. 2020, doi: 10.1007/S13042-020-01155-X.

[339] D. Wilimitis and C. G. Walsh, “Practical Considerations and Applied Examples of Cross-Validation for Model Development and Evaluation in Health Care: Tutorial.,” *JMIR AI*, vol. 2, no. 1, p. e49023, Dec. 2023, doi: 10.2196/49023.

[340] T. J. Bradshaw, Z. Huemann, J. Hu, and A. Rahmim, “A Guide to Cross-Validation for Artificial Intelligence in Medical Imaging,” *Radiol. Artif. Intell.*, vol. 5, no. 4, p. e220232, Jul. 2023, doi: 10.1148/RYAI.220232.

[341] P. A. Lachenbruch, “McNemar Test,” *Wiley StatsRef: Statistics Reference Online*, Sep. 2014, doi: 10.1002/9781118445112.STAT04876.

[342] O. Kramer, “Scikit-Learn,” *Studies in Big Data*, vol. 20, pp. 45–53, 2016, doi: 10.1007/978-3-319-33383-0_5/FIGURES/2.

[343] F. A. Wolf, P. Angerer, and F. J. Theis, “SCANPY: Large-scale single-cell gene expression data analysis,” *Genome Biol.*, vol. 19, no. 1, pp. 1–5, Feb. 2018, doi: 10.1186/S13059-017-1382-0/FIGURES/1.

[344] S. Imambi, K. B. Prakash, and G. R. Kanagachidambaresan, “PyTorch,” *EAI/Springer Innovations in Communication and Computing*, pp. 87–104, 2021, doi: 10.1007/978-3-030-57077-4_10/FIGURES/17.

[345] K. A. Frazer *et al.*, “A second generation human haplotype map of over 3.1 million SNPs,” *Nature*, vol. 449, no. 7164, pp. 851–861, 2007, doi: 10.1038/nature06258.

[346] M. Barker *et al.*, “Introducing the FAIR Principles for research software,” *Sci. Data*, vol. 9, no. 1, pp. 1–6, Dec. 2022, doi: 10.1038/S41597-022-01710-X;SUBJMETA.

[347] I. Peters, P. Kraker, E. Lex, C. Gumpenberger, and J. I. Gorraiz, “Zenodo in the Spotlight of Traditional and New Metrics,” *Front. Res. Metr. Anal.*, vol. 2, p. 318745, Dec. 2017, doi: 10.3389/FRMA.2017.00013/BIBTEX.

[348] W. Zhang, S. Shi, and Q. Qi, “Deep graph convolutional neural network for one-dimensional hepatic vascular haemodynamic prediction,” *bioRxiv*, p. 2024.08.13.607720, Aug. 2024, doi: 10.1101/2024.08.13.607720.

[349] H. Cui *et al.*, “scGPT: toward building a foundation model for single-cell multi-omics using generative AI,” *Nat. Methods*, vol. 21, no. 8, pp. 1470–1480, Aug. 2024, doi: 10.1038/S41592-024-02201-0;SUBJMETA.

[350] J. Banus, A. C. Ogier, R. Hullin, P. Meyer, R. B. van Heeswijk, and J. Richiardi, “Spatiotemporal graph neural process for reconstruction, extrapolation, and classification of cardiac trajectories,” Sep. 2025, Accessed: Sep. 26, 2025. [Online]. Available: https://arxiv.org/pdf/2509.12953v1

APPENDICES

APPENDIX A – MATHEMATICAL EQUATIONS

Introduction

This document presents the complete mathematical formulation of the Hybrid Graph Neural Network and Recurrent Neural Network (GNN-RNN) model for predicting cardiomyocyte differentiation trajectories. The model integrates spatial transcriptomics data through GNN processing and temporal gene expression patterns via RNN processing, achieving superior classification performance through multimodal fusion strategies.

Graph Neural Network (GNN) Component

Graph Attention Network (GAT) Node Update

The node representation update in the Graph Attention Network follows:

$$\mathbf{h}_i^{(l+1)} = \sigma\left(\sum_{j \in \mathcal{N}(i)} \alpha_{ij}^{(l)} \mathbf{W}^{(l)} \mathbf{h}_j^{(l)}\right)$$

where:

- $\mathbf{h}_i^{(l)} \in \mathbb{R}^{d^{(l)}}$ is the feature vector of node i at layer l
- $\mathcal{N}(i)$ denotes the spatial neighborhood of node i
- $\alpha_{ij}^{(l)}$ is the attention coefficient between nodes i and j at layer l
- $\mathbf{W}^{(l)} \in \mathbb{R}^{d^{(l+1)} \times d^{(l)}}$ is the learnable weight matrix
- $\sigma(\cdot)$ is the activation function (LeakyReLU)

Attention Mechanism

The attention coefficients are computed using the attention mechanism:

$$\alpha_{ij} = \frac{\exp\left(\text{LeakyReLU}\left(\mathbf{a}^T [\mathbf{W}\mathbf{h}_i \parallel \mathbf{W}\mathbf{h}_j]\right)\right)}{\sum_{k \in \mathcal{N}(i)} \exp\left(\text{LeakyReLU}(\mathbf{a}^T [\mathbf{W}\mathbf{h}_i \parallel \mathbf{W}\mathbf{h}_k])\right)}$$

where:

- $\mathbf{a} \in \mathbb{R}^{2d'}$ is the learnable attention parameter vector

- $\|$ denotes the concatenation operation
- $\text{Lawyerly}(x) = \max(0.01x, x)$ is the LeakyReLU activation function

Spatial Graph Construction

The spatial adjacency matrix is constructed based on physical proximity:

$$A_{ij} = \begin{cases} 1 & \text{if } d(\mathbf{s}_i, \mathbf{s}_j) \leq \tau \\ 0 & \text{otherwise} \end{cases}$$

where:

- $d(\mathbf{s}_i, \mathbf{s}_j) = \| \mathbf{s}_i - \mathbf{s}_j \|_2$ is the Euclidean distance
- $\mathbf{s}_i, \mathbf{s}_j \in \mathbb{R}^2$ are spatial coordinates
- $\tau = 55\mu\text{m}$ is the distance threshold for 10X Visium technology

Recurrent Neural Network (RNN) Component

Bidirectional LSTM Architecture

The BiLSTM processes temporal sequences in both forward and backward directions. The LSTM cell operations are defined by:

Gate Computations

$$\begin{aligned}
\mathbf{f}_t &= \sigma(\mathbf{W}_f \cdot [\mathbf{h}_{t-1}, \mathbf{x}_t] + \mathbf{b}_f) \quad \text{(Forget Gate)} \\
\mathbf{i}_t &= \sigma(\mathbf{W}_i \cdot [\mathbf{h}_{t-1}, \mathbf{x}_t] + \mathbf{b}_i) \quad \text{(Input Gate)} \\
\tilde{\mathbf{C}}_t &= \tanh(\mathbf{W}_C \cdot [\mathbf{h}_{t-1}, \mathbf{x}_t] + \mathbf{b}_C) \quad \text{(Candidate Values)} \\
\mathbf{C}_t &= \mathbf{f}_t \odot \mathbf{C}_{t-1} + \mathbf{i}_t \odot \tilde{\mathbf{C}}_t \quad \text{(Cell State)} \\
\mathbf{o}_t &= \sigma(\mathbf{W}_o \cdot [\mathbf{h}_{t-1}, \mathbf{x}_t] + \mathbf{b}_o) \quad \text{(Output Gate)} \\
\mathbf{h}_t &= \mathbf{o}_t \odot \tanh(\mathbf{C}_t) \quad \text{(Hidden State)}
\end{aligned}$$

where:

- $\mathbf{W}_*, \mathbf{b}_*$ are learnable parameters for each gate
- $\sigma(\cdot)$ is the sigmoid function
- $\odot$ denotes element-wise multiplication
- $[\cdot,\cdot]$ represents concatenation

Bidirectional Processing

$$\vec{\mathbf{h}}_t = \text{LSTM}_{\text{forward}}(\mathbf{x}_t, \vec{\mathbf{h}}_{t-1})$$
$$\overleftarrow{\mathbf{h}}_t = \text{LSTM}_{\text{backward}}(\mathbf{x}_t, \overleftarrow{\mathbf{h}}_{t+1})$$
$$\mathbf{h}_t = [\vec{\mathbf{h}}_t; \overleftarrow{\mathbf{h}}_t]$$

Hybrid Fusion Strategies

Early Fusion (Concatenation)

The concatenation fusion strategy combines embeddings at the feature level:

$$\mathbf{h}_{\text{fused}} = [\mathbf{h}_{\text{GNN}}; \mathbf{h}_{\text{RNN}}]$$
$$\mathbf{y} = \text{MLP}(\mathbf{h}_{\text{fused}})$$

where $\text{MLP}(\cdot)$ represents a multi-layer perceptron classifier.

Attention Fusion (Dynamic Weighting)

The attention-based fusion learns dynamic weights for each modality:

$$\boldsymbol{\alpha} = \text{softmax}(\text{MLP}([\mathbf{h}_{\text{GNN}}; \mathbf{h}_{\text{RNN}}]))$$
$$\mathbf{h}_{\text{fused}} = \alpha_{\text{GNN}} \cdot \mathbf{W}_{\text{GNN}}\mathbf{h}_{\text{GNN}} + \alpha_{\text{RNN}} \cdot \mathbf{W}_{\text{RNN}}\mathbf{h}_{\text{RNN}}$$

where:

- $\boldsymbol{\alpha} = [\alpha_{\text{GNN}}, \alpha_{\text{RNN}}]^T$ with $\alpha_{\text{GNN}} + \alpha_{\text{RNN}} = 1$
- $\mathbf{W}_{\text{GNN}}, \mathbf{W}_{\text{RNN}}$ are learnable projection matrices

Late Fusion (Ensemble)

The ensemble fusion combines predictions from separate modality-specific classifiers:

$$\mathbf{y}_{\text{GNN}} = \text{MLP}_{\text{GNN}}(\mathbf{h}_{\text{GNN}})$$
$$\mathbf{y}_{\text{RNN}} = \text{MLP}_{\text{RNN}}(\mathbf{h}_{\text{RNN}})$$
$$\mathbf{y}_{\text{final}} = \lambda \cdot \mathbf{y}_{\text{GNN}} + (1 - \lambda) \cdot \mathbf{y}_{\text{RNN}}$$

where $\lambda = \sigma(w)$ is a learnable ensemble weight parameter.

Loss Functions and Optimization

Weighted Cross-Entropy Loss

To handle class imbalance, we employ weighted cross-entropy loss:

$$\mathcal{L}_{\text{CE}} = -\frac{1}{N}\sum_{i=1}^{N} w_{y_i} \log(\text{softmax}(\mathbf{f}(\mathbf{x}_i))_{y_i})$$

where:

- w_{y_i} is the class weight for the true class y_i
- $\mathbf{f}(\mathbf{x}_i)$ is the model output for sample i
- N is the total number of samples

Focal Loss

For severe class imbalance, we implement focal loss:

$$\mathcal{L}_{\text{focal}} = -\alpha_t(1 - p_t)^{\gamma}\log(p_t)$$

where:

- p_t is the predicted probability for the true class
- α_t is the class weighting factor
- $\gamma = 2.0$ is the focusing parameter

Monte Carlo Dropout for Uncertainty Quantification

For uncertainty estimation, we employ Monte Carlo dropout:

$$p(\mathbf{y}|\mathbf{x}) = \frac{1}{T}\sum_{t=1}^{T} \text{softmax}\left(\mathbf{f}(\mathbf{x}, \boldsymbol{\theta}_t)\right)$$

$$\text{Uncertainty} = -\sum_{c=1}^{C} p\left(y = c|\mathbf{x}\right)\log p(y = c|\mathbf{x})$$

where:

- T is the number of Monte Carlo samples
- $\boldsymbol{\theta}_t$ represents model parameters with dropout enabled
- C is the number of classes

Evaluation Metrics

Classification Accuracy

$$\text{Accuracy} = \frac{1}{N}\sum_{i=1}^{N} \mathbb{1}\left[y_i = \hat{y}_i\right]$$

where $\mathbb{1}[\cdot]$ is the indicator function.

F1-Score

The weighted F1-score is computed as:

$$\text{Precision}_c = \frac{TP_c}{TP_c + FP_c}$$

$$\text{Recall}_c = \frac{TP_c}{TP_c + FN_c}$$

$$\text{F1}_c = \frac{2 \times \text{Precision}_c \times \text{Recall}_c}{\text{Precision}_c + \text{Recall}_c}$$

$$\text{F1}_{\text{weighted}} = \sum_{c=1}^{C} \frac{n_c}{N} \text{F1}_c$$

where n_c is the number of samples in class c.

Area Under the ROC Curve (AUC-ROC)

For multi-class classification, we use macro-averaged AUC:

$$\text{AUC}_{\text{macro}} = \frac{1}{C}\sum_{c=1}^{C} \text{AUC}_c$$

where AUC_c is the AUC for class c in a one-vs-rest setting.

Activation Functions

Sigmoid Function

$$\sigma(x) = \frac{1}{1 + e^{-x}}$$

Softmax Function

$$\text{softmax}(\mathbf{x})_i = \frac{e^{x_i}}{\sum_{j=1}^{K} e^{x_j}}$$

LeakyReLU

$$\text{LeakyReLU}(x) = \begin{cases} x & \text{if } x > 0 \\ 0.01x & \text{if } x \leq 0 \end{cases}$$

Hyperbolic Tangent

$$\tanh(x) = \frac{e^{x} - e^{-x}}{e^{x} + e^{-x}}$$

Data Preprocessing

Min-Max Normalization

$$x_{\text{norm}} = \frac{x - x_{\min}}{x_{\max} - x_{\min}}$$

Standard Scaling (Z-score)

$$x_{\text{scaled}} = \frac{x - \mu}{\sigma}$$

where μ is the mean and σ is the standard deviation.

Log Transformation

$$x_{\log} = \log(x + 1)$$

Summary

This document presents the complete mathematical framework underlying the Hybrid GNN-RNN model for cardiomyocyte differentiation prediction. The integration of spatial graph neural networks and temporal recurrent neural networks through attention-based fusion achieves state-of-the-art performance (96.67% accuracy) while providing uncertainty quantification and biological interpretability.

The mathematical formulations demonstrate how spatial relationships in tissue architecture (captured by GAT) and temporal gene expression dynamics (modeled by BiLSTM) can be effectively combined through learnable attention mechanisms to predict complex biological processes with high accuracy and reliability.

APPENDIX B – DATA SPLITTING AND LEAKAGE CHECKLIST

Splitting is performed once on the aligned joint indices, so no sample appears in more than one partition across either modality. All hyperparameter decision (early stopping, LR scheduling, model selection) use the validation set only; the test set is evaluated once at the end.

#	Control category	Specific Control	Implementation Detail
Data Splitting			
1	Stratified Train/Val/Test split	Class-proportional partitioning	"train_test_split(..., stratify=y)" ensures each split preserves the original class distribution
2	Three-way split (60/20/20)	Separate validation and held-out test sets	Train 64%, Val 16%, Test 20% via two successive stratified splits ("test_size=0.2" then "test_size=0.2" of train)
3	Mask-based GNN splitting	Boolean mask isolation for graph data	"train_mask", "val_mask", "test_mask" as non-overlapping Boolean tensors over nodes
4	K-fold cross-validation	5-fold CV for robust estimation	"KFold(n_splits=5, shuffle=True, random_state=42)" with per-fold model re-initialisation
5	Temporal split seeding	Deterministic random split for temporal data	"torch.Generator().manual_seed(42)" used in "random_split()" for RNN temporal data
Multimodal Alignment			
6	Sample-ID-based alignment	Cross-modal identity matching	GNN and RNN embeddings joined on "sample_ids.npy" via "np.intersect1d()" before any splitting (ensures same sample in both modalities)
7	Class-stratified alignment (fallback)	Fallback when IDs unavailable	Per-class "min(gnn_count, rnn_count)" samples drawn with "np.random.seed(42)"
8	Joint split after alignment	Single split governs both modalities	"X_gnn[train_idx], X_rnn[train_idx], y[train_idx]" (the same index array is applied to GNN, RNN, and labels simultaneously)
Regularisation			

(Overfitting Prevention)			
9	Early stopping	Halt training when validation stalls	Patience – 15 epochs; requires >1% relative improvement in val loss to reset counter
10	L2 weight decay (AdamW)	Parameter norm penalty	“weight_decay=5e-4” via “AdamW” optimiser
11	Dropout (multi-layer, tapered)	Stochastic unit silencing	Tapered dropout across classifier: “0.3, 0.21, 0.15, 0.09” (progressive reduction)
12	MC Dropout	Uncertainty-aware dropout at test time	“MCDropout” module with “training=True” always; 50-sample Monte Carlo inference
13	Batch Normalisation	Internal covariate shift reduction	“nn.BatchNorm1d” after Linear layers in both RNN input processor and classifier head
14	Label smoothing	Soft target regularisation	“CrossEntropyLoss(label_smoothing=0.1)” as alternative to focal loss
15	Focal loss	Down-weight easy examples	“FocalLoss(alpha, gamma)” for class-imbalanced training
16	Learning rate scheduling	Adaptive LR reduction	“ReduceLROnPlateau(patience=10, factor=0.5)” + cosine annealing scheduler
Class Imbalance Controls			
17	Weight random sampling	Over-sample minority classes	“WeightedRandomSampler” with “compute_class_weight(‘balanced’)” per-sample weights
18	Class-weighted loss	Cost-sensitive training	“CrossEntropyLoss(weight=class_weights)” where weights are inversely proportional to class frequency
Normalisation / Preprocessing			
19	Standard scaling of embeddings	Zero-mean, unit-variance	“StandardScaler().fit_transform()” applied separately to GNN and RNN embeddings
20	Log-normalisatio	Library-size correction	“log1p(X / X.sum() * 10000)” applied to raw expression before any modelling

	n of gene counts		
Reproducibility			
21	Global random seed fixing	Deterministic execution	“torch.manual_seed(42)”, “np.random.seed(42)”, “cudnn.deterministic=True”, “cudnn.benchmark=False”
22	Fixed random_state=4	Consistent splits across runs	All “train_test_split”, “KFold”, and “random_split” calls use “random_state=42” or “seed”
Overfitting Diagnosis			
23	Train-val gap monitoring	Quantify overfitting severity	“gap_mean = mean (train_acc – val_acc)”; flagged High if gap > 10% or val_std > 5%
24	Learning curve analysis	Detect underfitting/overfitting	Train at 20% - 100% of data with 3 runs per size; plot convergence of train vs. val scores
25	MC Dropout uncertainty	Confidence calibration at test time	50-sample stochastic forward passes → predictive entropy and confidence intervals per prediction
26	Best-checkpoint selection	Avoid evaluating overfit late-epoch models	Model state dict saved only at best val loss; final evaluation loads best checkpoint